Optimization of giant unilamellar vesicle electroformation for different lipid mixtures with a focus on high cholesterol concentrations

Boban, Zvonimir

Sveučilište u Splitu

Prirodoslovno-matematički fakultet

Doktorski studij Biofizika

Doktorski rad

Optimizacija elektroformacije divovskih unilamelarnih vezikula za različite lipidne smjese uz naglasak na visoke koncentracije kolesterola

Zvonimir Boban

Split, travanj 2023.

University of Split

Faculty of Science

Doctoral Study of Biophysics

Doctoral thesis

Optimization of giant unilamellar vesicle electroformation for different lipid mixtures with a focus on high cholesterol concentrations

Zvonimir Boban

Split, April 2023

University of Split, Faculty of Science, Doctoral Study of Biophysics

Optimization of giant unilamellar vesicle electroformation for different lipid mixtures with a focus on high cholesterol concentrations

A thesis by Zvonimir Boban under the supervision of Assoc. Prof. Marija Raguž, Ph.D. submitted in Partial Fulfilment of the Requirements for the Degree of Doctor of Philosophy. Achieved academic title: Ph.D. in Science, field of Physics

Composition of the Expert Panel for the Assessment and Defence of the Doctoral Thesis:

1. Prof. Mile Dželalija , Ph.D. _____

2. Prof. Damir Sapunar, Ph.D. _____

3. Assist. Prof. Lucija Krce, Ph.D. _____

4. Assoc. Prof. Laris Zoranić, Ph.D. (substitute member) _____

confirms that the Ph.D. thesis has been defended on _____.

Acting Chairman of the Doctoral Study

_____

Assoc. Prof. Damir Kovačić. Ph.D.

DEAN:

_____

Prof. Mile Dželalija, Ph.D.

Sveučilište u Splitu, Prirodoslovno-matematički fakultet, Doktorski studij Biofizika

Optimizacija elektroformacije divovskih unilamelarnih vezikula za različite lipidne smjese uz naglasak na visoke koncentracije kolesterola

Doktorski rad autora Zvonimir Bobana pod vodstvom izv. prof. dr. sc. Marije Raguž kao dio obaveza potrebnih da se dobije doktorat znanosti, mjesec i godina.
Dobiveni akademski naziv i stupanj: doktor prirodnih znanosti iz polja fizika.

Povjerenstvo za ocjenu i obranu doktorskog rada u sastavu:

1. prof. dr. sc. Mile Dželalija _____

2. prof. dr. sc. Damir Sapunar _____

3. doc. dr. sc. Lucija Krce _____

4. izv. prof. dr. sc. Laris Zoranić. (zamjenski član) _____

potvrđuje da je disertacija obranjena dana _____.

Vršitelj dužnosti voditelja doktorskog studija

_____

izv. prof. dr. sc. Damir Kovačić

DEKAN:

_____

prof. dr. sc. Mile Dželalija

BASIC DOCUMENTATION CARD

University of Split
Faculty of Science

Ph.D. thesis

Optimization of giant unilamellar vesicle electroformation for different lipid mixtures with a focus on high cholesterol concentrations

Zvonimir Boban

Thesis performed at: University of Split, School of Medicine

Abstract

Giant unilamellar vesicles (GUVs) are widely used as artificial cell membrane models. Electroformation is the most commonly used method for their production. The method depends on multiple parameters, so reproducible production of high quality GUVs can be challenging, especially when working with lipid mixtures containing cholesterol concentrations reaching and surpassing the bilayer saturation threshold. After analyzing existing electroformation protocols, we identified two key issues for such mixtures. The first issue is related to experiment reproducibility. Most protocols use the drop-deposition method which produces lipid films of nonuniform thickness, resulting in lower experiment reproducibility and efficiency of GUV formation. The second is cholesterol demixing in the form of anhydrous crystals during lipid film drying, resulting in an artifactual decrease of cholesterol concentration in GUVs compared to the initial lipid mixture. To deal with the first problem, we first tested electroformation from such mixtures with replacement of the drop-deposition step by spin-coating. Optimizing this process improved the GUV size and yield, but the cholesterol demixing issue remained. To address this issue, we developed a new protocol which combines the rapid solvent exchange, plasma cleaning and spin-coating techniques to produce GUVs by electroformation from damp lipid films. We believe that this new improved electroformation protocol will allow us to successfully study models of eye lens fiber cell membranes with their very high Chol content.

(84 pages, 27 figures, 125 references, original in English)
Thesis deposited in: National and University Library in Zagreb, University Library in Split and Library of the Faculty of Science, University of Split

Keywords: GUV, electroformation, cholesterol, phospholipid, film thickness, rapid solvent exchange, spin-coating, plasma cleaning, damp lipid film, fluorescence microscopy

Supervisor: Assoc. Prof. Marija Raguž, Ph.D.

Reviewers: 1. Prof. Mile Dželalija, Ph.D.
2. Prof. Damir Sapunar, Ph.D.
3. Assist. Prof. Lucija Krce, Ph.D.

Thesis accepted: April 12, 2023

TEMELJNA DOKUMENTACIJSKA KARTICA

Sveučilište u Splitu
Prirodoslovno-matematički fakultet

Doktorski rad

Optimizacija elektroformacije divovskih unilamelarnih vezikula za različite lipidne smjese uz naglasak na visoke koncentracije kolesterola

Zvonimir Boban

Rad je izrađen u: Medicinski fakultet Sveučilišta u Splitu

Sažetak

Divovske unilamelarne vezikule (DUV) naširoko se koriste kao modeli staničnih membrana. Elektroformacija je najčešće korištena metoda za njihovu proizvodnju. Metoda ovisi o više parametara, tako da ponovljiva proizvodnja visokokvalitetnih DUV-ova može biti izazovna, osobito pri radu s lipidnim smjesama koje sadrže koncentracije kolesterola koje dosežu i premašuju prag zasićenja membranskog dvosloja. Nakon analize postojećih protokola elektroformacije, identificirali smo dva ključna problema za takve smjese. Prvi se odnosi na ponovljivost eksperimenata. Većina protokola koristi metodu nakapavanja koja proizvodi lipidne filmove nejednake debljine, što rezultira smanjenom ponovljivošću eksperimenata i učinkovitošću stvaranja DUV-ova. Drugi je izlučivanje kolesterola u obliku dehidriranih kristala tijekom sušenja lipidnog filma, što dovodi do artefaktualnog smanjenja koncentracije kolesterola u DUV-ovima u usporedbi s početnom lipidnom smjesom. Kako bismo umanjili prvi problem, testirali smo elektroformaciju iz takvih smjesa uz zamjenu koraka nakapavanja tehnikom brzog razmazivanja. Optimizacija ovog procesa poboljšala je veličinu i prinos DUV-ova, ali i dalje je preostalo pitanje izlučivanja kolesterola. Potaknuti time, razvili smo novi protokol koji kombinira tehnike brze izmjene otapala, čišćenja plazmom i brzog razmazivanja za proizvodnju DUV-ova elektroformacijom iz vlažnih lipidnih filmova. Smatramo da će nam ovaj novi protokol pomoći u daljnjem istraživanju svojstava membrana s vrlo visokim udjelom kolesterola, poput vlaknastih stanica leće oka.

(84 stranice, 27 slika, 125 literaturnih navoda, jezik izvornika: engleski)
Rad je pohranjen u: Nacionalnoj sveučilišnoj knjižnici u Zagrebu, Sveučilišnoj knjižnici u Splitu i Knjižnici Prirodoslovno-matematičkog fakulteta Sveučilišta u Splitu

Ključne riječi: GUV, elektroformacija, kolesterol, fosfolipid, debljina filma, brza izmjena otapala, tehnika brzog razmazivanja, čišćenje plazmom, vlažni lipidni film, fluorescencijska mikroskopija

Mentor: izv. prof. dr. sc. Marija Raguž

Ocjenjivači: 1. prof. dr. sc. Mile Dželalija
2. prof. dr. sc. Damir Sapunar
3. doc. dr. sc. Lucija Krce

Rad prihvaćen: 12.4.2023.

ACKNOWLEDGMENTS

Hvala mojoj mentorici izv. prof. dr. sc. Mariji Raguž na potpori i omogućenju uvjeta za izradu ovog doktorata unatoč mnogim preprekama i zahtjevnim okolnostima koje su se pojavile na putu.
Hvala mojim kolegama, posebno Ivanu Mardešiću i Ani Puljas koji su mi najviše pomagali oko mjerenja.
Hvala i svima s Prirodoslovno-matematičkog fakulteta u Splitu koji su nam izašli u susret u vezi korištenja prostora i opreme.

Posebno hvala mojoj supruzi i djeci koja svemu što radim daju smisao i široj obitelji na podršci u teškim trenutcima.

CONTENTS

ABSTRACT

Giant unilamellar vesicles (GUVs) are widely used as artificial cell membrane models. Chol concentrations of around 30 - 40 mol% are most commonly experimented with, since most biological membranes do not exceed this level. Our work concentrates on membrane models with cholesterol content reaching and surpassing the Chol saturation threshold which correspond to a Chol concentration of approximately 50 mol% in phospholipid membranes. After the saturation threshold is reached, the excess Chol is incorporated into pure Chol bilayer domains up to a solubility threshold after which Chol crystals are formed outside the membrane. Membrane models with such high Chol content are of special interest to researchers investigating the fiber cell plasma membranes of the eye lens or the role of Chol in the development of atherosclerosis. In the case of fiber cells of eye lenses, the Chol/phospholipid molar ratios can be up to 2 in the lens cortex and up to 4 in the nucleus.

Electroformation is the most commonly used method for production of GUVs. The method depends on multiple parameters, so reproducible production of high quality GUVs can be challenging, especially when working with lipid mixtures containing cholesterol (Chol) concentrations reaching and surpassing the bilayer saturation threshold. After analyzing existing electroformation protocols, we identified two key issues for such mixtures. The first issue is related to experiment reproducibility. Traditional protocols use the drop-deposition method which produces lipid films of nonuniform thickness, resulting in lower experiment reproducibility and efficiency of GUV formation. The second is Chol demixing in the form of anhydrous crystals during lipid film drying, resulting in an artifactual decrease of Chol concentration in GUVs compared to the initial lipid mixture.

To deal with the first problem, we tested electroformation from binary phosphatidlcholine/Chol and ternary phosphatidylcholine/sphingomyelin/Chol mixtures with high Chol concentrations. Replacement of the drop-deposition step by spin-coating and optimization of the electrical parameters improved the GUV size and yield. The optimal film thickness was found to be ~ 30 nm, and the results were obtained for frequency–voltage combinations in the range of 2–6 V and 10–100 Hz.

However, the Chol demixing issue remained. To address this issue, we developed a new protocol which combines the rapid solvent exchange, plasma cleaning and spin-coating techniques to produce GUVs through electroformation from damp lipid films. We believe that this new improved electroformation protocol will enable

successful studies of models of eye lens fiber cell membranes with their very high Chol content. Furthermore, both using aqueous solutions and treating the electrodes with plasma have been proven beneficial for electroformation efficiency, allowing for production of GUVs with charged lipids and solutions containing high ion concentrations. Since it avoids organic solvents and lipid film drying, the protocol could also be adapted for protein reconstitution into GUVs.

LIST OF PUBLICATIONS RELEVANT TO THE THESIS

The following publications constitute the main part of the thesis:

1. Boban, Z.; Puljas, A.; Kovač, D.; Subczynski, W.K.; Raguz, M. Effect of Electrical Parameters and Cholesterol Concentration on Giant Unilamellar Vesicles Electroformation. Cell Biochem. Biophys. 2020, 78, 157–164, doi:10.1007/s12013-020-00910-9.

2. Boban, Z.; Mardešić, I.; Subczynski, W.K.; Raguz, M. Giant Unilamellar Vesicle Electroformation: What to Use, What to Avoid, and How to Quantify the Results. Membranes (Basel). 2021, 11, 860, doi:10.3390/MEMBRANES11110860.

3. Boban, Z.; Mardešić, I.; Subczynski, W.K.; Jozić, D.; Raguz, M. Optimization of Giant Unilamellar Vesicle Electroformation for Phosphatidylcholine/Sphingomyelin/ Cholesterol Ternary Mixtures. Membranes (Basel). 2022, 12, 525, doi:10.3390/membranes12050525.

4. Boban, Z.; Mardešić, I.; Perinović Jozić, S.; Šumanovac, J.; Subczynski, W.K.; Raguz, M. Electroformation of Giant Unilamellar Vesicles from Damp Lipid Films Formed by Vesicle Fusion. Membranes (Basel). 2023, 13, 352, doi: 10.3390/membranes13030352.

1 INTRODUCTION

1.1 Plasma membranes with a high cholesterol content

The plasma membrane is a complex structure separating the cell interior from its environment. It consists of various different lipids, mostly phospholipids, sphingolipids and cholesterol (Chol), but also membrane proteins and carbohydrates [1,2]. Phospholipids differ with respect to the headgroup, hydrocarbon chain length and degree of unsaturation. Physical properties of the membrane change depending on its phospholipid composition and differences in Chol content [3]. Chol concentration influences the membrane thickness and rigidity [4,5], domain formation [6], and cell signaling [7]. The Chol molecule consists of a polar head, a rigid steroid ring structure and a nonpolar hydrocarbon tail. It is positioned with its head among the polar heads of other phospholipids and the rigid ring structure alongside the acyl chain region of lipids. Consequently, the Chol molecule can regulate the lateral organization and physical properties of the membrane.

Artificial vesicles are often grown from single phospholipid species. Aside from phospholipids, Chol and/or sphingomyelin are most frequently incorporated into vesicles since they are the other two most abundant eukaryotic plasma membrane components [8–10]. Chol concentrations of up to ~50 mol% are most commonly experimented with, since most biological membranes do not exceed this level [8,11], and the maximum solubility limit of Chol in phospholipid membranes seems to be around 66 mol% [12,13].

Our work concentrates on membrane models with Chol content reaching and surpassing the Chol saturation threshold which correspond to a Chol concentration of approximately 50 mol% in phospholipid membranes. After the saturation threshold is reached, the excess Chol is incorporated into pure Chol bilayer domains (CBDs) up to a solubility threshold after which Chol crystals are formed outside the membrane [14,15]. Membranes with such high Chol content are of special interest to researchers investigating the fiber cell plasma membranes of the eye lens [14,16–21] or the role of Chol in the development of atherosclerosis [22,23]. The fiber cells of eye lenses exhibit Chol/phospholipid molar ratios of up to 2 in the lens cortex and up to 4 in its nucleus [24,25]. Such high Chol contents are thought to be crucial for maintaining lens transparency by enabling the formation of CBDs which ensure that the surrounding phospholipid bilayer is saturated with Chol. High Chol content is a sign of pathology in most tissues and organs [11,23]. Eye lenses are the only system in which such high Chol

concentrations and CBDs are needed to maintain fiber cell membranes, fiber cells, and whole lens homeostasis.

1.2 Liposomes as artifical membrane models

Artificial vesicles have become an important research tool due to their similarity to biological membranes [26–31]. Being lab-created, they enable the study of membrane properties under controlled conditions. Based on their structure, we classify vesicles into unilamellar, multilamellar (MLVs) and oligolamellar vesicles (Figure 1). Unilamellar vesicles only have a single outer bilayer, multilamellar vesicles contain multiple bilayers arranged in concentric circles, and oligolamellar vesicles enclose smaller vesicles inside. Unilamellar vesicles are further sorted by size into small (SUVs, < 100 nm), large (LUVs, 100 nm – 1 μm), and giant unilamellar vesicles (GUVs, > 1 μm) (Figure 1). Small and large unilamellar vesicles are more often studied in the context of drug delivery applications [32–34] and GUVs are more interesting to researchers studying membrane properties and organization because of similarity in size to eukaryotic cells. An additional advantage of GUV size is the possibility to observe them using light microscopy techniques.

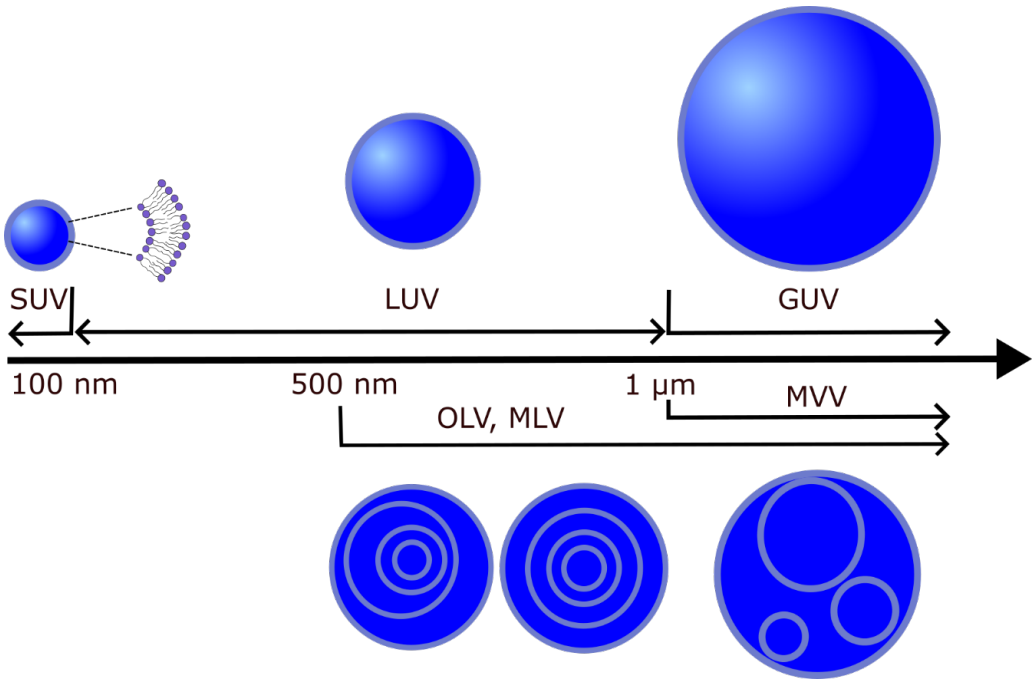

Figure 1. Different types of lipid vesicles based on their size and structure. Reproduced from [35].

1.3 Traditional electroformation protocol

One of the earliest attempts at forming GUVs was the natural swelling method introduced by Reeves and Dowben in 1969 [28]. There, a lipid solution is deposited on a surface and dried to form a lipid film. The lipid film is then rehydrated, and the obtained solution gently stirred to form vesicles. The vesicles are formed mainly due to the osmotic pressure driving the aqueous solution in between the stacked lipid bilayers. Exposing the hydrophobic portion of the bilayer to aqueous solutions is unfavourable and causes them to close up into vesicles. However, the proportion of GUVs that can be generated using this method is small as most of them are either multilamellar or display other types of defects [36]. In their efforts to devise a protocol that reliably produces a high proportion of cell-sized unilamellar vesicles, Angelova and Dimitrov applied an external electric field during lipid swelling and thus invented the electroformation method [37]. Although the exact theoretical mechanism behind the method is not yet completely understood, it is believed that the electric field affects lipid swelling through direct electrostatic interactions, redistribution of counterions, changes in membrane surface and line tension and electroosmotic flow effects [38–41].

Although Angelova and Dimitrov used platinum wires for electroformation, indium tin oxide (ITO) electrodes are most commonly used nowadays. The only difference between these two protocols is the electroformation chamber layout. The protocol starts with droplets of lipids dissolved in an organic solvent being deposited onto the electrode (Figure 2a). In addition to lipids, fluorescent dyes are present in the mixture in small quantities to enable the usage of fluorescent microscopy later on. The solvent is evaporated under vacuum or a stream of inert gas (Figure 2b). A spacer is attached to the electrode using vacuum grease (Figure 2c). Another electrode is then attached to the spacer with its conductive side facing inward. Following that, the chamber is filled with an internal solution of choice and connected to a voltage source while maintaining a temperature higher than the phase transition temperature of deposited lipids. Copper tape is often attached to the electrodes to provide better contact with the alternating current function generator (Figure 2d). The combination of the electric field and lipid film hydration leads to creation of lipid vesicles that can be observed under a microscope (Figure 2e).

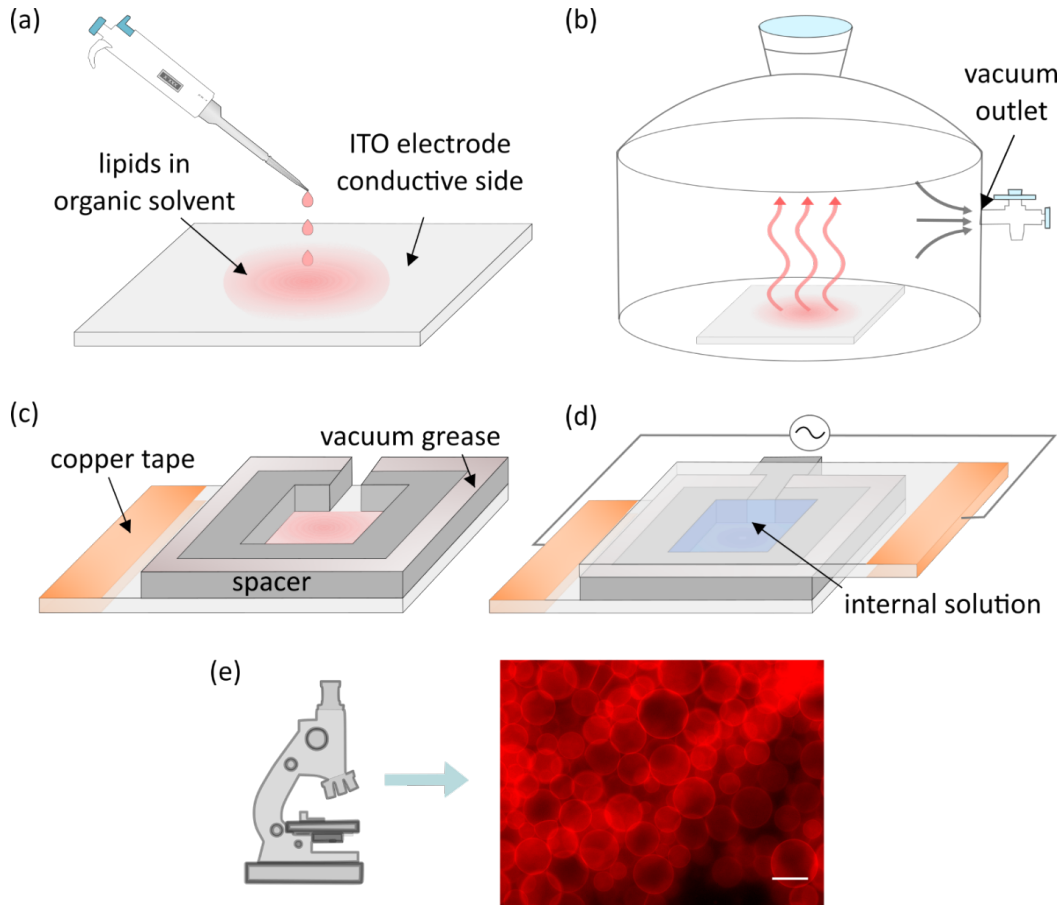

Figure 2. (**a**) Deposition of lipid droplets onto the electrode surface. (**b**) Evaporation of organic solvent under vacuum. (**c**) Construction of the electroformation chamber. (**d**) Electroformation chamber filled with an internal solution and connected to an alternating current function generator. (**e**) An image of fluorescently labeled giant unilamellar vesicles (GUVs) obtained using fluorescence microscopy. The scale bar denotes 50 μm. Reproduced from [42].

1.4 Modifications of the traditional protocol

1.4.1 Electrode material and cleaning

Alongside platinum electrodes, ITO-coated glass slides are most commonly used nowadays. In comparison to platinum electrodes, ITO electrodes provide a larger and flatter surface, so a higher GUV yield can be obtained. Also, owing to their transparency, microscopic techniques are easier to apply.

Compared to ITO electrodes, platinum electrode aging seems to affect the average diameter of vesicles less, but the proportion of GUVs (i.e., the proportion of defect-free unilamellar vesicles) also drops. Steel syringe and copper electrodes also have been suggested as cost-friendly alternatives [43,44]. Furthermore, titanium electrodes have

been advocated by some groups since their usage seems to decrease lipid peroxidation when compared to ITO electrodes [45–48].

In order to remove contaminants from the electrode surface, researchers use a variety of cleaning protocols. In general, they consist of cleaning the electrodes using organic solvents and then drying them. Of course, there are a lot of variations of these general steps, and some articles do not even include the cleaning protocol [49–51]. Variations include sonication in conjunction with organic solvents [41,52–54], repeated rinsing with organic solvents [55] and swabbing electrodes using lint-free wipes [56–59]. Electrodes are either dried under a stream of inert gas [41,52,54,56] or just wiped and air dried [57]. Plasma cleaning has also been tested on ITO glass [41,52] and has proved to be very effective, since it both cleans the surface and makes it more hydrophilic. Moreover, plasma cleaning could aid hydration of the solid lipid film and formation of lipid bilayers [41].

1.4.2 Lipid film deposition

The traditional electroformation protocol contains a step in which the lipids dissolved in chloroform or other organic solvents are deposited onto the electrodes simply by dropping the solution and evaporating the solvent later [37,60] (Figure 3a). In order to efficiently produce GUVs, the lipid film is suggested to be around 5–10 bilayers thick (around 30–60 nm) [37,54,61]. When using drop deposition, regions of different thicknesses will form. Although this means that at least some portion of the deposited film will be suitable for electroformation at given parameters, other regions will inevitably be too thin or too thick. These nonuniformities result in lack of reproducibility.

In order to make the deposition process more efficient and reproducible, other approaches were investigated as well. Some groups used needles or thin rods to smear the solution after dropping it in order to increase the film homogeneity [41,59,62,63] (Figure 3b). Others tried to create non-overlapping snakelike patterns of the lipid film using a Hamilton syringe [56]. A more systematic approach was tested by stamping the lipid solution onto the ITO electrode using a customized polydimethylsiloxane (PDMS) stamp [64] (Figure 3c). This approach resulted in GUVs of a size similar to the width of the gaps in the PDMS stamp. However, the authors report that the thickness of the lipid film was not uniform over the lipid patches in the gaps. Dip coating (immersing the ITO electrode in the lipid solution and holding it vertically to dry) was explored as well, but

due to different rates of solvent evaporation across the glass, the film proved to be inhomogeneous [54].

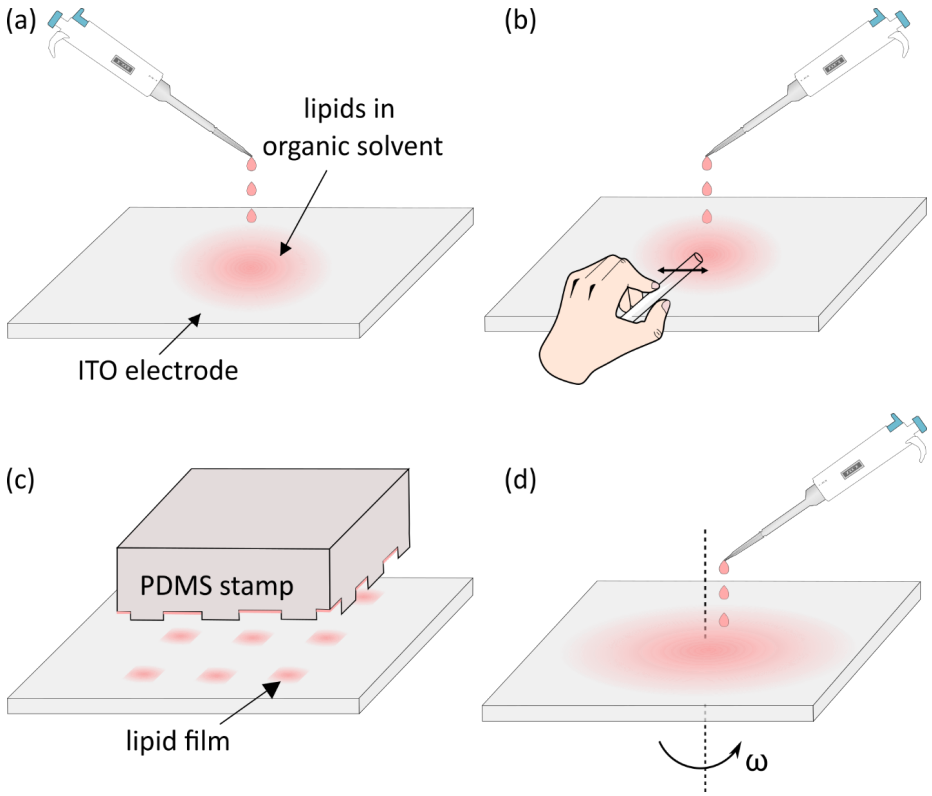

Figure 3. (**a**) Droplet deposition. (**b**) Droplet deposition with smearing afterward to better spread the lipid film. (**c**) Deposition of lipids by pressing a patterned silicon stamp on the electrode surface. (**d**) Spin-coating of lipid solution by fast rotation of the electrode immediately after the deposition. Reproduced from [42].

Reproducibly controllable lipid film thickness was achieved by Estes and Mayer using the spin-coating method. The lipid solution is dropped onto the flat electrode surface, which is subsequently rotated very fast in order to create a homogenous lipid film [54] (Figure 3d). The uniformity of films and method reproducibility were confirmed using ellipsometry and atomic force microscopy techniques. The method was proven to be effective by several groups using a wide range of lipid compositions [54,55,57]. The only disadvantage is that it requires a much larger amount of lipids compared to traditional methods, since much of the solution is washed away during electrode spinning [54].

Another attempt at achieving uniform lipid films was tested by Le Berre et al. [65]. They drag-dropped an organic solution of lipids on a solid substrate. Constant substrate velocity and temperature were maintained while simultaneously controlling the vapor aspiration. Reproducible results with variations of ± 5 nm were obtained, but the

method has not been widely adopted, probably due to the device used being relatively complicated.

Oropeza-Guzman et al. suggested an approach utilizing the coffee ring effect to address this issue [66]. The effect describes a process during which most lipid material in a drying droplet is being deposited on the periphery of the droplet, forming a ring-like stain. They took advantage of the effect by consecutively depositing progressively larger droplets on top of one another. Adding more material created rings of progressively larger diameters. Each consecutive ring would smear and flatten the ring from the previous droplet, thus leaving an area of uniform lipid thickness inside. Although the method has not resulted in an increase of the mean diameter of vesicle populations when compared to the single droplet deposition, the multi-droplet preparations displayed a much lower percentage of defects and nonunilamellar vesicles.

Before chamber construction, the organic solvent needs to be removed from the deposited lipid solution. This is most commonly achieved by placing the electrodes under vacuum. Alternatively, drying can be performed by placing the electrode with the lipid solution under a stream of an inert gas such as nitrogen or argon. More rarely encountered, lyophilization can also be used to eliminate traces of the organic solvent [12,67].

Some researchers went in another direction and instead of trying to improve the existing approach, replaced the organic solution of lipids with aqueous liposome suspensions (SUVs, LUVs, or multilamellar vesicles) [29,50,53,66,68–70]. Using this approach, Pott et al. concluded that GUV formation was better when using aqueous liposome solutions than when using organic lipid solutions [29]. They attribute this to the ability of such dispersions to produce well-oriented membrane stacks immediately after evaporation of water. Although they have completely removed any excess water from the deposits, an alternative approach was suggested in which the deposits would be only partially dehydrated prior to internal solution addition. The effect of using damp lipid films on GUV properties was explored in more detail by Baykal-Caglar et al. [50]. By measuring their miscibility transition temperature, they have shown that such an approach produces more compositionally uniform populations of GUVs. This result is explained by reduction in lipid demixing—a common artifact appearing when drying the lipid solution completely. The artifact is especially pronounced when using mixtures with a Chol content near to or over the maximum solubility threshold for that mixture [12].

Furthermore, avoiding the dry phase and use of organic solvents benefits protocols aimed at protein incorporation into GUVs, since these steps damage the protein structure. The first proof of successful protein reconstitution using this approach came from Girard et al. [70] and the most recent protocol is described by Witkowska et al. [53].

1.4.3 Electrical parameters

Most studies are not concerned with electroformation parameters giving the best GUV yield, but only require a certain number of stable vesicles for further research. It is no wonder then that most of them choose established voltage and frequency values from common references such as Angelova et al. or Veatch where peak-to-peak voltage is usually kept between 1 and 10 V and frequency around 10 Hz [37,59,71].

Of course, since the property of interest here is the electric field and not the voltage by itself, the voltage values should always be accompanied by electrode separation in order to provide some context for the field strength. Common interelectrode separations range from 0.5 to 3 mm. Most often, a separation value from this interval is used without special explanation, and the voltage is modified accordingly. In combination with ITO electrodes, the separation is achieved through the use of spacers usually made from silicon (PDMS) [27,37,40,54–56,60] or teflon (polytetrafluoroethylen) [45,57,72,73]. Another alternative is specifiying the electric field strength instead of the voltage from the beginning [29,55,57].

Significant deviations from conventional parameters are usually explored only in studies specifically trying to improve a certain aspect of the electroformation protocol. GUVs were obtained using egg phosphatidylcholine or DOPA (1,2-dioleoyl-*sn*-glycero-3-phosphate) using electric field values of up to 40 V/mm and frequencies up to 1 MHz [55]. Another study used a mixture of phosphatidylcholine and cholesterol and found the optimal values to be 5 V/mm and 10 kHz [40]. Considering such large differences depending on the specific lipid composition and experimental setup, it is prudent to optimize the electrical parameters every time a different lipid composition (or one not yet explored by other researchers) is used. However, using electric field strengths up to a couple V/mm and frequencies of 10–100 Hz seems to give satisfying results for many different lipid compositions (positive, negative and zwitterionic lipids compositions were tested) when deionized water is used as an internal solution [62].

If physiological salt concentration buffers are used as the internal solution, higher frequencies tend to be needed [29,41,58,74]. Pott et al., Montes et al. and Lefrancois et al.

all had success forming vesicles at physiological conditions using a frequency of 500 Hz [29,49,74]. Li et al. did a systematic frequency-voltage sweep for three lipid compostions (two zwitterionic and one negatively charged lipid species) and found the ideal frequency to be in the range of 100–1000 Hz as well [41]. The preference for higher frequencies is attributed to disruption of the electric double layer under those conditions [41,55,58,75].

Some groups alter the voltage values during electroformation [29,43,49,53,63,70,72,74]. The reasoning behind such protocols is well described by Pott et al. [29]. First, the electric field is progressively being increased up to a maximum value at a fixed frequency in order to maintain a sphere-like shape of growing vesicles. Second, depending on the chamber solution and the duration of the first step, the electric field is kept constant in order to allow an increase in size through swelling. An additional step can be included in which the electric field remains the same as in the previous step, but the frequency is reduced in order to promote vesicle fusion and detachment from the electrodes.

Drabik et al. compared the approach of increasing the voltage by 1 V every hour from 1 to 4 V with a constant 2.5 V applied for 4 h. The obtained vesicles were bigger when using the sequential voltage approach, but both the amount of lipids used for electroformation and the ratio of unilamellar to oligolamellar vesicles remained unchanged [72]. It is important to note that this research only used a zwitterionic monounsaturated phospholipid, so the results might differ when using different lipids or more complex compositions. Breton et al. utilized a protocol involving an initial stepwise increase in voltage up to a maximum value that was then maintained for a certain amount of time [76]. Using three lipid species with different levels of unsaturation, they have shown that even at relatively low electric field values (< 1 V/mm), lipid oxidation occurs for moderately and highly oxidizable lipids (two double bonds or more). This is in agreement with a previous study on the oxidative effect of electric field on lipids from Zhou et al. [47]. The increase in maximum voltage did not change the rate of oxidation for monounsaturated lipid species [76]. The size of the vesicles increased up to an oxidation level of 25 % after which it started to decrease [76]. The fact that oxidation of 25 % will be reached at different voltages for different lipid species again underlines the necessity of optimizing the protocol for each different lipid composition used.

1.5 Chol demixing issue

In order to investigate the properties of CBDs in a controlled environment, GUVs of adequate compositions should be produced. However, because of the high Chol content, preparation of such GUVs is problematic using the traditional electroformation protocol due to the lipid film drying step. During lipid film drying, some Chol demixes and forms anhydrous Chol crystals [17,50,77]. Once the film is rehydrated, these crystals do not participate in the formation of the lipid bilayer, resulting in an artifactual decrease of Chol concentration in the bilayer compared to the initial mixing ratio in the lipid solution.

A good example of Chol demixing was provided in a study utilizing confocal microscopy to detect CBDs in GUVs formed from a mixture of Chol and POPC (1-palmitoyl-2-oleoyl-glycero-3-phosphocholine) using the traditional electroformation method (with the dry lipid film step) [17]. CBDs were observed only for Chol content greater than the Chol saturation limit and Chol solubility threshold, at about 75 mol% of Chol (Chol/POPC mixing ratio of 3/1), and not as expected at 50 mol%.

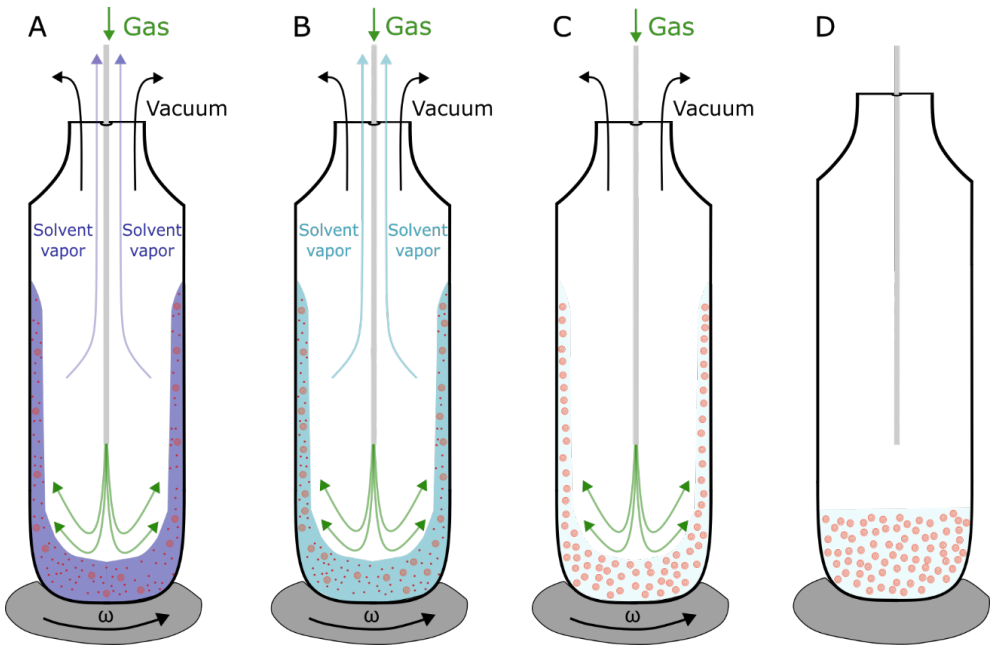

Figure 4. Schematic depiction of the rapid solvent exchange method. A) Organic solvent (blue) containing lipids (red) is mixed with an aqueous solution, and removal is achieved by vortexing the solution under vacuum. The process can be made more efficient by adding a flow of inert gas (green) pushing the organic solvent vapors out. B) MLVs start to form. The vacuum pressure is set below the organic solvent evaporation point, but higher than the evaporation point of water. C) Exchange is finished when all the organic solution is evaporated and only aqueous solution containing formed MLVs is left. D) When MLVs are formed vortex is turned off, and vacuum and gas flow pipes are closed. Reproduced from [35].

A method called the rapid solvent exchange (RSE) can be utilized to bypass the dry phase [78]. During the procedure, chloroform dissolved lipids are first mixed with an aqueous medium and then the chloroform is rapidly evaporated, leaving behind an aqueous suspension of vesicles (Figure 4) [78].

The method has been proven effective against the Chol demixing artifact [14,50,77]. However, it results in formation of smaller multilamellar vesicles (MLVs), not GUVs. By performing electron paramagnetic resonance measurements on MLVs produced using the RSE method, it was shown that CBDs start to form at 50 mol% of Chol (at a Chol/phospholipid molar ratio of 1/1) [14,15]. The difference in amount of Chol in the initial lipid mixture needed for detection of CBDs attests to the severity of Chol demixing during the lipid film drying step.

2 AIMS AND SCOPES OF THE THESIS

The research presented in this thesis was motivated by studies on the fiber cell plasma membranes of the eye lens which contain Chol in concentrations reaching and surpassing the Chol saturation threshold. In order to better understand the properties of such systems, we optimized and advanced the electroformation of GUVs made from mixtures containing different phospholipids and high Chol concentrations. After trying out the traditional electroformation protocol, several issues arose. The reproducibility of the method was quite low and GUV populations with a wide size distribution were produced. Additionally, since the traditional protocol uses lipids dissolved in an organic solvent during the film deposition step, the traces of the solvent have to be removed after deposition in order to not harm the GUV formation process. When large amounts of Chol are incorporated to the lipid mixture, the complete drying of the film leads to Chol precipitation in the form of anhydrous crystals. These crystals do not participate in subsequent bilayer formation, resulting in an artifactual decrease of Chol concentration in the bilayer compared to the initial lipid mixture.

We addressed the first issue by improving the layout of the electroformation chamber and modifying the lipid film deposition step. Instead of using the drop-deposition technique of the traditional protocol, we opted for the spin-coating method. Using this modified protocol, we produced lipid films with different Chol concentrations from binary POPC/Chol [57] and ternary POPC/sphingomyelin/Chol [79] lipid mixtures. Ternary phospholipid/sphingomyelin/Chol mixtures are of interest to researchers studying the properties of lipid rafts [80–82]. The thickness and uniformity of the lipid film were quantified using atomic force microscopy, X-ray reflectometry and fluorescence microscopy. The optimal thickness was determined to be around 30 - 35 nm. However, it should be noted that the best lipid film thickness will always depend on the specific lipid composition, so optimization should be carried out for each mixture for which there are no previous measurements on scientific record. The lipid film thickness showed a linear dependance on the amount of lipids, so it could be reproducibly controlled by altering the total lipid concentration.

Since lipid mixtures with such high Chol concentrations were rarely experimented with before, in order to successfully produce GUVs and maximize their yield and size uniformity, we also had to test various frequency-voltage combinations to find the one that produced the best results. The amount of defects, and size distribution of the GUV

population were assessed using fluorescence microscopy. The best results were obtained for frequency–voltage combinations in the range of 2–6 V and 10–100 Hz.

Even after all these modifications, the Chol demixing artifact remained. In order to resolve this issue, the dry film step should be bypassed. A study by Baykal-Caglar et al. managed to produce GUVs from damp lipid films after incomplete drying of an RSE produced aqueous liposome suspension on the surface [50]. However, their protocol lasted very long since they had to wait for approximately 24 hours for the film to become sufficiently dry.

In the final article incorporated into the thesis, we proposed a novel improved protocol which combines the plasma-cleaning, RSE, and spin-coating techniques for production of GUVs from aqueous damp lipid films obtained through vesicle fusion [83]. Our approach was inspired by the vesicle fusion method which is often used for preparation of supported bilayer membranes [84]. The method involves the deposition of an aqueous suspension of vesicles on a hydrophilized surface. The interaction of the hydrophilic surface with the vesicles causes them to rupture, creating a surface bilayer.

The protocol consists of 6 main steps:

1. The lipid solution is prepared from chloroform dissolved lipid stocks
2. The obtained solution is mixed with deionized water and RSE is then used to obtain the MLV suspension (Figure 5a)
3. MLVs are extruded by passing the solution through a polycarbonate filter in order to produce a homogeneous LUV solution (Figure 5b, c)
4. The ITO electrodes which were stored in deionized water are cleaned by swabbing with ethanol moistened wipes and then plasma cleaned for additional cleaning and surface hydrophilization (Figure 6a)
5. The LUV suspension is deposited onto the hydrophilic ITO electrode surface and spin-coated to produce a lipid film. The film is created due to vesicles rupturing in contact with the hydrophilic surface (Figure 6b)
6. The coated electrode is used in construction of the electroformation chamber which is subsequently connected to an alternatincg current source in order to produce GUVs (Figure 6c)

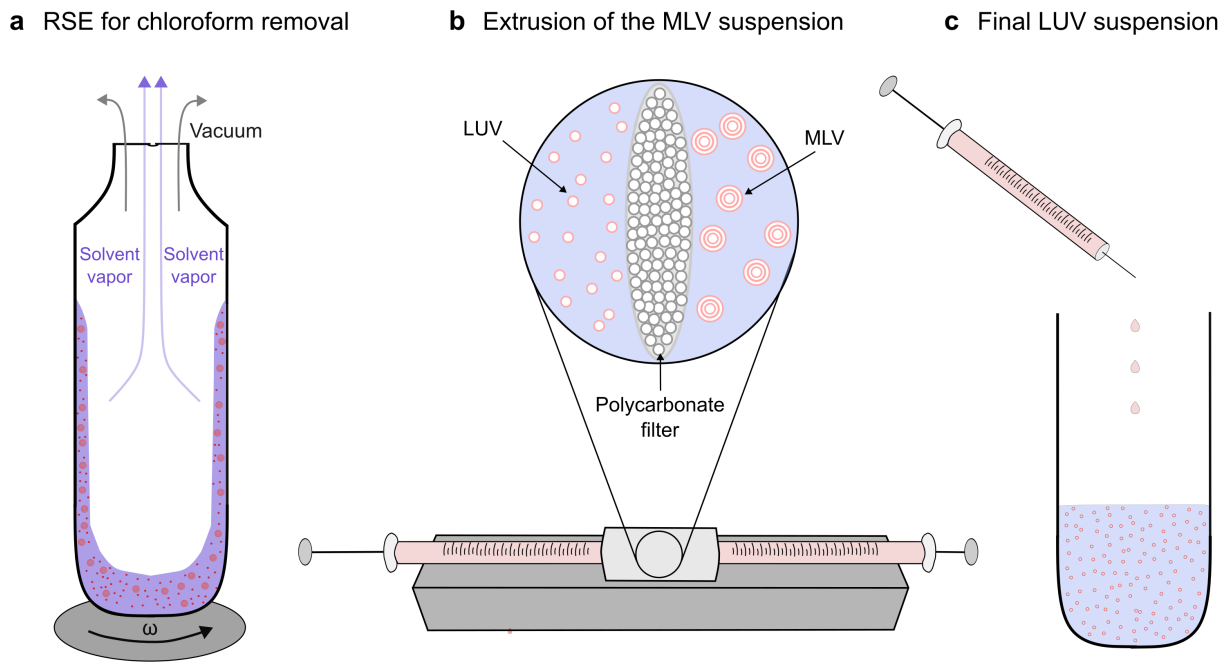

Figure 5. Preparation of the LUV solution. **(a)** MLVs are first prepared using the RSE method by rapidly evaporating chloroform from the mixture. **(b)** MLVs are passed through a polycarbonate filter an uneven number of times in order to obtain LUVs. **(c)** The obtained LUV solution is stored for later use in preparation of the damp lipid film. Reproduced from [83].

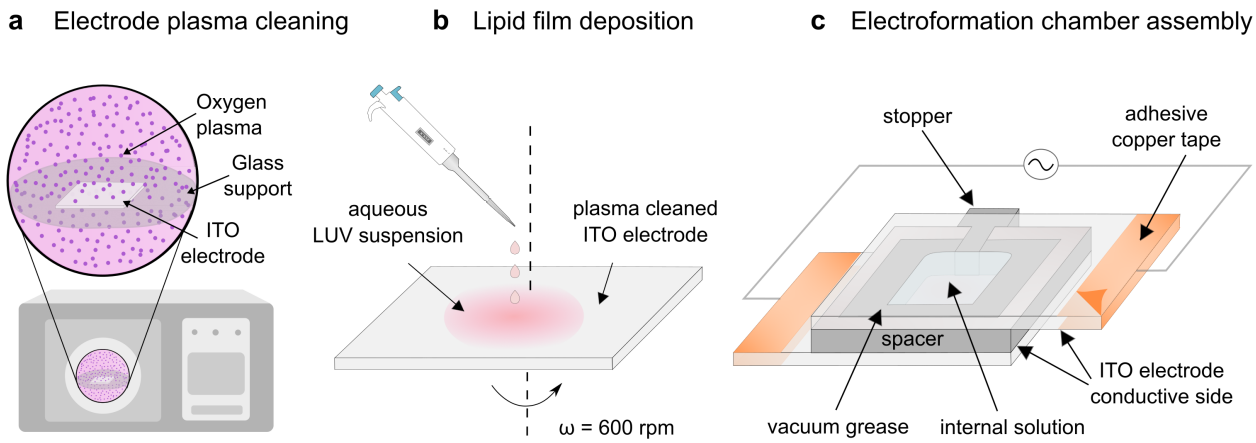

Figure 6. Electroformation from a damp lipid film. **(a)** The ITO electrode is hydrophilized using a plasma cleaner. **(b)** The LUV suspension is deposited onto a plasma cleaned ITO coated glass and spin-coated to obtain a damp lipid film. **(c)** The coated electrode is used to assemble the electroformation chamber. Reproduced from [83].

The successful removal of the organic solvent and film dampness were confirmed using attenuated total reflection Fourier transform infrared spectroscopy. The duration

of the protocol was significantly reduced - from 24 hours of drying to a couple of minutes of spin-coating. Moreover, compared to protocols that include the dry film step, the sizes and quality of vesicles determined from fluorescence microscopy images were similar or better, confirming the benefits of our protocol in that regard as well.

The proposed protocol should help reduce the Chol demixing artifact and improve the ability to produce high quality GUV populations under different conditions and from different lipid mixtures. However, a tradeoff seems to be involved. On one hand, in order to increase the certainty that Chol will not crystallize, the lipid film should remain as wet as possible. On the other hand, we have shown that shorter drying times result in lower yields and smaller average GUV diameters. If the lipid mixture contains no Chol, or small quantities of Chol, there is no reason not to dry the lipid film. However, if that is not the case, since the gentle hydration protocol also involves a lipid film drying step, the Chol demixing will certainly be an issue. The RSE technique is included to assure that the Chol concentration in MLVs is the same as the concentration of Chol in the initial mixture of lipids dissolved in an organic solvent.

We believe that this new improved electroformation protocol will allow us to successfully study models of eye lens fiber cell membranes with their very high Chol content. Furthermore, both using aqueous solutions and treating the electrodes with plasma have been proven beneficial for electroformation efficiency, allowing for production of GUVs with charged lipids and solutions containing high ion concentrations. Since it avoids organic solvents and lipid film drying, the protocol could also be adapted for protein reconstitution into GUVs.

3 REFERENCES

1. Harayama, T.; Riezman, H. Understanding the Diversity of Membrane Lipid Composition. *Nat. Rev. Mol. Cell Biol.* **2018**, *19*, 281–296, doi:10.1038/nrm.2017.138.
2. Nicolson, G.L. The Fluid—Mosaic Model of Membrane Structure: Still Relevant to Understanding the Structure, Function and Dynamics of Biological Membranes after More than 40years. *Biochim. Biophys. Acta - Biomembr.* **2014**, *1838*, 1451–1466, doi:10.1016/j.bbamem.2013.10.019.
3. Casares, D.; Escribá, P. V.; Rosselló, C.A. Membrane Lipid Composition: Effect on Membrane and Organelle Structure, Function and Compartmentalization and Therapeutic Avenues. *Int. J. Mol. Sci.* **2019**, *20*, 2167, doi:10.3390/ijms20092167.
4. Róg, T.; Pasenkiewicz-Gierula, M.; Vattulainen, I.; Karttunen, M. Ordering Effects of Cholesterol and Its Analogues. *Biochim. Biophys. Acta - Biomembr.* **2009**, *1788*, 97–121, doi:10.1016/j.bbamem.2008.08.022.
5. Gumí-Audenis, B.; Costa, L.; Carlá, F.; Comin, F.; Sanz, F.; Giannotti, M. Structure and Nanomechanics of Model Membranes by Atomic Force Microscopy and Spectroscopy: Insights into the Role of Cholesterol and Sphingolipids. *Membranes (Basel).* **2016**, *6*, 58, doi:10.3390/membranes6040058.
6. Harder, T. Formation of Functional Cell Membrane Domains: The Interplay of Lipid– and Protein–Mediated Interactions. *Philos. Trans. R. Soc. London. Ser. B Biol. Sci.* **2003**, *358*, 863–868, doi:10.1098/rstb.2003.1274.
7. Incardona, J.P.; Eaton, S. Cholesterol in Signal Transduction. *Curr. Opin. Cell Biol.* **2000**, *12*, 193–203, doi:10.1016/S0955-0674(99)00076-9.
8. Van Meer, G.; Voelker, D.R.; Feigenson, G.W. Membrane Lipids: Where They Are and How They Behave. *Nat. Rev. Mol. Cell Biol.* **2008**, *9*, doi:10.1038/nrm2330.
9. Lorent, J.H.; Levental, K.R.; Ganesan, L.; Rivera-Longsworth, G.; Sezgin, E.; Doktorova, M.; Lyman, E.; Levental, I. Plasma Membranes Are Asymmetric in Lipid Unsaturation, Packing and Protein Shape. *Nat. Chem. Biol.* **2020**, *16*, 644–652, doi:10.1038/s41589-020-0529-6.
10. Watson, H. Biological Membranes. *Essays Biochem.* **2015**, *59*, 43–70, doi:10.1042/BSE0590043.
11. Subczynski, W.K.; Justyna, M.P.; Mainali, L.; Raguz, M. High Cholesterol / Low Cholesterol : Effects in Biological Membranes Review. *Cell Biochem. Biophys.* **2017**, 1–16, doi:10.1007/s12013-017-0792-7.
12. Huang, J.; Buboltz, J.T.; Feigenson, G.W. Maximum Solubility of Cholesterol in Phosphatidylcholine and Phosphatidylethanolamine Bilayers. *Biochim. Biophys. Acta (BBA)-Biomembranes* **1999**, *1417*, 89–100, doi:10.1016/s0005-2736(98)00260-0.
13. Stevens, M.M.; Honerkamp-Smith, A.R.; Keller, S.L. Solubility Limits of Cholesterol, Lanosterol, Ergosterol, Stigmasterol, and β-Sitosterol in Electroformed Lipid Vesicles. *Soft Matter* **2010**, *6*, 5882–5890, doi:10.1039/c0sm00373e.
14. Mainali, L.; Raguz, M.; Subczynski, W.K. Formation of Cholesterol Bilayer

Domains Precedes Formation of Cholesterol Crystals in Cholesterol/Dimyristoylphosphatidylcholine Membranes: EPR and DSC Studies. *J. Phys. Chem. B* **2013**, *117*, 8994–9003, doi:10.1021/jp402394m.

15. Mainali, L.; Pasenkiewicz-Gierula, M.; Subczynski, W.K. Formation of Cholesterol Bilayer Domains Precedes Formation of Cholesterol Crystals in Membranes Made of the Major Phospholipids of Human Eye Lens Fiber Cell Plasma Membranes. *Curr. Eye Res.* **2020**, *45*, 162–172, doi:10.1080/02713683.2019.1662058.
16. Mainali, L.; Raguz, M.; O'Brien, W.J.; Subczynski, W.K. Properties of Membranes Derived from the Total Lipids Extracted from Clear and Cataractous Lenses of 61–70-Year-Old Human Donors. *Eur. Biophys. J.* **2014**, *44*, 91–102, doi:10.1007/s00249-014-1004-7.
17. Raguz, M.; Kumar, S.N.; Zareba, M.; Ilic, N.; Mainali, L.; Subczynski, W.K. Confocal Microscopy Confirmed That in Phosphatidylcholine Giant Unilamellar Vesicles with Very High Cholesterol Content Pure Cholesterol Bilayer Domains Form. *Cell Biochem. Biophys.* **2019**, *77*, 309–317, doi:10.1007/s12013-019-00889-y.
18. Subczynski, W.K.; Raguz, M.; Widomska, J.; Mainali, L.; Konovalov, A. Functions of Cholesterol and the Cholesterol Bilayer Domain Specific to the Fiber-Cell Plasma Membrane of the Eye Lens. *J. Membr. Biol.* **2012**, *245*, 51–68, doi:10.1007/s00232-011-9412-4.
19. Mainali, L.; Raguz, M.; O'Brien, W.J.; Subczynski, W.K. Properties of Membranes Derived from the Total Lipids Extracted from the Human Lens Cortex and Nucleus. *Biochim. Biophys. Acta - Biomembr.* **2013**, *1828*, 1432–1440, doi:10.1016/j.bbamem.2013.02.006.
20. Subczynski, W.K.; Mainali, L.; Raguz, M.; O'Brien, W.J. Organization of Lipids in Fiber-Cell Plasma Membranes of the Eye Lens. *Exp. Eye Res.* **2017**, *156*, 79–86, doi:10.1016/j.exer.2016.03.004.
21. Widomska, J.; Subczynski, W.K.; Mainali, L.; Raguz, M. Cholesterol Bilayer Domains in the Eye Lens Health: A Review. *Cell Biochem. Biophys.* **2017**, doi:10.1007/s12013-017-0812-7.
22. Mason, R.P.; Tulenko, T.N.; Jacob, R.F. Direct Evidence for Cholesterol Crystalline Domains in Biological Membranes: Role in Human Pathobiology. *Biochim. Biophys. Acta (BBA)-Biomembranes* **2003**, *1610*, 198–207, doi:10.1016/S0005-2736(03)00018-X.
23. Subczynski, W.K.; Pasenkiewicz-Gierula, M. Hypothetical Pathway for Formation of Cholesterol Microcrystals Initiating the Atherosclerotic Process. *Cell Biochem. Biophys.* **2020**, *78*, 241–247, doi:10.1007/s12013-020-00925-2.
24. Li, L.-K.; So, L.; Spector, A. Membrane Cholesterol and Phospholipid in Consecutive Concentric Sections of Human Lenses. *J. Lipid Res.* **1985**, *26*, 600–609.
25. Li, L.K.; So, L. Age Dependent Lipid and Protein Changes in Individual Bovine Lenses. *Curr. Eye Res.* **1987**, doi:10.3109/02713688709025219.
26. Menger, F.M.; Angelova, M.I. Giant Vesicles: Imitating the Cytological Processes of Cell Membranes. *Acc. Chem. Res.* **1998**, *31*, 789–797, doi:10.1021/ar970103v.
27. Veatch, S.L.; Keller, S.L. Organization in Lipid Membranes Containing

Cholesterol. *Phys. Rev. Lett.* **2002**, *89*, 268101, doi:10.1103/PhysRevLett.89.268101.
28. Reeves, J.P.; Dowben, R.M. Formation and Properties of Thin-Walled Phospholipid Vesicles. *J. Cell. Physiol.* **1969**, *73*, 49–60.
29. Pott, T.; Bouvrais, H.; Méléard, P. Giant Unilamellar Vesicle Formation under Physiologically Relevant Conditions. *Chem. Phys. Lipids* **2008**, *154*, 115–119, doi:10.1016/j.chemphyslip.2008.03.008.
30. Valkenier, H.; López Mora, N.; Kros, A.; Davis, A.P. Visualization and Quantification of Transmembrane Ion Transport into Giant Unilamellar Vesicles. *Angew. Chemie Int. Ed.* **2015**, *54*, 2137–2141, doi:10.1002/anie.201410200.
31. Subczynski, W.; Raguz, M.; Widomska, J. Subczynski WK, Raguz M, Widomska J. Studying Lipid Organization in Biological Membranes Using Liposomes and EPR Spin Labeling. *Methods Mol. Biol.* **2010**, *606*, 247–269, doi:10.1007/978-1-60761-447-0.
32. Zylberberg, C.; Matosevic, S. Pharmaceutical Liposomal Drug Delivery: A Review of New Delivery Systems and a Look at the Regulatory Landscape. *Drug Deliv.* **2016**, *23*, 3319–3329, doi:10.1080/10717544.2016.1177136.
33. Sercombe, L.; Veerati, T.; Moheimani, F.; Wu, S.Y.; Sood, A.K.; Hua, S. Advances and Challenges of Liposome Assisted Drug Delivery. *Front. Pharmacol.* **2015**, *0*, 286, doi:10.3389/FPHAR.2015.00286.
34. Akbarzadeh, A.; Rezaei-Sadabady, R.; Davaran, S.; Joo, S.W.; Zarghami, N.; Hanifehpour, Y.; Samiei, M.; Kouhi, M.; Nejati-Koshki, K. Liposome: Classification, Preparation, and Applications. *Nanoscale Res. Lett.* **2013**, *8*, 102, doi:10.1186/1556-276X-8-102.
35. Mardešić, I.; Boban, Z.; Subczynski, W.K.; Raguz, M. Membrane Models and Experiments Suitable for Studies of the Cholesterol Bilayer Domains. *Membranes (Basel).* **2023**, *13*, 320, doi:10.3390/membranes13030320.
36. Rodriguez, N.; Pincet, F.; Cribier, S. Giant Vesicles Formed by Gentle Hydration and Electroformation: A Comparison by Fluorescence Microscopy. *Colloids Surfaces B Biointerfaces* **2005**, *42*, 125–130.
37. Angelova, M.I.; Dimitrov, D.S. Liposome Electroformation. *Faraday Discuss. Chem. Soc.* **1986**, *81*, 303–311, doi:10.1039/DC9868100303.
38. Dimitrov, D.S.; Angelova, M.I. Lipid Swelling and Liposome Formation on Solid Surfaces in External Electric Fields. In *New Trends in Colloid Science*; Springer, 1987; pp. 48–56.
39. Has, C.; Pan, S. Vesicle Formation Mechanisms: An Overview. *J. Liposome Res.* 2020.
40. Li, W.; Wang, Q.; Yang, Z.; Wang, W.; Cao, Y.; Hu, N.; Luo, H.; Liao, Y.; Yang, J. Impacts of Electrical Parameters on the Electroformation of Giant Vesicles on ITO Glass Chips. *Colloids Surfaces B Biointerfaces* **2016**, *140*, 560–566, doi:10.1016/j.colsurfb.2015.11.020.
41. Li, Q.; Wang, X.; Ma, S.; Zhang, Y.; Han, X. Electroformation of Giant Unilamellar Vesicles in Saline Solution. *Colloids Surfaces B Biointerfaces* **2016**, *147*, 368–375, doi:10.1016/j.colsurfb.2016.08.018.

42. Boban, Z.; Mardešić, I.; Subczynski, W.K.; Raguz, M. Giant Unilamellar Vesicle Electroformation: What to Use, What to Avoid, and How to Quantify the Results. *Membranes (Basel).* **2021**, *11*, 860, doi:10.3390/MEMBRANES11110860.
43. Pereno, V.; Carugo, D.; Bau, L.; Sezgin, E.; Bernardino De La Serna, J.; Eggeling, C.; Stride, E. Electroformation of Giant Unilamellar Vesicles on Stainless Steel Electrodes. *ACS Omega* **2017**, *2*, 994–1002, doi:10.1021/acsomega.6b00395.
44. Behuria, H.G.; Biswal, B.K.; Sahu, S.K. Electroformation of Liposomes and Phytosomes Using Copper Electrode. *J. Liposome Res.* **2021**, *31*, 255–266, doi:10.1080/08982104.2020.1800729.
45. Ayuyan, A.G.; Cohen, F.S. Lipid Peroxides Promote Large Rafts: Effects of Excitation of Probes in Fluorescence Microscopy and Electrochemical Reactions during Vesicle Formation. *Biophys. J.* **2006**, *91*, 2172–2183, doi:10.1529/biophysj.106.087387.
46. Morales-Penningston, N.F.; Wu, J.; Farkas, E.R.; Goh, S.L.; Konyakhina, T.M.; Zheng, J.Y.; Webb, W.W.; Feigenson, G.W. GUV Preparation and Imaging: Minimizing Artifacts. *Biochim. Biophys. Acta - Biomembr.* **2010**, *1798*, 1324–1332, doi:10.1016/j.bbamem.2010.03.011.
47. Zhou, Y.; Berry, C.K.; Storer, P.A.; Raphael, R.M. Peroxidation of Polyunsaturated Phosphatidyl-Choline Lipids during Electroformation. *Biomaterials* **2007**, *28*, 1298–1306, doi:10.1016/j.biomaterials.2006.10.016.
48. Farkas, E.R.; Webb, W.W. Multiphoton Polarization Imaging of Steady-State Molecular Order in Ternary Lipid Vesicles for the Purpose of Lipid Phase Assignment. *J. Phys. Chem. B* **2010**, *114*, 15512–15522, doi:10.1021/jp107025h.
49. Lefrançois, P.; Goudeau, B.; Arbault, S. Electroformation of Phospholipid Giant Unilamellar Vesicles in Physiological Phosphate Buffer. *Integr. Biol. (United Kingdom)* **2018**, *10*, 429–434, doi:10.1039/c8ib00074c.
50. Baykal-Caglar, E.; Hassan-Zadeh, E.; Saremi, B.; Huang, J. Preparation of Giant Unilamellar Vesicles from Damp Lipid Film for Better Lipid Compositional Uniformity. *Biochim. Biophys. Acta - Biomembr.* **2012**, *1818*, 2598–2604, doi:10.1016/j.bbamem.2012.05.023.
51. Zhao, J.; Wu, J.; Shao, H.; Kong, F.; Jain, N.; Hunt, G.; Feigenson, G. Phase Studies of Model Biomembranes: Macroscopic Coexistence of Lα + Lβ, with Light-Induced Coexistence of Lα + Lo Phases. **2007**, *1768*, 2777–2786, doi:10.1016/j.bbamem.2007.07.009.
52. Bi, H.; Yang, B.; Wang, L.; Cao, W.; Han, X. Electroformation of Giant Unilamellar Vesicles Using Interdigitated ITO Electrodes. *J. Mater. Chem. A* **2013**, *1*, 7125–7130, doi:10.1039/c3ta10323d.
53. Witkowska, A.; Jablonski, L.; Jahn, R. A Convenient Protocol for Generating Giant Unilamellar Vesicles Containing SNARE Proteins Using Electroformation. *Sci. Rep.* **2018**, *8*, 9422, doi:10.1038/s41598-018-27456-4.
54. Estes, D.J.; Mayer, M. Electroformation of Giant Liposomes from Spin-Coated Films of Lipids. *Colloids Surfaces B Biointerfaces* **2005**, *42*, 115–123, doi:10.1016/j.colsurfb.2005.01.016.

55. Politano, T.J.; Froude, V.E.; Jing, B.; Zhu, Y. AC-Electric Field Dependent Electroformation of Giant Lipid Vesicles. *Colloids Surfaces B Biointerfaces* **2010**, *79*, 75–82, doi:10.1016/j.colsurfb.2010.03.032.
56. Herold, C.; Chwastek, G.; Schwille, P.; Petrov, E.P. Efficient Electroformation of Supergiant Unilamellar Vesicles Containing Cationic Lipids on ITO-Coated Electrodes. *Langmuir* **2012**, *28*, 5518–5521, doi:10.1021/la3005807.
57. Boban, Z.; Puljas, A.; Kovač, D.; Subczynski, W.K.; Raguz, M. Effect of Electrical Parameters and Cholesterol Concentration on Giant Unilamellar Vesicles Electroformation. *Cell Biochem. Biophys.* **2020**, *78*, 157–164, doi:10.1007/s12013-020-00910-9.
58. Stein, H.; Spindler, S.; Bonakdar, N.; Wang, C. Production of Isolated Giant Unilamellar Vesicles under High Salt Concentrations. *Front. Physiol.* **2017**, *8*, 1–16, doi:10.3389/fphys.2017.00063.
59. Veatch, S.L. Electro-Formation and Fluorescence Microscopy of Giant Vesicles with Coexisting Liquid Phases. *Methods Mol. Biol.* **2007**, *398*, 59–72, doi:10.1007/978-1-59745-513-8_6.
60. Angelova, M.I.; Soléau, S.; Méléard, P.; Faucon, F.; Bothorel, P. Preparation of Giant Vesicles by External AC Electric Fields. Kinetics and Applications. In *Trends in Colloid and Interface Science VI*; Springer, 1992; pp. 127–131.
61. Boban, Z.; Mardešić, I.; Subczynski, W.K.; Jozić, D.; Raguz, M. Optimization of Giant Unilamellar Vesicle Electroformation for Phosphatidylcholine/Sphingomyelin/Cholesterol Ternary Mixtures. *Membr. 2022, Vol. 12, Page 525* **2022**, *12*, 525, doi:10.3390/MEMBRANES12050525.
62. Ghellab, S.E.; Mu, W.; Li, Q.; Han, X. Prediction of the Size of Electroformed Giant Unilamellar Vesicle Using Response Surface Methodology. *Biophys. Chem.* **2019**, *253*, 106217, doi:10.1016/j.bpc.2019.106217.
63. Gracià, R.S.; Bezlyepkina, N.; Knorr, R.L.; Lipowsky, R.; Dimova, R. Effect of Cholesterol on the Rigidity of Saturated and Unsaturated Membranes: Fluctuation and Electrodeformation Analysis of Giant Vesicles. *Soft Matter* **2010**, *6*, 1472–1482, doi:10.1039/b920629a.
64. Taylor, P.; Xu, C.; Fletcher, P.D.I.; Paunov, V.N. A Novel Technique for Preparation of Monodisperse Giant Liposomes. *Chem. Commun.* **2003**, *44*, 1732–1733, doi:10.1039/B304059C.
65. Berre, L.; Chen, Y.; Baigl, D. From Convective Assembly to Landau - Levich Deposition of Multilayered Phospholipid Films of Controlled Thickness. *Langmuir* **2009**, 2554–2557, doi:10.1021/la803646e.
66. Oropeza-Guzman, E.; Riós-Ramírez, M.; Ruiz-Suárez, J.C. Leveraging the Coffee Ring Effect for a Defect-Free Electroformation of Giant Unilamellar Vesicles. *Langmuir* **2019**, *35*, 16528–16535, doi:10.1021/acs.langmuir.9b02488.
67. Bagatolli, L.A.; Parasassi, T.; Gratton, E. Giant Phospholipid Vesicles: Comparison among the Whole Lipid Sample Characteristics Using Different Preparation Methods: A Two Photon Fluorescence Microscopy Study. *Chem. Phys. Lipids* **2000**, *105*, 135–147, doi:doi.org/10.1016/S0009-3084(00)00118-3.

68. Collins, M.D.; Gordon, S.E. Giant Liposome Preparation for Imaging and Patch-Clamp Electrophysiology. *J. Vis. Exp.* **2013**, 1–9, doi:10.3791/50227.
69. Bhatia, T.; Husen, P.; Brewer, J.; Bagatolli, L.A.; Hansen, P.L.; Ipsen, J.H.; Mouritsen, O.G. Preparing Giant Unilamellar Vesicles (GUVs) of Complex Lipid Mixtures on Demand: Mixing Small Unilamellar Vesicles of Compositionally Heterogeneous Mixtures. *Biochim. Biophys. Acta - Biomembr.* **2015**, *1848*, 3175–3180, doi:10.1016/j.bbamem.2015.09.020.
70. Girard, P.; Pécréaux, J.; Lenoir, G.; Falson, P.; Rigaud, J.L.; Bassereau, P. A New Method for the Reconstitution of Membrane Proteins into Giant Unilamellar Vesicles. *Biophys. J.* **2004**, *87*, 419–429, doi:10.1529/biophysj.104.040360.
71. Angelova, M.; Dimitrov, D.S. A Mechanism of Liposome Electroformation. In *Trends in colloid and interface science II*; Springer, 1988; pp. 59–67.
72. Drabik, D.; Doskocz, J.; Przybyło, M. Effects of Electroformation Protocol Parameters on Quality of Homogeneous GUV Populations. *Chem. Phys. Lipids* **2018**, *212*, 88–95, doi:10.1016/j.chemphyslip.2018.01.001.
73. Betaneli, V.; Worch, R.; Schwille, P. Effect of Temperature on the Formation of Liquid Phase-Separating Giant Unilamellar Vesicles (GUV). *Chem. Phys. Lipids* **2012**, *165*, 630–637, doi:10.1016/j.chemphyslip.2012.06.006.
74. Montes, L.-R.; Alonso, A.; Goni, F.M.; Bagatolli, L.A. Giant Unilamellar Vesicles Electroformed from Native Membranes and Organic Lipid Mixtures under Physiological Conditions. *Biophys. J.* **2007**, *93*, 3548–3554, doi:10.1529/biophysj.107.116228.
75. Hossain, R.; Adamiak, K. Dynamic Properties of the Electric Double Layer in Electrolytes. *J. Electrostat.* **2013**, *71*, 829–838, doi:10.1016/j.elstat.2013.06.006.
76. Breton, M.; Amirkavei, M.; Mir, L.M. Optimization of the Electroformation of Giant Unilamellar Vesicles (GUVs) with Unsaturated Phospholipids. *J. Membr. Biol.* **2015**, *248*, 827–835, doi:10.1007/s00232-015-9828-3.
77. Huang, J.; Buboltz, J.T.; Feigenson, G.W. Maximum Solubility of Cholesterol in Phosphatidylcholine and Phosphatidylethanolamine Bilayers. *Biochim. Biophys. Acta - Biomembr.* **1999**, *1417*, 89–100, doi:10.1016/S0005-2736(98)00260-0.
78. Buboltz, J.T. A More Efficient Device for Preparing Model-Membrane Liposomes by the Rapid Solvent Exchange Method. *Rev. Sci. Instrum.* **2009**, *80*, 124301, doi:10.1063/1.3264073.
79. Boban, Z.; Mardešić, I.; Subczynski, W.K.; Jozić, D.; Raguz, M. Optimization of Giant Unilamellar Vesicle Electroformation for Phosphatidylcholine/Sphingomyelin/Cholesterol Ternary Mixtures. *Membranes (Basel).* **2022**, *12*, 525, doi:10.3390/membranes12050525.
80. Veatch, S.L.; Keller, S.L. Miscibility Phase Diagrams of Giant Vesicles Containing Sphingomyelin. *Phys. Rev. Lett.* **2005**, *94*, 3–6, doi:10.1103/PhysRevLett.94.148101.
81. de Almeida, R.F.M.; Fedorov, A.; Prieto, M. Sphingomyelin/Phosphatidylcholine/Cholesterol Phase Diagram: Boundaries and Composition of Lipid Rafts. *Biophys. J.* **2003**, *85*, 2406–2416, doi:10.1016/S0006-3495(03)74664-5.

82. Kusumi, A.; Fujiwara, T.K.; Tsunoyama, T.A.; Kasai, R.S.; Liu, A.; Hirosawa, K.M.; Kinoshita, M.; Matsumori, N.; Komura, N.; Ando, H.; et al. Defining Raft Domains in the Plasma Membrane. *Traffic* **2020**, *21*, 106–137, doi:10.1111/tra.12718.
83. Boban, Z.; Mardešić, I.; Perinović Jozić, S.; Šumanovac, J.; Subczynski, W.K.; Raguz, M. Electroformation of Giant Unilamellar Vesicles from Damp Lipid Films Formed by Vesicle Fusion. *Membranes (Basel).* **2023**, *13*, 352, doi: 10.3390/membranes13030352.
84. Hardy, G.J.; Nayak, R.; Zauscher, S. Model Cell Membranes: Techniques to Form Complex Biomimetic Supported Lipid Bilayers via Vesicle Fusion. *Curr. Opin. Colloid Interface Sci.* **2013**, *18*, 448–458, doi:10.1016/j.cocis.2013.06.004.

4 EFFECT OF ELECTRICAL PARAMETERS AND CHOLESTEROL CONCENTRATION ON GIANT UNILAMELLAR VESICLES ELECTROFORMATION

Reproduced with permission from Springer, Nature from Boban, Z.; Puljas, A.; Kovač, D.; Subczynski, W.K.; Raguz, M. Effect of Electrical Parameters and Cholesterol Concentration on Giant Unilamellar Vesicles Electroformation. Cell Biochem. Biophys. 2020, 78, 157–164, doi:10.1007/s12013-020-00910-9.

Cell Biochemistry and Biophysics (2020) 78:157–164
https://doi.org/10.1007/s12013-020-00910-9

ORIGINAL PAPER

Effect of Electrical Parameters and Cholesterol Concentration on Giant Unilamellar Vesicles Electroformation

Zvonimir Boban[1,2] · Ana Puljas[1] · Dubravka Kovač[3] · Witold Karol Subczynski[4] · Marija Raguz[1]

Received: 17 January 2020 / Accepted: 30 March 2020 / Published online: 21 April 2020

Abstract

Giant unilamellar vesicles (GUVs) are used extensively as models that mimic cell membranes. The cholesterol (Chol) content in the fiber cell plasma membranes of the eye lens is extremely high, exceeding the solubility threshold in the lenses of old humans. Thus, a methodological paper pertaining to preparations of model lipid bilayer membranes with high Chol content would significantly help the study of properties of these membranes. Lipid solutions containing 1-palmitoyl-2-oleoyl-glycero-3-phosphocholine (POPC) and Chol were fluorescently labeled with phospholipid analog 1,1′-dioctadecyl-3,3,3′,3′-tetramethylindocarbocyanine perchlorate ($DiIC_{18}(3)$) and spin-coated to produce thin lipid films. GUVs were formed from these films using the electroformation method and the results were obtained using fluorescent microscopy. Electroformation outcomes were examined for different electrical parameters and different Chol concentrations. A wide range of field frequency–field strength (ff–fs) combinations was explored: 10–10,000 Hz and 0.625–9.375 V/mm peak-to-peak. Optimal values for GUVs preparation were found to be 10–100 Hz and 1.25–6.25 V/mm, with largest vesicles occurring for 10 Hz and 3.75 V/mm. Chol:POPC mixing ratios (expressed as a molar ratio) ranged from 0 to 3.5. We show that increasing the Chol concentration decreases the GUVs size, but this effect can be reduced by choosing the appropriate ff–fs combination.

Keywords GUVs · Cholesterol · Phospholipids · Electroformation · Frequency · Field strength

Introduction

Giant unilamellar vesicles (GUVs) have been an important topic of research lately due to their similarity to biological membranes [1–6] and their potential as drug carriers [7–9]. Preparation methods for GUVs are still being perfected in order to obtain the best result, which in turn depends on the selected application of lipid vesicles [10]. One of the first methods used for GUVs formation was controlled hydration (known also as gentle hydration, natural swelling, or spontaneous swelling), developed by Reeves and Dowben, which includes spontaneous swelling of phospholipids in aqueous solution of nonelectrolytes [11]. An advancement in preparation of GUVs came from Angelova and Dimitrov [12] who introduced liposome electroformation as an alternative to the traditional swelling method. The initial procedure was further improved by involving alternating current (AC) instead of direct current (DC) electric fields [13]. Electroformation features that made it the most commonly used method [14] are high percentage of formed unilamellar vesicles [15, 16], homogeneous size distribution [17], simple manipulation, and short preparation time [16].

Since then, effects of many parameters have been examined in order to improve the yield, size, and homogeneity of the obtained GUVs. Most notable parameters include the AC-field frequency and strength, lipid composition, electroformation duration, temperature, and thickness of the lipid films. However, the interplay of these parameters has not yet

Supplementary information The online version of this article (https://doi.org/10.1007/s12013-020-00910-9) contains Supplementary material, which is available to authorized users.

✉ Marija Raguz
marija.raguz@mefst.hr

[1] Department of Medical Physics and Biophysics, University of Split School of Medicine, Split, Croatia

[2] University of Split, Faculty of Science, Doctoral study of Biophysics, Split, Croatia

[3] Department of Physics, Faculty of Science, University of Split, Split, Croatia

[4] Department of Biophysics, Medical College of Wisconsin, Milwaukee, WI, USA

been fully explored. For instance, most studies used frequencies of about 10 Hz and electric fields of about 1 V/mm [13, 18–21]. Conversely, when exploring the field frequency–field strength (ff–fs) combinations effect on electroformation efficiency, some groups reported higher frequencies and AC-field strengths than those used before [22–24]. Li et al. found the optimal combination to be 11,000 Hz and 5 V/mm. For 10 V/mm best results were also obtained using a 11,000 Hz frequency, but some irregular vesicles appeared [23]. Similar results were obtained by Wang et al. [24]. Politano et al. [22] showed that electroformation can be successful at frequencies as high as 10,000 Hz (at field values of 0.212–2.12 V/mm) and field strengths of up to 20 V/mm (for frequencies 1–100 Hz).

One of the reasons for optimization of electroformation parameters is their strong dependance on the lipid composition in preparation mixtures [22]. Because of its biological significance [25, 26], cholesterol (Chol) was often added to different phospholipid mixtures. However, because the Chol proportion in most mammalian cell membranes is lower than 50% [27], Chol:Phospholipid (PL) ratio used in these studies was usually lower than 1:1 [13, 14, 18, 22–24, 28, 29]. Examples of systems with high Chol content are fiber cell plasma membranes of the eye-lenses [30–33] and atherosclerotic smooth muscle cells [25]. Within the human eye lens, the Chol:PL molar ratio of the fiber cell membrane ranges from 1 to 2 in the lens cortex and from 3 to 4 in the lens nucleus [30, 31]. Chol is hypothesized to be crucial for maintaining lens transparency by creating Chol bilayer domains (CBDs), which ensure that the surrounding phospholipid bilayer is saturated with Chol. This keeps the bulk physical properties of the membrane consistent and unaffected by phospholipid composition changes [34–43]. In contrast, cholesterol bilayer enrichment is related to negative effects during the development of atherosclerosis.

In order to cover the range of Chol concentrations mentioned above, here we will compare samples with Chol:POPC mixing ratios ranging from 0 to 3.5. Throughout the text, we will use the term mixing ratio to define the molar concentration ratio before evaporating the solvent. The need for differentiation between mixing ratios and molar ratios in investigated membranes of GUVs arises due to possible demixing of Chol during sample preparation. This process can lead to a decreased Chol:POPC molar ratio in the bilayer when compared with the mixing ratio. The highest molar ratio was determined from the maximum solubility limit observed previously to be around 66 mol% [44, 45].

This issue could be addressed by using preparation methods that avoid those stages, such as rapid solvent exchange (RSE) [46]. A study using RSE and electroformation to create vesicles with phospholipids and Chol was already conducted [29]. However, the lipid composition was chosen to achieve a coexisting liquid ordered-liquid disordered phase in the membrane (the highest Chol concentration was 46 mol%), while we are aiming for lipid compositions with Chol content higher than 50 mol%. At this high Chol content, CBDs are embedded into the surrounding PL bilayer saturated with Chol forming a structured (or dispersed) liquid ordered phase. Consequently, the Chol:PL ratio used was too low to provide insight into systems such as the eye lens cortex and nucleus. Also, the electroformation field frequency and strength used in the study were kept constant at around 0.5 V/mm and 10 Hz, and in our experiment we explored a much broader range of electrical parameters.

Other electroformation studies mainly focused on providing the best electroformation parameters for different phospholipid compositions while keeping the Chol level constant. Here, however, we determined the optimal electroformation parameters for lipid membranes with Chol:PL ratios suitable for modeling the cortical and nuclear fiber cell plasma membranes of the human eye lens.

Materials and Methods

Materials

One-palmitoyl-2-oleoyl-glycero-3-phosphocholine (POPC) and cholesterol (Chol) were obtained from Avanti Polar Lipids Inc. (Alabaster, AL). Fluorescent dye 1,1′-dioctadecyl-3,3,3′,3′-tetramethylindocarbocyanine perchlorate ($DiIC_{18}(3)$) was purchased from Invitrogen, Thermo Fisher Scientific (Waltham, MA). When not used, the lipids were stored at −20 °C. Chemical structures and their approximate locations in the membrane bilayer are presented in Fig. 1. Other chemicals of at least reagent grade were obtained from Sigma-Aldrich (St. Louis, MO). Indium-tin oxide coated glass (ITO, CG-90 INS 115) was purchased from Delta

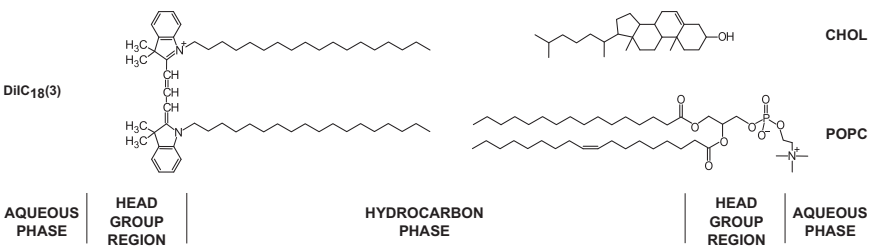

Fig. 1 Chemical structures of lipids and fluorescent dye and their approximate locations in the lipid bilayer membrane

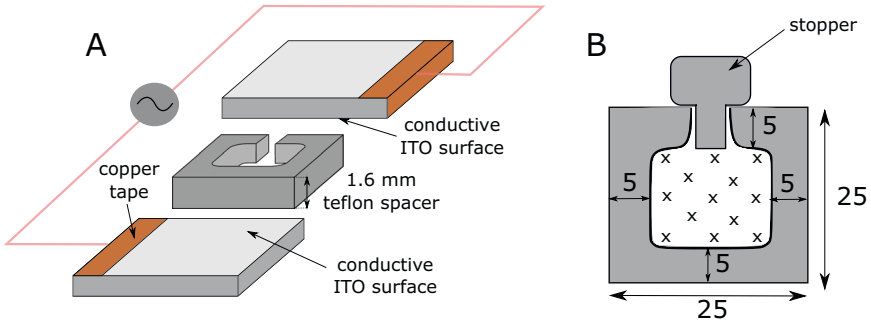

Fig. 2 Experimental setup. **a** Illustration of the electroformation chamber. **b** Positions on the chamber surface at which microscope images were taken. All numeric values are expressed in mm

Technologies (Loveland, LO). Glass dimensions were 25 × 75 × 1.1 mm. New ITO glass was used for each preparation in order to prevent coating deterioration. Mili-Q deionized water was used as a chamber solution.

Deposition of the Lipid Film

A common concern in electroformation protocols is uniform lipid film deposition on the electrode surface. Deposition is traditionally done by dropping the lipid solution on the ITO electrode and letting it dry [13]. This method can be further improved by spreading the film using a small object (e.g., a glass pipette or rod) before the solvent has a chance to evaporate [18, 47, 48]. Although this does increase the film thickness homogeneity, the method is not precise enough to guarantee reproducibility since film thickness cannot be accurately controlled. This issue was addressed using the spin-coating method as described by Estes and Mayer, where a lipid film is spread over the electrode surface by spinning the electrode at very large angular velocities [19]. Here, prior to spin-coating, the glass was immersed in deionized water for at least 45 min before being wiped four times with 70% ethanol moistened wipes. Properties of samples with Chol:POPC mixing ratios ranging from 0 to 3.5 were compared. The POPC:DiIC$_{18}$(3) molar ratio was always kept at 1:0.002. Consequently, for different Chol:POPC ratio used here, the dye:lipid concentration ratios ranged from 0.002:1 (for sample without Chol) to 0.0004:1 (for highest Chol content). A mixture containing 3.75 mg/mL of lipids in 95% chloroform, 5% acetonitrile solution was prepared [19]. The solution (350 µL) was deposited onto the ITO surface and a thin lipid layer was created using a spin-coater (Sawatec SM-150). The glass was spun for 4 min at 600 rpm. The final velocity was reached in 1 s. After coating, the lipid film was placed under vacuum for 30 min to evaporate any remaining solvent.

Electroformation Chamber

The electroformation chamber consisted of two 25 × 37.5 mm ITO coated glass electrodes separated by a 1.6 mm thick teflon spacer. Electrodes were made by cutting a 25 × 75 mm ITO glass slide using a diamond pen cutter. After one of the electrodes was lipid-coated, the chamber was assembled by attaching the spacer to the electrodes using vacuum grease (Fig. 2a). The opening inside the spacer is square shaped with rounded corners so air bubbles are less likely to be trapped. The entrance to the chamber was blocked using a teflon stopper (Fig. 2b). The stopper is rectangularly shaped and a bit narrower than the neck of the gap in the spacer. This small difference in width allowed for ejection of remaining air bubbles along with the surplus of fluid from the chamber. Upon insertion, the stopper was also sealed with vacuum grease. This way, there was no contact between the grease and the lipid solution inside, so the probability of contamination was decreased. After sealing, the chamber was attached to a voltage source (UNI-T UTG9005C pulse generator) and placed inside an incubator at a temperature of 60 °C. In order to assure good contact between conductor wires and the electrodes, the outer edges of the chamber were covered with copper tape (Fig. 2a). After 2 h, the voltage was turned off and the chamber was kept in the incubator for another hour.

Image and Data Analysis

In order to search the entire volume of the chamber, we scanned 13 points on the chamber surface at three different depths as indicated in Fig. 2b. Images were obtained using a fluorescence microscope (Zeiss Axio—imager M1 or Olympus BX51). Vesicle diameters were measured using the line tool in Fiji software [49] and data analysis was performed using R programming language [50].

Sample distribution normality was tested through qq-plots and Shapiro–Wilk test. If the normality assumption was violated, appropriate nonparametric tests were used. Goodness of linear fit was estimated using the coefficient of determination R^2.

Results and Discussion

GUVs Formation for Different Field Frequency–Field Strength Combinations

Electroformation successfulness averaged over the whole sample depends on a variety of parameters as listed in the

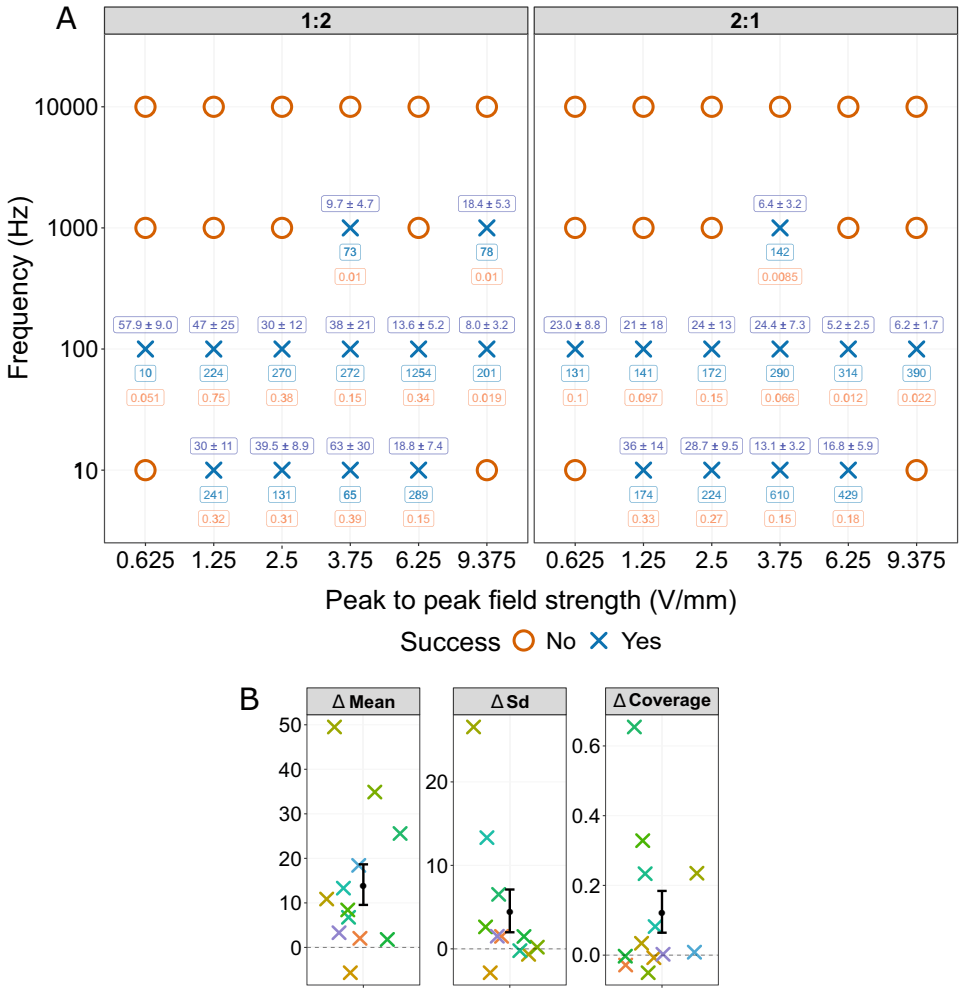

Fig. 3 GUVs electroformation successfulness. **a** ff–fs diagram for two different Chol:POPC ratios. In cases where vesicles were successfully formed (X points), the number above is the vesicle diameter denoted as mean ± sd, expressed in μm. Numbers given below are the number and coverage of tracked vesicles, respectively. All numbers pertain to the best frame observed for a particular sample. **b** Mean, sd, and coverage value differences between 1:2 and 2:1 Chol:POPC ratios. ΔMean and ΔSd are expressed in μm. X symbols denote individual sample parameter differences. Black dot and error bars denote the mean difference and standard error of the differences

introduction, one of which is film thickness [12, 19, 24]. Even though the spin-coating method creates macroscopically homogeneous lipid films, there are microscopic differences in thickness over the sample [19]. In addition, the ITO layer is not perfectly smooth, so it can contribute to variations in thickness as well (Supplementary Fig. S1).

Depending on those differences, we can have varying degrees of electroformation successfulness throughout the sample. Consequentially, averaging over the whole sample can decrease our ability to identify the best possible ff–fs combination. Therefore, we compared only the best frames in each sample. To reduce the influence of local variations in film thickness, we used a small magnification objective (10×) to make the quantification area as large as possible.

Electroformation outcomes were described using the mean and standard deviation (sd) of GUVs diameters and the number of GUVs. Even though the vesicle number is indicative of electroformation successfulness, it can be misleading when interpreted by itself because the maximum number of vesicles that can fit inside a limited area is dependent on their diameter (Supplementary Fig. S2).

This is why, alongside the GUVs number, we also calculated the coverage N/N_{max} for each sample, where N_{max} is the maximum number of vesicles that could fit inside the observed region. N_{max} is derived assuming all vesicles are spherical and have a diameter equal to the average diameter measured in that sample. Therefore, it is calculated solely from geometrical considerations as explained in the Supplementary. Obviously, coverage should be a positive value ranging from zero to one. An additional benefit of using coverage is the ability to compare results when using different microscope magnifications, which cannot be said for comparing the number of vesicles. Figure 3a shows that electroformation seems to be most successful for ff–fs combinations of 10–100 Hz and 1.25–6.25 V/mm. Increasing the frequency further leads to a decrease in successfulness for both Chol:POPC ratios (1:2, 2:1), so after setting the frequency at 10,000 Hz, electroformation efficacy dropped to zero. Comparing the means between all pairs for two different Chol:POPC ratios confirms the assumption that very high Chol contents reduce the electroformed GUVs diameter (mean ± standard error (sem) = 14 ± 5 μm, $p = 0.01$, Student's paired

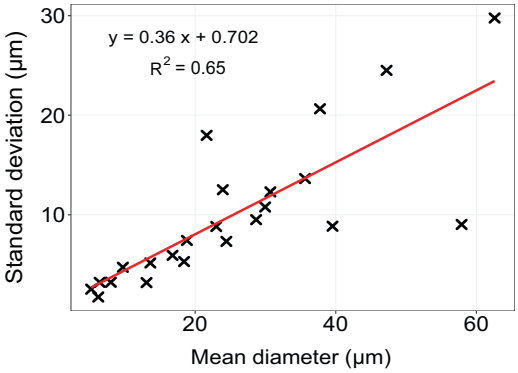

Fig. 4 GUVs standard deviation vs mean diameter, $y = 0.36 \times +0.70\,\mu m$, $R^2 = 0.65$

t-test) (Fig. 3b). Although not statistically significant, increasing Chol concentration seems to also decrease the coverage of the observed region (mean ± sem = 0.12 ± 0.06, $p = 0.09$, Wilcoxon signed-rank test) (Fig. 3b, Supplementary Fig. S3). We have also observed vesicle diameter distribution becoming narrower with decreasing average vesicle size (Fig. 4). Although such a behavior has been noted before [22], here we show that there seems to be a linear dependence between the two parameters.

Effect of Cholesterol Concentration on GUVs Formation

Here we show how Chol concentration impacts GUVs formation at 10 and 100 Hz for field strengths covering the optimal electroformation region—1.25, 3.75, and 6.25 V/mm (Fig. 5). Increasing Chol concentration shifted vesicle diameter distributions toward lower values. The phenomenon is probably due to Chol changing the elasticity of the lipid bilayer, thus making the bending required for GUVs formation much harder. Interestingly though, the change of Chol concentration impacts GUVs formation differently depending on the electric field parameters.

As mentioned earlier, the shift in size is accompanied by narrower distributions with an almost identical regression line slope (Figs. 4, 5a, Supplementary Fig. S4). Also, GUVs formed at higher frequencies have smaller or similar average diameters than their lower frequency counterparts (Fig. 5). This is especially visible at low voltages. The effect could possibly be explained from the lipid vibration amplitude formula derived by Dimitrov and Angelova [15]. The general form of the expression is $A = \frac{U}{af(1+bf)}$, where A, U, and f are the vibration amplitude, voltage, and frequency, and a, b constants describing other system properties. The formula predicts smaller amplitudes for lower voltages and higher frequencies. Therefore, it is possible that higher frequencies in combination with lower voltages prevent the formation of very large GUVs by decreasing the vibration amplitude too much. Although the same formula predicts a higher amplitude (and therefore possibly a larger GUVs diameter), the GUVs diameter seems to grow as we increase the voltage and then drops as the voltage gets too high. The decrease might be caused by an overly high mechanical stress or by excessive oxidation of lipid molecules [51].

One of the authors (Witold Karol Subczynski), using the RSE method to prepare POPC multilamellar liposomes, shows that the formation of pure CBDs in POPC membranes starts at a Chol:POPC molar ratio of 1:1 [52]. However, as we demonstrated in our recent paper, in GUVs CBDs started to be observed only at Chol:POPC mixing ratios greater than 2:1 [53]. In that investigation, GUVs were prepared using the electroformation method from the lipid film formed using the film deposition method. This indicates that the demixing of Chol in the form of Chol crystals during the preparation using the film deposition method significantly decreases the true Chol:POPC molar ratio in membranes of GUVs. Such high cholesterol concentrations affect electroformed GUVs diameters the least for the field strength of 3.75 V/mm (Fig. 5). However, between the two explored frequencies (10 and 100 Hz), the 10 Hz frequency led to a more stable mean diameter–Chol concentration dependence. Consequently, the 10 Hz–3.75 V/mm ff–fs combination seems to be the best when creating model membranes containing CBDs.

Summary

Due to their role as biological membrane models, GUVs have been extensively studied lately. Nowadays, the most popular method for their creation is electroformation. Consequently, optimization of electroformation parameters for GUVs formation is very important. In our experiment, electroformation of GUVs containing varying Chol:POPC mixing ratios was conducted (from 0 to 3.5). Electroformation was characterized by calculating the vesicles diameter mean value and sd, vesicle number and coverage. Coverage was added to the characterization because the number of vesicles by itself can lead to effectiveness misinterpretation due to not taking into account the diameter dependance. A wide range of ff–fs combinations was explored: 10–10,000 Hz and 0.625–9.375 V/mm peak-to-peak, with average vesicle diameters ranging approximately from 5 to 60 µm. The optimal ff–fs combinations for investigated lipid compositions are around 10–100 Hz and 1.25–6.25 V/mm. The upper electroformation limit is around 1,000 Hz for frequency and around 9.375 V/mm peak-to-peak for field strength. Comparing pairwise differences in mean diameters between two Chol:POPC ratios (1:2 and 2:1) for multiple ff–fs combinations, we determined that there is a significant difference between the two Chol concentrations ($p = 0.01$, Student's *t*-test). Although

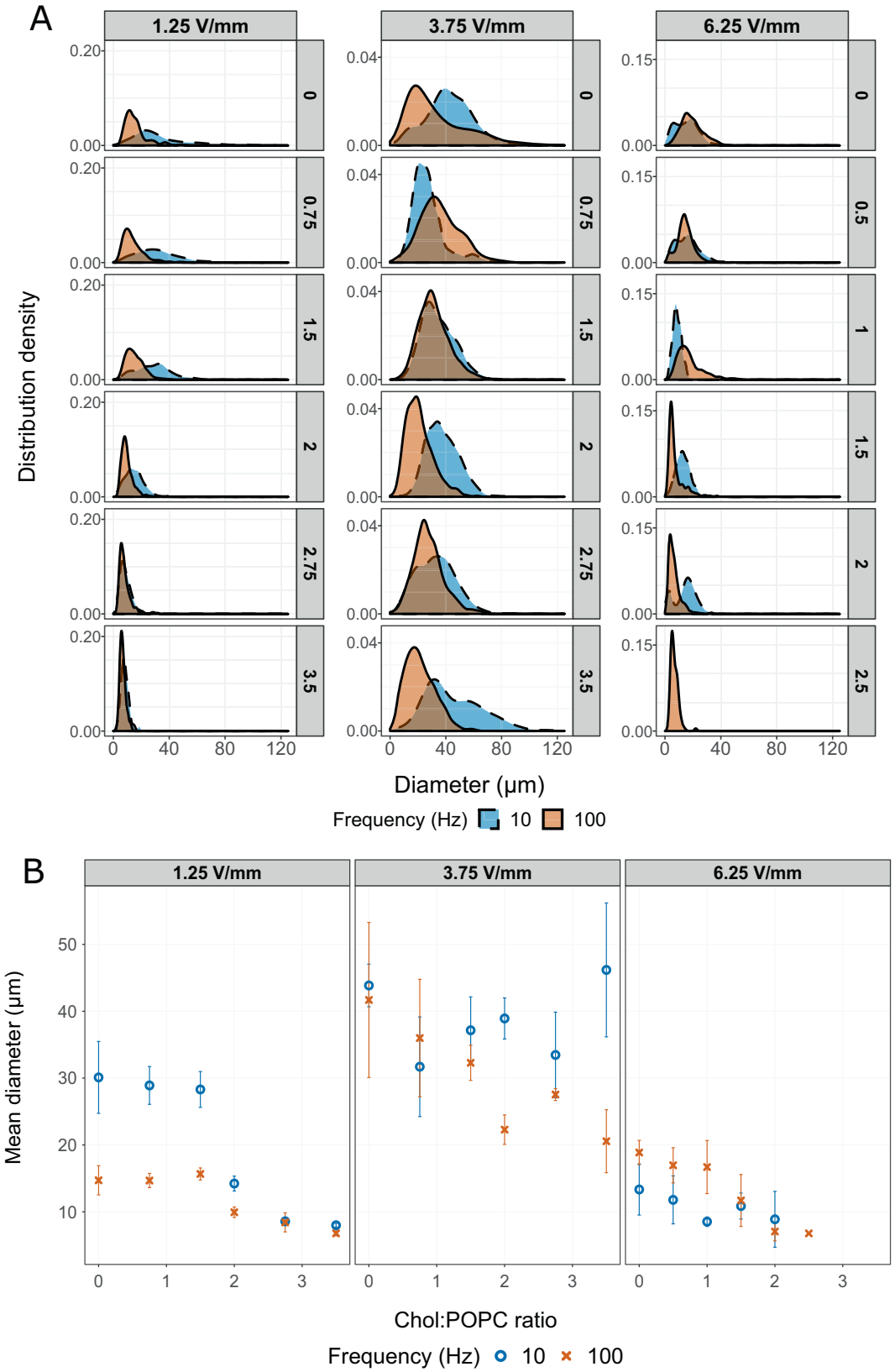

Fig. 5 Effect of Chol concentration on electroformation successfulness. **a** Change of vesicle diameter distribution with change in Chol:POPC ratio. **b** Vesicle diameter as a function of Chol:POPC ratio. Points and bars represent means and their standard errors

not enough to be statistically significant, vesicle coverage also seems to be negatively affected by increasing Chol concentration ($p = 0.09$, Wilcoxon signed-rank test).

In order to further inspect the impact of Chol concentration, we observed the change in GUVs formation for five different Chol concentrations and three different field strengths covering the optimal electroformation region (1.25, 3.75, and 6.25 V/mm). The conclusions were in line with our initial hypothesis. High Chol concentrations decreased the average GUVs diameters, although the effect strength varied depending on the ff–fs combination. High Chol concentrations affected electroformed GUVs diameters the least in the case of 10 Hz–3.75 V/mm ff–fs combination. Consequently, that combination seems to be the best one when dealing with model membranes containing very large amounts of Chol.

Because of the large number of variables included in the electroformation process, there is still room for improvement. For instance, incubation temperature and duration, chamber dimensions and lipid film thickness could be altered in order to get better results. Also, this study used deionized water as a chamber solution. The effects of using physiological solutions under these Chol concentrations remain to be tested. When using film deposition methods, another problem to be tackled is the potential artifactual solid-state demixing of Chol during sample preparation. The problem could be solved by using preparation methods that avoid those stages, such as RSE.

Acknowledgements We thank Ante Bilušić, Katarina Vukojević, Damir Sapunar, Sandra Kostić, Jasna Puizina, Ivana Bočina, Ivica Aviani, and Lucija Krce for access to their lab equipment and helpful discussions and comments.

Funding Research reported in this publication was supported by the Croatian Science Foundation (Croatia) under Grant [IP-2019-04-1958], by the National Institutes of Health (USA) under Grant R01 EY 015526, and by the Polish National Science Center under Grant [2016/22/M/NZ1/00187].

Compliance with Ethical Standards

Conflict of Interest The authors declare that they have no conflict of interest.

Publisher's note Springer Nature remains neutral with regard to jurisdictional claims in published maps and institutional affiliations.

References

1. Menger, F. M., & Angelova, M. I. (1998). Giant vesicles: imitating the cytological processes of cell membranes. *Accounts of Chemical Research*, *31*, 789–797.
2. Veatch, S. L., & Keller, S. L. (2002). Organization in lipid membranes containing cholesterol. *Physical Review Letters*, *89*, 268101.
3. Montes, L.-R., Alonso, A., Goni, F. M., & Bagatolli, L. A. (2007). Giant unilamellar vesicles electroformed from native membranes and organic lipid mixtures under physiological conditions. *Biophysical Journal*, *93*, 3548–3554.
4. Valkenier, H., López Mora, N., Kros, A., & Davis, A. P. (2015). Visualization and quantification of transmembrane ion transport into giant unilamellar vesicles. *Angewandte Chemie*, *54*, 2137–2141.
5. Li, Q., Wang, X., Ma, S., Zhang, Y., & Han, X. (2016). Electroformation of giant unilamellar vesicles in saline solution. *Colloids Surfaces B Biointerfaces*, *147*, 368–375.
6. Pott, T., Bouvrais, H., & Méléard, P. (2008). Giant unilamellar vesicle formation under physiologically relevant conditions. *Chemistry and Physics of Lipids*, *154*, 115–119.
7. Nacka, F., Cansell, M., Méléard, P., & Combe, N. (2001). Incorporation of α-tocopherol in marine lipid-based liposomes: in vitro and in vivo studies. *Lipids.*, *36*, 1313–1320.
8. Patil, Y. P., & Jadhav, S. (2015). Preparation of Liposomes for drug delivery applications by extrusion of giant unilamellar vesicles. In *Nanoscale and microscale phenomena* (pp. 17–29). Springer, India.
9. Alavi, M., Karimi, N., & Safaei, M. (2017). Application of various types of liposomes in drug delivery systems. *Advanced Pharmaceutical Bulletin*, *7*, 3.
10. van Swaay, D., et al. (2013). Microfluidic methods for forming liposomes. *Lab on a Chip*, *13*, 752–767.
11. Reeves, J. P., & Dowben, R. M. (1969). Formation and properties of thin-walled phospholipid vesicles. *Journal of Cellular Physiology*, *73*, 49–60.
12. Angelova, M. I., & Dimitrov, D. S. (1986). Liposome electroformation. *Faraday Discussions of the Chemical Society*, *81*, 303–311.
13. Angelova, M. I., Soléau, S., Méléard, P., Faucon, F., & Bothorel, P. (1992). Preparation of giant vesicles by external AC electric fields. Kinetics and applications. *Progress in Colloid and Polymer Science*, *89*, 127–131.
14. Walde, P., Cosentino, K., Engel, H., & Stano, P. (2010). Giant vesicles: preparations and applications. *ChemBioChem*, *11*, 848–865.
15. Dimitrov, D. S., & Angelova, M. I. (1987). Lipid swelling and liposome formation on solid surfaces in external electric fields. *Progress in Colloid and Polymer Science*, *73*, 48–56.
16. Rodriguez, N., Pincet, F., & Cribier, S. (2005). Giant vesicles formed by gentle hydration and electroformation: a comparison by fluorescence microscopy. *Colloids Surfaces B Biointerfaces*, *42*, 125–130.
17. Bagatolli, L. A., Parasassi, T., & Gratton, E. (2000). Giant phospholipid vesicles: comparison among the whole lipid sample characteristics using different preparation methods: a two photon fluorescence microscopy study. *Chemistry and Physics of Lipids*, *105*, 135–147.
18. Veatch, S. L. (2007). Electro-formation and fluorescence microscopy of giant vesicles with coexisting liquid phases. In: McIntosh, T. J. (ed.), *Methods in Molecular Biology in Lipid Rafts*, (vol. 398, pp. 59–72). Humana Press Inc., Totowa, NJ, Springer.
19. Estes, D. J., & Mayer, M. (2005). Electroformation of giant liposomes from spin-coated films of lipids. *Colloids Surfaces B Biointerfaces*, *42*, 115–123.
20. Riske, K. A., & Dimova, R. (2005). Electro-deformation and poration of giant vesicles viewed with high temporal resolution. *Biophysical Journal*, *88*, 1143–1155.
21. Gudheti, M. V., Mlodzianoski, M., & Hess, S. T. (2007). Imaging and shape analysis of GUVs as model plasma membranes: effect of trans DOPC on membrane properties. *Biophysical Journal*, *93*, 2011–2023.

22. Politano, T. J., Froude, V. E., Jing, B., & Zhu, Y. (2010). AC-electric field dependent electroformation of giant lipid vesicles. *Colloids Surfaces B Biointerfaces*, *79*, 75–82.
23. Li, W., Wang, Q., Yang, Z., Wang, W., Cao, Y., Hu, N., Luo, H., Liao, Y., & Yang, J. (2016). Impacts of electrical parameters on the electroformation of giant vesicles on ITO glass chips. *Colloids Surfaces B Biointerfaces*, *140*, 560–566.
24. Wang, Q., Zhang, X., Fan, T., Yang, Z., Chen, X., Wang, Z., Xu, J., Li, Y., Hu, N., & Yang, J. (2017). Frequency-dependent electroformation of giant unilamellar vesicles in 3D and 2D microelectrode systems. *Micromachines*, *8*, 24.
25. Mason, R. P., Tulenko, T. N., & Jacob, R. F. (2003). Direct evidence for cholesterol crystalline domains in biological membranes: role in human pathobiology. *Biochimica et Biophysica Acta (BBA)-Biomembranes*, *1610*, 198–207.
26. Silvius, J. R. (2003). Role of cholesterol in lipid raft formation: lessons from lipid model systems. *Biochimica et Biophysica Acta (BBA)-Biomembranes*, *1610*, 174–183.
27. Van Meer, G., Voelker, D. R., & Feigenson, G. W. (2008). Membrane lipids: where they are and how they behave. *Nature Reviews Molecular Cell Biology*. https://doi.org/10.1038/nrm2330.
28. Portet, T., Mauroy, C., Démery, V., Houles, T., Escoffre, J.-M., Dean, D. S., & Rols, M.-P. (2012). Destabilizing giant vesicles with electric fields: an overview of current applications. *The Journal of Membrane Biology*, *245*, 555–564.
29. Baykal-Caglar, E., Hassan-Zadeh, E., Saremi, B., & Huang, J. (2012). Preparation of giant unilamellar vesicles from damp lipid film for better lipid compositional uniformity. *Biochimica et Biophysica Acta (BBA)-Biomembranes*, *1818*, 2598–2604.
30. Li, L.-K., So, L., & Spector, A. (1985). Membrane cholesterol and phospholipid in consecutive concentric sections of human lenses. *Journal of Lipid Research*, *26*, 600–609.
31. Li, L.-K., So, L., & Spector, A. (1987). Age-dependent changes in the distribution and concentration of human lens cholesterol and phospholipids. *Biochimica et Biophysica Acta (BBA)-Lipids Lipid Metab*, *917*, 112–120.
32. Rujoi, M., Jin, J., Borchman, D., Tang, D., & Yappert, M. C. (2003). Isolation and lipid characterization of cholesterol-enriched fractions in cortical and nuclear human lens fibers. *Investigative Ophthalmology and Visual Science*, *44*, 1634–1642.
33. Zelenka, P. S. (1984). Lens lipids. *Current Eye Research*, *3*, 1337–1359.
34. Subczynski, W. K., Raguz, M., Widomska, J., Mainali, L., & Konovalov, A. (2012). Functions of cholesterol and the cholesterol bilayer domain specific to the fiber-cell plasma membrane of the eye lens. *The Journal of Membrane Biology*. https://doi.org/10.1007/s00232-011-9412-4.
35. Mainali, L., Raguz, M., O'Brien, W. J., & Subczynski, W. K. (2017). Changes in the properties and organization of human lens lipid membranes occurring with age. *Current Eye Research*, *42*, 721–731.
36. Mainali, L., Raguz, M., O'Brien, W. J., & Subczynski, W. K. (2015). Properties of membranes derived from the total lipids extracted from clear and cataractous lenses of 61–70-year-old human donors. *European Biophysics Journal*, *44*, 91–102.
37. Mainali, L., Raguz, M., O'Brien, W. J., & Subczynski, W. K. (2013). Properties of membranes derived from the total lipids extracted from the human lens cortex and nucleus. *Biochimica et Biophysica Acta (BBA)-Biomembranes*, *1828*, 1432–1440.
38. Widomska, J., Subczynski, W. K., Mainali, L., & Raguz, M. (2017). Cholesterol bilayer domains in the eye lens health: a review. *Cell Biochemistry and Biophysics*. https://doi.org/10.1007/s12013-017-0812-7.
39. Mainali, L., Raguz, M., Camenisch, T. G., Hyde, J. S., & Subczynski, W. K. (2011). Spin-label saturation-recovery EPR at W-band: applications to eye lens lipid membranes. *Journal of Magnetic Resonance*. https://doi.org/10.1016/j.jmr.2011.06.014.
40. Raguz, M., Widomska, J., Dillon, J., Gaillard, E. R., & Subczynski, W. K. (2009). Physical properties of the lipid bilayer membrane made of cortical and nuclear bovine lens lipids: EPR spin-labeling studies. *Biochimica et Biophysica Acta*. https://doi.org/10.1016/j.bbamem.2009.09.005.
41. Raguz, M., Widomska, J., Dillon, J., Gaillard, E. R., & Subczynski, W. K. (2008). Characterization of lipid domains in reconstituted porcine lens membranes using EPR spin-labeling approaches. *Biochimica et Biophysica Acta. Biomembrane*. https://doi.org/10.1016/j.bbamem.2008.01.024.
42. Widomska, J., Raguz, M., & Subczynski, W. K. (2007). Oxygen permeability of the lipid bilayer membrane made of calf lens lipids. *Biochimica et Biophysica Acta. Biomembrane*. https://doi.org/10.1016/j.bbamem.2007.06.018.
43. Widomska, J., Raguz, M., Dillon, J., Gaillard, E. R., & Subczynski, W. K. (2007). Physical properties of the lipid bilayer membrane made of calf lens lipids: EPR spin labeling studies. *Biochimica et Biophysica Acta. Biomembrane*. https://doi.org/10.1016/j.bbamem.2007.03.007.
44. Huang, J., Buboltz, J. T., & Feigenson, G. W. (1999). Maximum solubility of cholesterol in phosphatidylcholine and phosphatidylethanolamine bilayers. *Biochimica et Biophysica Acta (BBA)-Biomembranes*, *1417*, 89–100.
45. Stevens, M. M., Honerkamp-Smith, A. R., & Keller, S. L. (2010). Solubility limits of cholesterol, lanosterol, ergosterol, stigmasterol, and β-sitosterol in electroformed lipid vesicles. *Soft Matter.*, *6*, 5882–5890.
46. Buboltz, J. T., & Feigenson, G. W. (1999). A novel strategy for the preparation of liposomes: rapid solvent exchange. *Biochimica et Biophysica Acta (BBA)-Biomembranes*, *1417*, 232–245.
47. Ratanabanangkoon, P., Gropper, M., Merkel, R., Sackmann, E., & Gast, A. P. (2002). Two-dimensional streptavidin crystals on giant lipid bilayer vesicles. *Langmuir.*, *18*, 4270–4276.
48. Bernard, A.-L., Guedeau-Boudeville, M.-A., Jullien, L., & Di Meglio, J.-M. (2000). Strong adhesion of giant vesicles on surfaces: dynamics and permeability. *Langmuir.*, *16*, 6809–6820.
49. Schindelin, J., Arganda-Carreras, I., Frise, E., Kaynig, V., Longair, M., Pietzsch, T., Preibisch, S., Rueden, C., Saalfeld, S., & Schmid, B., et al. (2012). Fiji: an open-source platform for biological-image analysis. *Nature Methods.*, *9*, 676.
50. R Development Core Team (2008). R: A language and environment for statistical computing. http://www.r-project.org.
51. Breton, M., Amirkavei, M., & Mir, L. M. (2015). Optimization of the electroformation of giant unilamellar vesicles (GUVs) with unsaturated phospholipids. *The Journal of Membrane Biology*. (2015). https://doi.org/10.1007/s00232-015-9828-3.
52. Mainali, L., Pasenkiewicz-Gierula, M., & Subczynski, W. K. (2020). Formation of cholesterol Bilayer domains precedes formation of cholesterol crystals in membranes made of the major phospholipids of human eye lens fiber cell plasma membranes. *Current Eye Research*. (2020). https://doi.org/10.1080/02713683.2019.1662058.
53. Raguz, M., Kumar, S. N., Zareba, M., Ilic, N., Mainali, L., & Subczynski, W. K. (2019). Confocal microscopy confirmed that in phosphatidylcholine giant unilamellar vesicles with very high cholesterol content pure cholesterol bilayer domains form. *Cell Biochemistry and Biophysics*. https://doi.org/10.1007/s12013-019-00889-y.

Impact of high cholesterol content on properties of electroformed giant unilamellar vesicles

Zvonimir Boban[a], Dubravka Kovač[b], Witold Karol Subczynski[c], Ana Puljas[a], Marija Raguz[a,+]

[a]Department of Medical Physics and Biophysics, University of Split School of Medicine, Split, Croatia

[b]Department of Physics, Faculty of Science, University of Split, Split, Croatia

[c]Department of Biophysics, Medical College of Wisconsin, Milwaukee, USA

[+] Corresponding author: e-mail: marija.raguz@mefst.hr, Šoltanska 2, 21000 Split, Croatia

Supplementary

If we consider a rectangular area covered completely by vesicles of same diameter so that there are m vesicles in each column and n columns, we can calculate the number of vesicles in that area by knowing lengths a and b of the rectangle sides. Looking at Supp. Fig. S1a, we can see that $b = (2m+1) \cdot \Delta y = (2m+1) \cdot r$. Since all vesicles are of equal size, Δx is equal to the height of an equilateral triangle with sides equal to the vesicles diameter. It follows that $a = (n-1) \cdot \Delta x + 2r = (n-1) \cdot \frac{2r\sqrt{3}}{2} + 2r = ((n-1)\sqrt{3}+2) \cdot r$. Once we have m and n, we can multiply them to obtain the maximum possible number of vesicles $N_{max} = m \cdot n$. This number is obviously heavily dependent on vesicle diameter as shown in Supp. Fig. S1b.

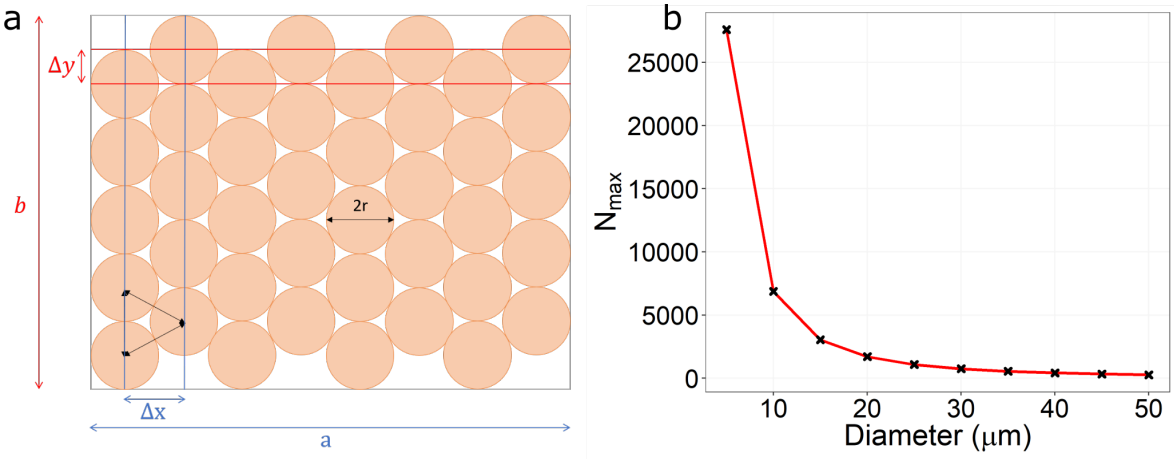

Fig. S1 Derivation of coverage parameter. a Densest vesicle layout. b Maximum number of vesicles with varying vesicle diameters for coverage = 1. Region size is set at the same area as the one observed under the microscope

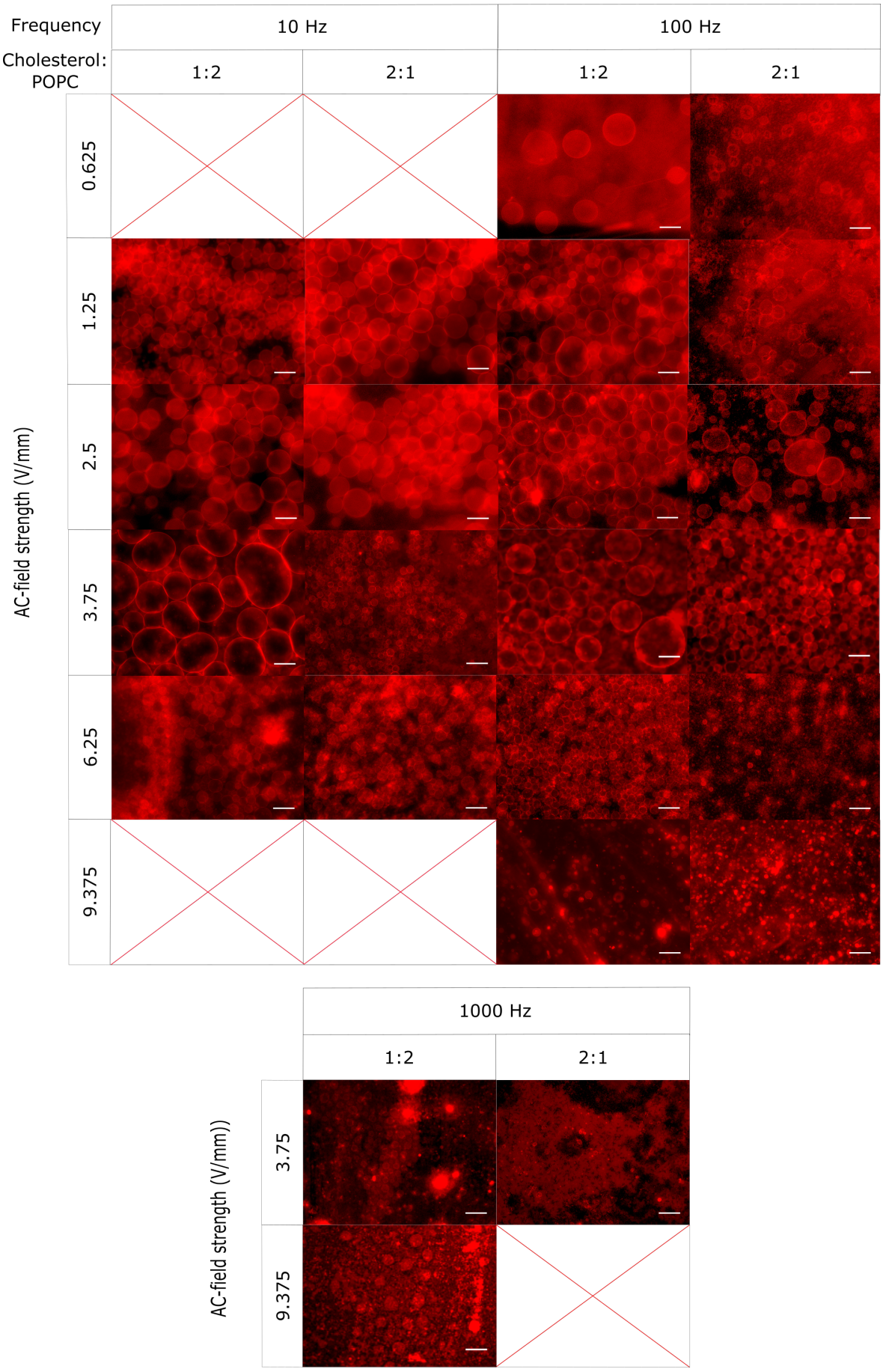

Fig. S2 AC-field frequency-strength diagram for GUV electroformation. Scale bar in the bottom right corner denotes 50 μm. The images are zoomed in compared to original microscope images so that vesicles are more discernible

5 GIANT UNILAMELLAR VESICLE ELECTROFORMATION: WHAT TO USE, WHAT TO AVOID, AND HOW TO QUANTIFY THE RESULTS

Reproduced from Boban, Z.; Mardešić, I.; Subczynski, W.K.; Raguz, M. Giant Unilamellar Vesicle Electroformation: What to Use, What to Avoid, and How to Quantify the Results. Membranes (Basel). 2021, 11, 860, doi:10.3390/membranes11110860.ect

membranes

MDPI

Review

Giant Unilamellar Vesicle Electroformation: What to Use, What to Avoid, and How to Quantify the Results

Zvonimir Boban [1,2], Ivan Mardešić [1,2], Witold Karol Subczynski [3] and Marija Raguz [1,*]

[1] Department of Medical Physics and Biophysics, University of Split School of Medicine, 21000 Split, Croatia; zvonimir.boban@mefst.hr (Z.B.); ivan.mardesic@mefst.hr (I.M.)
[2] Doctoral Study of Biophysics, Faculty of Science, University of Split, 21000 Split, Croatia
[3] Department of Biophysics, Medical College of Wisconsin, Milwaukee, WI 53226, USA; subczyn@mcw.edu
* Correspondence: marija.raguz@mefst.hr; Tel.: +385-98-768-819

Abstract: Since its inception more than thirty years ago, electroformation has become the most commonly used method for growing giant unilamellar vesicles (GUVs). Although the method seems quite straightforward at first, researchers must consider the interplay of a large number of parameters, different lipid compositions, and internal solutions in order to avoid artifactual results or reproducibility problems. These issues motivated us to write a short review of the most recent methodological developments and possible pitfalls. Additionally, since traditional manual analysis can lead to biased results, we have included a discussion on methods for automatic analysis of GUVs. Finally, we discuss possible improvements in the preparation of GUVs containing high cholesterol contents in order to avoid the formation of artifactual cholesterol crystals. We intend this review to be a reference for those trying to decide what parameters to use as well as an overview providing insight into problems not yet addressed or solved.

Keywords: electroformation; GUVs; cholesterol; lipid composition; lipid deposition; electrical parameters; temperature; electroformation duration; internal solution; quantitative analysis

Citation: Boban, Z.; Mardešić, I.; Subczynski, W.K.; Raguz, M. Giant Unilamellar Vesicle Electroformation: What to Use, What to Avoid, and How to Quantify the Results. *Membranes* **2021**, *11*, 860. https://doi.org/10.3390/membranes11110860

Academic Editors: Joanna Kotyńska and Monika Naumowicz

Received: 14 October 2021
Accepted: 5 November 2021
Published: 7 November 2021

1. Introduction

Artificial vesicles have become an important research tool due to their similarity to biological membranes [1–6]. Being lab-created, they enable the study of membrane properties under controlled conditions. When mimicking the biological membrane, we are interested mainly in unilamellar vesicles (only one outer bilayer), but multilamellar (bilayers arranged in concentric circles) and oligolamellar vesicles (containing smaller ones inside) can also be created. Depending on their size, unilamellar vesicles are commonly divided into three groups: small (SUVs, <100 nm), large (LUVs, 100 nm–1 μm), and giant unilamellar vesicles (GUVs, >1 μm). SUVs and LUVs are more often studied in the context of drug delivery applications [7–9]. GUVs are more useful as artificial cell models for eukaryotic cells due to similarity in size. Additionally, their size enables observation of membrane domain structure using light microscopy.

Here, we will focus on the electroformation method in the context of GUV formation. Although other reviews have covered similar topics, they are either not up to date [10], focus on just one segment of a specific method [11,12], or cover a much broader range of topics/methods, thus not exploring any particular approach in enough detail [13–16].

Due to a large number of electroformation parameters, it is easy to overlook some of them or underestimate the importance of a seemingly trivial step in the protocol. This motivated us to collectively analyze their impact on GUV growth in order to better understand their importance and interplay. Special emphasis is placed on GUVs with cholesterol (Chol) contents exceeding their membrane saturation limits. Membranes with such high Chol contents are of special interest to researchers investigating the involvement of Chol in the development of atherosclerosis [17,18] or to those, like our group, who investigate fiber cell

plasma membranes of the eye lens [19–25]. High Chol and formation of pure cholesterol bilayer domains (CBDs) are signs of pathology in most tissues and organs [18,26]. Eye lenses are the only system in which such high Chol concentrations and CBDs are needed to maintain fiber cell membranes, fiber cells, and whole lens homeostasis. However, because of the high Chol content, preparation of such GUVs is problematic due to Chol demixing resulting in the formation of Chol crystals [20,27–29]. These crystals do not participate in further membrane formation, which leads to a real membrane Chol content that is lower than the Chol mixing ratio. We have faced these problems in our work [20] and will discuss possible ways to solve them.

The review starts by defining the classic protocol steps and then goes through each of those steps, exploring developed variations and commenting on related artifacts. Additionally, methods for quantifying the size and count of obtained vesicles are discussed. The final section goes over conclusions from the review and discusses possible improvements in the preparation of GUVs with high cholesterol contents.

2. Classic Electroformation Protocol

One of the earliest attempts at forming GUVs was the natural swelling method introduced by Reeves and Dowben in 1969 [3]. According to this method, a lipid solution is deposited on a surface and dried to form a lipid film. The lipid film is then rehydrated and the obtained solution gently stirred to form vesicles. The vesicles are formed mainly due to the osmotic pressure driving the aqueous solution in between the stacked lipid bilayers. Exposing the hydrophobic portion of the bilayer to aqueous solutions is unfavourable and causes them to close up into vesicles. However, the proportion of GUVs that can be generated using this method is small, as most of them are either multilamellar or display other types of defects [30]. In their efforts to devise a protocol that reliably produces a high proportion of cell-sized unilamellar vesicles, Angelova and Dimitrov applied an external electric field during lipid swelling and thus invented the electroformation method [31]. Although the exact mechanism of the method is not yet completely understood, it is believed that the electric field affects lipid swelling through direct electrostatic interactions, redistribution of counterions, changes in membrane surface and line tension, and electroosmotic flow effects [32]. More detailed theoretical discussions on the electroformation mechanism can be found elsewhere [33–35]; here we focus mainly on exploring the optimal parameters and artifacts appearing when performing experimental work using this method.

Although Angelova and Dimitrov used platinum wires for electroformation, indium tin oxide (ITO) electrodes are most commonly used nowadays, so we utilize them in our description of the basic protocol. The only difference between these two protocols is the electroformation chamber layout. The protocol starts with droplets of lipids dissolved in an organic solvent being deposited onto the electrode (Figure 1a). In addition to lipids, fluorescent dyes are present in the mixture in small quantities to enable the usage of fluorescent microscopy later on.

The solvent is evaporated under vacuum or a stream of inert gas (Figure 1b). A spacer is attached to the electrode using vacuum grease (Figure 1c). Another electrode is then attached to the spacer with its conductive side facing inward. Following that, the chamber is filled with an internal solution of choice and connected to a voltage source while maintaining a temperature higher than the phase transition temperature of deposited lipids. Copper tape is often attached to the electrodes to provide better contact with the alternating current function generator (Figure 1d). The combination of the electric field and lipid film hydration leads to the creation of lipid vesicles which can be observed under a microscope (Figure 1e).

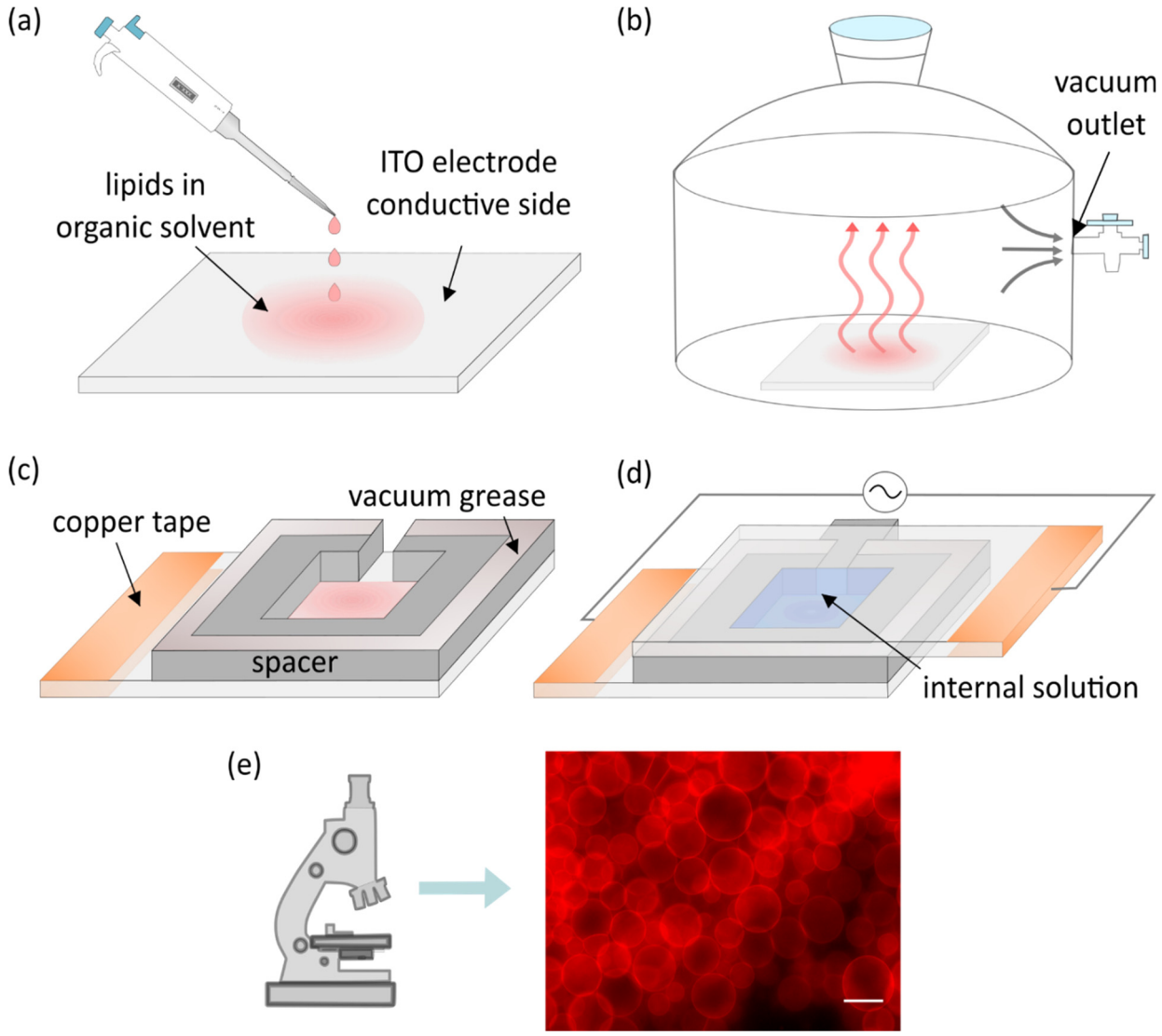

Figure 1. (**a**) Deposition of lipid droplets onto the electrode surface. (**b**) Evaporation of organic solvent under vacuum. (**c**) Construction of the electroformation chamber. (**d**) Electroformation chamber filled with an internal solution and connected to an alternating current function generator. (**e**) An image of fluorescently labeled giant unilamellar vesicles (GUVs) obtained using fluorescence microscopy. The scale bar denotes 50 µm.

At first, direct current was used, but water electrolysis led to formation of bubbles [31], so a transition to alternating currents was made [31,32]. Alternating currents also introduce electroosmotic motion of the fluid, which facilitates the destabilization of the lipid film, thus promoting the formation of vesicles [32,36]. Over the years, the initial protocol has been modified in order to increase the yield, homogeneity, and compositional uniformity of the vesicles or to enable preparation of GUVs from previously incompatible lipids and buffers. In the following sections, we will systematically discuss the advancement of each segment of the electroformation method.

3. Electrode Materials and Cleaning

Alongside platinum electrodes, ITO-coated glass slides are most commonly used nowadays. In comparison to platinum electrodes, ITO electrodes provide a larger and flatter surface, so a higher GUV yield can be obtained. Also, owing to their transparency, microscopic techniques are easier to apply. It is recommended to periodically replace ITO electrodes since they were proven to have limited reusability. Using the same ITO glass more than three times has been shown to decrease the average GUV diameter and their

quality. The effect seems to be less pronounced for zwitterionic and negatively charged lipids. Furthermore, the degradation seems to be reversible through annealing at high temperatures [37].

Compared with ITO electrodes, platinum electrode aging seems to affect the average diameter of vesicles less, but the proportion of GUVs (i.e., the proportion of defect-free unilamellar vesicles) also drops. Electrode replacement or annealing is recommended after approximately five experiments [38]. Steel syringes and copper electrodes have also been suggested as cost-friendly alternatives [39,40]. Furthermore, titanium electrodes have been advocated by some groups since their usage seems to decrease lipid peroxidation when compared to ITO electrodes [11,41–43].

In addition to changing the electrode material completely, various modifications to the existing electrode layouts were tested. Okumura and Sugiyama confirmed that GUVs can form on non-electroconductive materials, such as polymer meshes placed onto ITO electrodes and filled with lipid solutions [44,45]. Lefrançois et al. experimented with an asymmetrical ITO electrode layout (top electrode with a smaller surface area than the bottom one) [46] (Figure 2a). This layout proved to be more efficient when physiological salt concentrations were combined with interelectrode separations smaller than 2 mm. Small interelectrode separation did not cause problems when the same parameters were set, but deionized water was used as an internal solution. The effect appears because alternating-current electroosmosis assisted flow does not occur in the symmetrical configuration. However, since both symmetrical and asymmetrical layouts were tested under the same electrical parameters, it is not clear whether GUVs could be grown under physiological conditions for smaller electrode separations just by altering the electrical parameters and retaining the symmetrical ITO chamber layout. Bi et al. abandoned the principle of parallel opposing electrodes altogether and have shown that GUVs can be grown using coplanar interdigitated ITO electrodes [47] (Figure 2b).

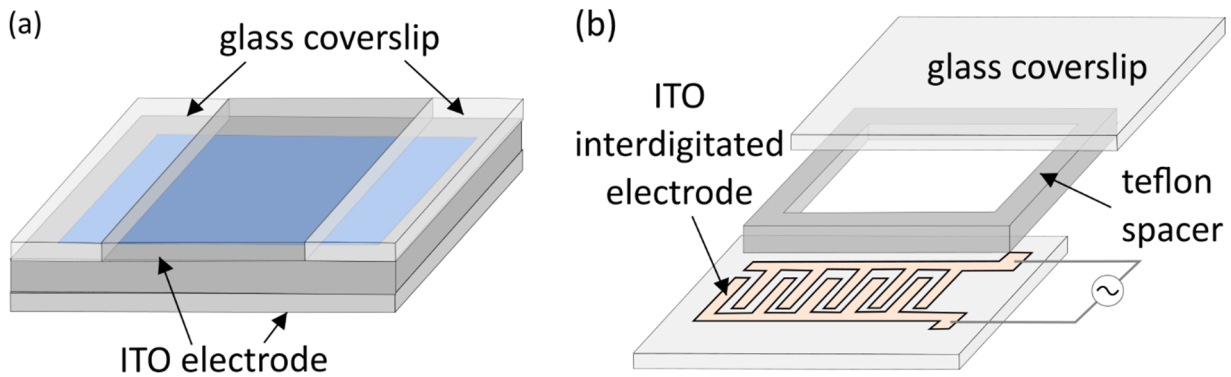

Figure 2. (**a**) Asymmetrical electrodes layout. The top indium tin oxide (ITO) electrode has a smaller surface than the bottom one, so it has to be surrounded by glass coverslips in order to close off the chamber. (**b**) Electroformation chamber with a coplanar interdigitated ITO electrode.

In order to remove contaminants from the electrode surface, researchers use a variety of cleaning protocols. In general, these consist of cleaning the electrodes using organic solvents and then drying them. Of course, there are many variations of these general steps, and some articles do not even include the cleaning protocol [29,46,48]. Variations include sonication in conjunction with organic solvents [35,47,49,50], repeated rinsing with organic solvents [51], and swabbing electrodes using lint-free wipes [10,12,28,37]. Electrodes are either dried under a stream of inert gas [35,37,47,50] or just wiped and air dried [28]. Plasma cleaning has also been tested on ITO glass [35,47] and has proved to be very effective, since it both cleans the surface and makes it more hydrophilic. Moreover, plasma cleaning could aid hydration of the solid lipid film and the formation of lipid bilayers [35].

4. Deposition of the Lipid Solution and Removal of the Solvent

In the early days of electroformation, the lipids dissolved in chloroform or other organic solvents were deposited onto the electrodes simply by dropping the solution and evaporating the solvent later [31,52] (Figure 3a). In order to efficiently produce GUVs, the lipid film is suggested to be around 5–10 bilayers thick (around 30–60 nm) [31,50]. When using drop deposition, regions of different thicknesses will be formed. Although this means that at least some portion of the deposited film will be suitable for electroformation at given parameters, other regions will inevitably be too thin or too thick. These nonuniformities lead to lack of reproducibility.

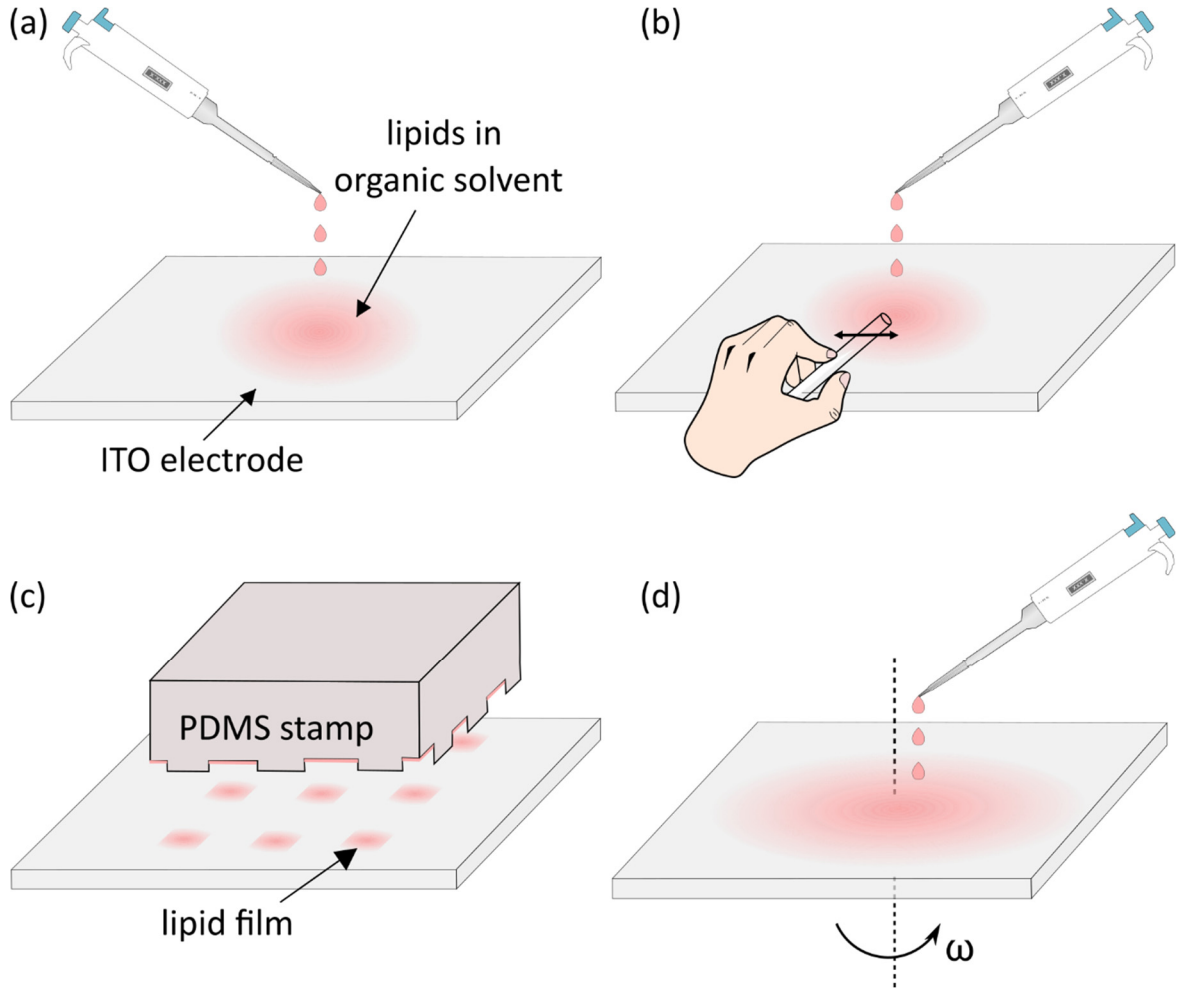

Figure 3. (**a**) Droplet deposition. (**b**) Droplet deposition with smearing afterward to better spread the lipid film. (**c**) Deposition of lipids by pressing a patterned silicon stamp on the electrode surface. (**d**) Spin-coating of lipid solution by fast rotation of the electrode immediately after the deposition.

In order to make the deposition process more efficient and reproducible, different approaches were investigated as well. Some groups used needles or thin rods to smear the solution after dropping it in order to increase the homogeneity of the film [10,35,53,54] (Figure 3b). Others used a Hamilton syringe to deposit non-overlapping snakelike patterns of lipids [37]. A more systematic approach was tested by stamping the lipid solution onto the ITO electrode using a customized polydimethylsiloxane (PDMS) stamp [55] (Figure 3c). This approach resulted in GUVs of a size similar to the width of the gaps in the PDMS stamp. However, the authors reported that the thickness of the lipid film was not uniform over the lipid patches in the gaps. Dip coating (immersing the ITO electrode in the lipid

solution and holding it vertically to dry) was explored as well, but due to different rates of solvent evaporation across the glass, the film proved to be inhomogeneous [50].

Reproducibly controllable lipid film thickness was achieved by Estes and Mayer using the spin-coating method. The lipid solution is dropped onto the flat electrode surface, which is subsequently rotated very fast ($\omega \sim 600$ rpm) in order to achieve a homogenous film [50] (Figure 3d). The uniformity of films and method reproducibility were confirmed using ellipsometry and atomic force microscopy techniques. The method was proven to be effective by several groups using a wide range of lipid compositions [28,50,51]. There are, however, disadvantages as well. First, it requires a much larger amount of lipids compared with traditional methods, since much of the solution is washed away during electrode rotation [50]. Second, it involves a spin-coater, which is not a standard device in labs investigating biological membranes.

Another attempt at achieving uniform lipid films was made by Le Berre et al. [56]. They drag-dropped an organic solution of lipids on a solid substrate. Constant substrate velocity and temperature were maintained while simultaneously controlling the vapor aspiration. Reproducible results with variations of ± 5 nm were obtained, but the method has not been widely adopted, probably due to the device used being relatively complicated.

Before chamber construction, the organic solvent needs to be removed from the deposited lipid solution. This is most commonly achieved by placing the electrodes under a vacuum [4,10,28,35,37,50,53]. Depending on the research group, the vacuum duration can range from just 5 min [53] to 2 h [35]. Alternatively, drying can be performed by placing the electrode with the lipid solution under a stream of an inert gas, such as nitrogen [31,51,52] or argon [41]. More rarely encountered, lyophilization can also be used to eliminate traces of the organic solvent [27,57].

Some researchers went in another direction and instead of trying to improve the existing approach, replaced the organic solution of lipids with aqueous liposome suspensions (SUVs, LUVs, or multilamellar vesicles) [4,29,49,58–61]. Using this approach, Pott et al. concluded that GUV formation was better when using aqueous liposome solutions than when using organic lipid solutions [4]. They attribute this to the ability of such dispersions to produce well-oriented membrane stacks immediately after the evaporation of water. Although any excess water was completely removed from the deposits, an alternative approach was suggested in which the deposits would be only partially dehydrated prior to internal solution addition. The effect of using damp lipid films on GUV properties was explored in more detail by Baykal-Caglar et al. [29]. By measuring their miscibility transition temperature, they have shown that such an approach produces more compositionally uniform populations of GUVs. This result is explained by a reduction in lipid demixing—a common artifact appearing when drying the lipid solution completely. The artifact is especially pronounced when using mixtures with a cholesterol content near to or above the maximum solubility threshold for that mixture [27].

Furthermore, avoiding the dry phase and use of organic solvents benefits protocols aimed at protein incorporation into GUVs, since these steps damage the protein structure. The first proof of successful protein reconstitution using this approach came from Girard et al. [61] and the most recent protocol is described by Witkowska et al. [49].

Since the deposition of aqueous liposome suspensions was a significant deviation from the classic protocol by itself, until recently, no one addressed the still existing problem of nonuniform film thickness. In 2019, Oropeza-Guzman et al. suggested using the coffee ring effect to solve this issue [59]. The effect describes a phenomenon in which a drying droplet deposits most of its material on the periphery, forming a ring-like stain. The group used the effect to their advantage by consecutively depositing progressively larger droplets on top of one another. Since a larger droplet has more material, it will create a larger diameter ring and, in the process, will smear and flatten the ring from the previous droplet, thus leaving an area of uniform lipid thickness inside (Figure 4). Although the mean diameter of vesicle populations hasn't significantly changed when compared to the single droplet deposition, the multi-droplet preparations displayed a much lower percentage

of nonunilamellar vesicles. These results combined with the low lipid mass used and a relatively simple experimental setup make the method a promising option for reproducible and uniform lipid deposition.

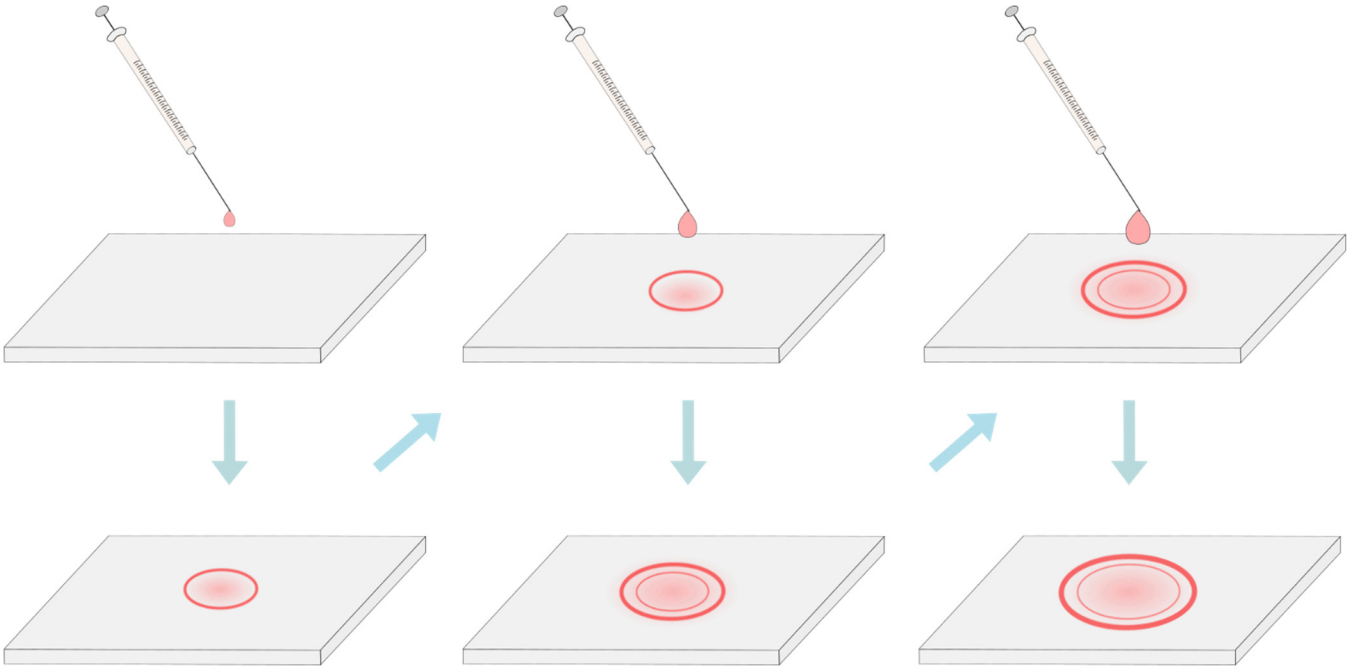

Figure 4. Deposition of lipids utilizing the coffee ring effect. After drying, most of the material is carried away toward the periphery and a ring-like stain is formed. This is known as the coffee-ring effect. By depositing progressively larger droplets, the ring from the previous droplets gets smeared and flattened, thus leaving behind an area of uniform lipid film thickness.

5. Lipid Compositions and Internal Solutions

Artificial vesicles are often grown from single phospholipid species. Vesicles made of different phospholipids [15,50] and hybrid phospholipid/polymer vesicles have been produced through electroformation [62–64]. Details about lipid/polymer vesicle electroformation can be found elsewhere [65]; here we will mainly focus on lipid composition. Among lipid mixtures, Chol and/or sphingomyelin are the most frequently employed since they are the other two most abundant eukaryotic plasma membrane components [66]. Chol concentrations of up to ~50 mol% are most commonly experimented with, since most biological membranes do not exceed this level [26,66], and the maximum solubility limit of Chol in phospholipid membranes seems to be around 66 mol% [27,67]. Nevertheless, biological systems, such as the fiber cells of eye lenses, exhibit Chol:phospholipid molar ratios of up to two in the lens cortex and up to four in the nucleus [68,69]. Excess Chol is incorporated into CBDs up to a solubility threshold after which cholesterol crystals are formed outside the membrane [22,70]. Modeling these systems requires GUVs of appropriate lipid composition, but they are not often used in experiments and additional obstacles, such as the previously mentioned demixing artifact, become more pronounced [20,27]. Phospholipid/sphingomyelin/Chol ternary mixtures have been more intensely researched of late, since these constituents are involved in the formation of lipid rafts [71].

For a long time, electroformation was deemed inappropriate for the growth of vesicles in a medium with physiological salt concentrations [72]. These difficulties have recently been linked to tighter lipid packing and decreased water permeability. Additionally, the electrohydrodynamic force decreases when using solutions with high ion concentrations [73,74]. Successful protocols for GUV electroformation under physiological conditions started appearing around 15 years ago [4,12,29,35,46,75,76]. Pott et al. successfully formed GUVs from a single lipid species in a 100–250 mM NaCl solution [4]. At their suggestion, using a similar protocol, Montes et al. also succeeded in forming GUVs from native mem-

branes or organic lipid mixtures at physiological conditions (25 mM HEPES + 150 mM NaCl pH 7.2) [76]. Using plasma cleaned ITO electrodes, Li et al. extended the concentration of NaCl up to 2 M and noticed that the diameters of GUVs increased in the 0–200 mM range and then decreased for 200 mM–2 M. Furthermore, they successfully formed GUVs in a PBS (phosphate buffered saline) and PCR (polymerase chain reaction) buffer [35]. Two years later, another protocol focusing solely on GUV growth in a PBS buffer was published. The same article also includes a discussion on microinjection of material into grown GUVs and concludes that the highest success rate is obtained when their mechanical stability is increased through the addition of 20 mol% of cholesterol to the mixture [46].

In addition to high salt concentrations, nonneutral lipid charge also seems to affect GUV growth [35,37,53,77,78]. Estes and Mayer successfully formed GUVs from neutrally and negatively charged lipids. However, they noticed that using high concentrations of negatively charged lipids resulted in an approximately 30% increase in the thickness of the coated lipid layer [50]. Ghellab et al. and Li et al. experimented with both negatively and positively charged lipid mixtures and were able to grow GUVs using all of the combinations [35,53]. Nevertheless, the average diameter of GUVs containing higher concentrations of charged lipids was much smaller. As a possible explanation for this effect, they mention the formation of an electric double layer due to the high concentrations of counter ions near the electrode.

Alongside water and physiological buffer, GUVs are sometimes grown in sucrose and then resuspended in glucose or a physiological buffer, resulting in their sinking to the bottom of the chamber [10,12,38,41]. This makes microscopy easier since all GUVs are in the same plane. Using sugars, such as sucrose, also seems to promote GUV formation by enhancing the hydrodynamic force on the lipids through an increase in interfacial viscosity between the solution and the lipid membrane [79].

Internal solution pH is also important since it is strongly linked with lipid hydrolysis. A study using partially hydrogenated egg yolk phosphatidylcholine showed that the hydrolysis rate is lowest at around pH 6.5–7 and then increases in both directions as the pH changes [80]. This is fortunate since physiological conditions assume near-neutral pH, so those values are desirable for cell mimicking experiments.

The most common method for observation of GUVs and their domains is fluorescence microscopy. However, the user has to be careful since production of peroxides due to excitation of the fluorescent dyes leads to light-induced lipid oxidation and subsequently to light-induced domains [10,11,41,48,81]. Zhao et al. compared two dye concentrations and found that it took more time for the light-induced domains to appear for the smaller concentration (10–20 s after illumination with a mercury lamp) [48]. On top of that, fluorescent probes can change the phase behavior of membranes with a miscibility transition [10,82]. Taking the above two effects into account, it is always best to use the smallest possible amount of lipid probe while still obtaining a good signal for microscopy. Additionally, when multiple fluorescent probes are used simultaneously (for some probes even in amounts as small as 0.05 mol%), their preferential partitioning can change when compared with a single fluorescent probe scenario [82].

6. Electrical Parameters

Most studies are not concerned with electroformation parameters giving the best GUV yield but only require a certain number of stable vesicles for further research. It is no wonder then that most studies choose established voltage and frequency values from common references, such as Angelova et al. or Veatch, where peak-to-peak voltage is usually kept between 1 and 10 V and frequency around 10 Hz [10,31,36].

Of course, since the property of interest here is the electric field and not the voltage by itself, the voltage values should always be accompanied by electrode separation in order to provide some context for the field strength. Common interelectrode separations range from 0.5 to 3 mm. Most often, a separation value from this interval is used without special explanation, and the voltage is modified accordingly. In combination with

ITO electrodes, the separation is achieved through the use of spacers usually made from silicon (PDMS) [2,31,34,37,50–52] or Teflon (polytetrafluoroethylene) [28,38,41,83]. Another alternative is specifying the electric field strength instead of the voltage from the beginning [4,28,51].

Significant deviations from conventional parameters are usually explored only in studies specifically trying to improve a certain aspect of the electroformation protocol. GUVs were obtained using egg phosphatidylcholine or DOPA (1,2-dioleoyl-*sn*-glycero-3-phosphate) using electric field values of up to 40 V/mm and frequencies up to 1 MHz [51]. Another study used a mixture of phosphatidylcholine and cholesterol and found the optimal values to be 5 V/mm and 10 kHz [34]. Considering such large differences depending on the specific lipid composition and experimental setup, it is prudent to optimize the electrical parameters every time a different lipid composition (or one not yet explored by other researchers) is used. However, using electric field strengths up to a couple V/mm and frequencies of 10–100 Hz seems to give satisfying results for many different lipid compositions (positive, negative, and zwitterionic lipids compositions were tested) when deionized water is used as an internal solution [53].

If physiological salt concentration buffers are used as the internal solution, higher frequencies tend to be needed [4,12,35,76]. Pott et al., Montes et al., and Lefrancois et al. all had success forming vesicles at physiological conditions using a frequency of 500 Hz [4,46,76]. Li et al. performed a systematic frequency-voltage sweep for three lipid compostions (two zwitterionic and one negatively charged lipid species) and found the ideal frequency to be in the range of 100–1000 Hz as well [35]. The preference for higher frequencies is attributed to disruption of the electric double layer under those conditions [12,35,51,84].

Some groups alter the voltage values during electroformation [4,38,39,46,49,54,61,76]. The reasoning behind such protocols is well described by Pott et al. [4]. First, the electric field is progressively being increased up to a maximum value at a fixed frequency in order to maintain a sphere-like shape of growing vesicles. Second, depending on the chamber solution and the duration of the first step, the electric field is kept constant in order to allow an increase in size through swelling. An additional step can be included in which the electric field remains the same as in the previous step, but the frequency is reduced in order to promote vesicle fusion and detachment from the electrodes.

Drabik et al. compared the approach of increasing the voltage by 1 V every hour from 1 to 4 V with a constant 2.5 V applied for 4 h. The vesicles obtained using the sequential voltage approach were bigger, but both the amount of lipids used for electroformation and the ratio of unilamellar to oligolamellar vesicles remained unchanged [38]. It is important to note that this research only used a zwitterionic monounsaturated phospholipid, so the results might differ when using different lipids or more complex compositions. Breton et al. utilized a protocol involving an initial stepwise increase in voltage up to a maximum value that was then maintained for a certain amount of time [85]. Using three lipid species with different levels of unsaturation, they have shown that even at relatively low electric field values (<1 V/mm), lipid oxidation occurs for moderately and highly oxidizable lipids (two double bonds or more). This is in agreement with a previous study on the oxidative effect of electric field on lipids from Zhou et al. [42]. The increase in maximum voltage did not change the rate of oxidation for monounsaturated lipid species [85]. The size of the vesicles increased up to an oxidation level of 25%, after which it started to decrease [85]. The fact that oxidation of 25% will be reached at different voltages for different lipid species again underlines the necessity of optimizing the protocol for each different lipid composition used.

7. Temperature and Electroformation Duration

Temperature is an important parameter in electroformation protocols since it governs the bilayer gel to liquid phase transition (melt/transition temperature). Moreover, a continuous increase in temperature (as opposed to a thresholding effect of the transition temperature) seems to be accompanied by an increase in the final diameter of produced

GUVs [35,47,53]. A probable explanation is that the temperature enhances the permeability of the membrane to the solvent through an increase in membrane fluidity [86]. Although increasing the GUV diameter is a desirable property, there is a disadvantage to increasing the temperature too much since prolonged exposure to high temperatures leads to increased lipid breakdown [10].

In order for the bilayer to be in the liquid phase and adequate mixing of components to be achieved, the electroformation temperature is usually kept above the transition temperature of the lipid with the highest transition temperature in the mixture. In some cases, the miscibility transition temperature can even exceed this highest transition temperature, so an even higher value is sometimes needed [10]. However, high temperatures can be harmful in scenarios such as those involving protein reconstitution. Regarding this issue, a study using a DOPC (1,2-dioleoyl-*sn*-glycero-3-phosphocholine)/sphingomyelin/Chol (2:2:1 molar mixture) compared the properties of GUVs grown at room temperature and 65 °C [83]. The proportion of liquid ordered–liquid disordered (Lo + Ld) phase separated vesicles was higher in the higher temperature batch. Nevertheless, the physical properties of vesicles that were phase separated were similar for both temperatures.

The rate of sample cooling after electroformation plays a significant role in the phase separation of membrane domains. First, sudden changes in temperature can break some vesicles [10]. Second, if cooled too quickly from a fluid one-phase region to the gel–fluid phase, the vesicles seem to be caught in a nonequilibrium state where phase separation has not yet been achieved [87,88]. On the other hand, in situations where the Ld phase is present in small amounts, cooling too slowly can lead to an artifactual decrease in the amount of Lo + Ld phase due to the Ld phase pinching off the parent GUV [11].

The duration of electroformation is variable between research groups as well and usually ranges from 0.5 to 7 h, though it can last up to 24 h in some cases [38]. The effect of prolonged electroformation duration (4–24 h) has been tested using fluorescence microscopy, flow cytometry, spectrofluorimetry, and colorimetric analysis to measure the diameter of vesicles, the proportion of oligolamellar vesicles, and the amount of lipid molecules in the GUV suspension after electroformation [38]. Prolonged electroformation duration did not significantly impact any of these parameters. However, the study only used a monounsaturated phospholipid, which is poorly oxidizable. Another study involving three lipids with different degrees of unsaturation was also conducted [85]. Using mass spectrometry and flow cytometry, a longer electroformation duration (5 vs. 20 h) was shown to induce lipid oxidation in more oxidizable lipids (two double bonds or more).

8. Vesicles Population Count and Size

8.1. Manual Analysis

Electroformation results are usually presented through the number and size of analyzed vesicles. The most common approaches use microscopic techniques and then count the vesicles and measure the diameters or intensities manually. Of course, since the number of GUVs in a chamber can be very high, it is not feasible to analyze every vesicle, so usually, a predetermined number of GUVs is selected. Unfortunately, this process is highly subjective and can lead to problems, such as biased selection or different criteria for selection. Consequently, there has been a recent surge in the development of automatic methods for GUV analysis. Based on the operating principle, methods for automated GUV detection and analysis can be divided into three larger groups: conventional microscopy aided by automatic detection algorithms, light scattering methods, and methods based on analysis of electrical impedance.

8.2. Automated Microscopy Analysis

Compared with manual analysis, automatic analysis can save a lot of time and reduce the possibility of bias while tracking the vesicle features. Nevertheless, many research groups still default to manual analysis, so studies using automated approaches do not appear often and are generally published within last 10 years. Numerous different ap-

proaches were used, such as circle detection using discrete differential evolution [89], Markov random field [90], and circular Hough transform [91]. The latest additions are offered as ImageJ [92] macros using (amongst others) techniques such as polar transformations [93,94] or a series of steps sometimes utilizing existing ImageJ functionalities [95,96].

3D reconstruction algorithms based on confocal microscopy stacks are available as well [97]. Although a 3D reconstruction is visually the best approach, we can never display the whole surface at once. In order to gain a complete information, we have to use multiple viewing angles. This problem can be solved by creating 2D projections from 3D image stacks through unfolding of the 3D surface (like projecting Earth's surface on a cartographic map) [98]. Additionally, since the 2D projection displays the whole surface at once, it is much easier to track the surface dynamics. Maybe the best approach would be to use these two methods together, since they complement each other; one gives us a familiar and visually appealing 3D representation and the other a possibility to monitor the whole surface at once.

8.3. Light Scattering Methods

Light scattering methods are a popular tool for determining the average diameter of particles suspended in a solution. For particles up to a diameter of around 1 μm, methods such as dynamic light scattering can be used to easily obtain the average diameter value [99]. Since GUVs fall out of this size category, the most commonly used light scattering method is flow cytometry [38,85,100–104]. Studies have been performed to confirm the correlation between the forward scatter (FSC) and side scatter (SSC) signal intensity and particle size. For example, the correlation for smaller particles (∼1 μm) has been confirmed using dynamic light scattering measurements [99] and for larger ones (∼10 μm) by observing liposomes under a microscope after fluorescence-activated cell sorting [101]. Consequently, to obtain the average liposome diameter, sample FSC and/or SSC signals are measured and compared with those of calibration beads (usually polystyrene or silica) of known size.

The problem with this approach is that the FSC and SSC signals depend on the internal structure of the particles as well as their refractive indices, giving rise to a certain amount of error in obtained diameters [99,105]. Usually, researchers are content with obtained relative sizing but comment on the possibility of error due to the refractive index mismatch. Possible solutions have been offered to account for the difference. One study first obtained the average refractive index of particles of interest and then corrected the calibration beads measurements using the Mie scattering theory [105]. Another study took a more direct approach and proposed artificial liposomes as calibrators instead of polystyrene beads [100]. An additional detail which is easily missed is that all of the articles above use FSC and/or SSC to extract the dimensions of the particles. However, when particles are approximately the same size as the height of the laser beam (as is the case for most GUVs), pulse width sizing is probably a better approach for determining the size of vesicles as it does not depend on many of the factors plaguing light scattering approaches for size measurements [106,107].

Recently, imaging flow cytometry devices started being used for GUV quantification [103]. This unites the best of both worlds by combining the rapid analysis of thousands of particles using flow cytometry with the capability of image-based approaches to identify the results.

8.4. Electrical Impedance-Based Analysis

Coulter counters detect particles suspended in an electrolyte based on the change of impedance due to the passing of a particle through an aperture between the two electrodes [108]. In terms of potential for analysis of GUVs, the method has an advantage of being able to detect the size of particles as well as their number.

With this possibility in mind, it is surprising that this device is not used more in GUV studies, so it is probably due to the device not being widely accessible. We were able to find only one recent GUV study using this method [109]. Even there, however, not a classic

Coulter counter but a handheld version was used. Although combining the principle with a handheld device is convenient, the drawback is that it can only be used to analyze particles ranging from 6 to 36 μm in diameter. However, depending on the aperture size, a classic Coulter counter can be adjusted to analyze objects as large as 1600 μm [108].

9. Final Conclusions and Future Directions

This section summarizes the most important modifications of the electroformation method and discusses future improvements regarding the formation of GUVs with a high Chol content.

Concerning electrodes, ITO and platinum remain the most common choices, but the same electrodes should not be used for too long due to the negative impact of electrode aging on GUV quality [37,38]. Traditional drop-deposition methods have been superseded due to their not being able to attain reproducibly uniform lipid films. The best alternatives seem to be the spin-coating method of Estes and Mayer [50] and deposition using the coffee-ring effect [59]. Of these two, the coffee-ring method offers the additional advantage of requiring fewer lipids. Replacing the organic solution of lipids with an aqueous liposome suspension during the deposition step has also been shown to improve GUV formation [4]. Bypassing the dry phase altogether by using damp lipid films for electroformation has been tested as well and shown to produce more compositionally uniform GUV populations [29]. The effect is attributed to a reduction in the lipid demixing artifact that occurs when the lipid film is dried completely.

In order to better emulate cell conditions, solutions with physiological pH and ion concentrations have to be used instead of deionized water. Using plasma cleaned ITO electrodes and higher electroformation frequencies (~500 Hz) seems to be beneficial for GUV growth in such environments [4,35,46,76]. Depending on the degree of unsaturation of used lipids, the voltage should be kept low enough to prevent oxidation. For highly oxidizable lipids, oxidation occurs even at relatively low field values such as 1 V/mm [85]. Overly long electroformation durations should also be avoided since they too increase lipid oxidation for polyunsaturated lipids [85].

Electroformation temperature should be kept well above the transition temperature of the lipid with the highest transition temperature in the mixture. Increasing the temperature has been shown to lead to an increase in final GUV diameter [35,47,53]. Nevertheless, temperature should not be set too high since prolonged exposure to high temperatures leads to increased lipid breakdown [10]. The rate of cooling should be monitored as well. Cooling too quickly can lead to vesicle rupture [10] and vesicles being caught in a nonequilibrium state [87,88]. However, if cooling occurs too slowly in situations where Lo + Ld phases are present, the Ld phase can pinch off the parent GUV, leading to artifactual results as well.

The most common method of quantifying vesicle yield is fluorescence microscopy followed by manual vesicle analysis. However, this approach can be highly subjective, leading to biased results. Consequently, numerous automated algorithms for GUV detection have recently been developed and implemented [89–91,93–95]. Aside from traditional image-based analysis, flow cytometry and impedance-based methods have also been used to assess the GUV yield. Flow cytometry provides information on both the size and structure of the analyzed population. However, the size measurements may be incorrect due to the cytometry signal dependance on the particle structure and refractive index [99,105]. Impedance-based analysis offers much more precise size measurements but lacks the additional information flow cytometry offers. Recently, imaging flow cytometry was applied to GUV analysis, combining the rapid population analysis of flow cytometry with the ability to identify the results through their images [103].

Applying classic electroformation protocols to produce GUVs from lipid mixtures containing high Chol concentrations leads to artifacts caused by Chol demixing and formation of Chol crystals. We faced these problems using confocal microscopy to confirm that pure CBDs are formed in GUVs made of a Chol/PL mixture [20]. We were able to

observe CBDs but only when the Chol/PL mixing ratio was equal or greater than 2.5 for DSPC (distearoylphosphatidylcholine) and 3 for POPC (1-palmitoyl-2-oleoyl-glycero-3-phosphocholine). We previously showed that for these phospholipids CBDs start to form at 50 mol% Chol concentration in lipid bilayer membranes of multilamellar liposomes (at a Chol/PL molar ratio of 1) [22,70]. At a membrane Chol content of 66 mol% (i.e., at a Chol/PL molar ratio of 2), Chol crystals start to form [22,70]. Thus, the real Chol content in the membranes of GUVs was significantly lower than the Chol/PL mixing ratio in the chloroform solution used for GUV preparation. The multilamellar liposomes were prepared using the rapid solvent exchange method [22,70], which protects against the demixing of Chol in the form of Chol crystals. Classic electroformation protocols contain steps of the film deposition method (see Section 2). During membrane preparation, using the film deposition method, the lipid mixture passes through the solid-state intermediate at which solid-state demixing of Chol in the form of Chol crystals take place. Chol crystals do not participate in the further membrane formation, resulting in a real membrane Chol content lower than the Chol mixing ratio [27]. This problem in the formation of GUVs could be solved by replacing the organic solutions of lipids with aqueous suspensions of compositionally uniform liposomes formed using the rapid solvent exchange method [22,110,111]. These liposome suspensions can then be used to form damp lipid films for electroformation. Baykal-Caglar et al. tested this approach, but only for liposome suspensions with lower Chol concentrations (up to ~40 mol%) [29]. We think that this approach can be extended to higher Chol contents reaching Chol saturation limits and Chol solubility thresholds.

Author Contributions: Z.B., conceptualization, investigation, writing—original draft preparation, writing—review and editing, visualization; I.M., investigation, writing—review and editing; W.K.S., writing—review and editing; M.R., writing—review and editing, project administration, funding acquisition. All authors have read and agreed to the published version of the manuscript.

Funding: Research reported in this publication was supported by the Croatian Science Foundation (Croatia) under Grant [IP-2019-04-1958].

Institutional Review Board Statement: Not applicable.

Data Availability Statement: Not applicable.

Conflicts of Interest: The authors declare no conflict of interest.

References

1. Menger, F.M.; Angelova, M.I. Giant vesicles: Imitating the cytological processes of cell membranes. *Acc. Chem. Res.* **1998**, *31*, 789–797. [CrossRef]
2. Veatch, S.L.; Keller, S.L. Organization in lipid membranes containing cholesterol. *Phys. Rev. Lett.* **2002**, *89*, 268101. [CrossRef]
3. Reeves, J.P.; Dowben, R.M. Formation and properties of thin-walled phospholipid vesicles. *J. Cell. Physiol.* **1969**, *73*, 49–60. [CrossRef]
4. Pott, T.; Bouvrais, H.; Méléard, P. Giant unilamellar vesicle formation under physiologically relevant conditions. *Chem. Phys. Lipids* **2008**, *154*, 115–119. [CrossRef]
5. Valkenier, H.; López Mora, N.; Kros, A.; Davis, A.P. Visualization and quantification of transmembrane ion transport into giant unilamellar vesicles. *Angew. Chemie Int. Ed.* **2015**, *54*, 2137–2141. [CrossRef] [PubMed]
6. Subczynski, W.; Raguz, M.; Widomska, J. Studying lipid organization in biological membranes using liposomes and EPR spin labeling. *Methods Mol. Biol.* **2010**, *606*, 247–269. [CrossRef]
7. Zylberberg, C.; Matosevic, S. Pharmaceutical liposomal drug delivery: A review of new delivery systems and a look at the regulatory landscape. *Drug Deliv.* **2016**, *23*, 3319–3329. [CrossRef]
8. Sercombe, L.; Veerati, T.; Moheimani, F.; Wu, S.Y.; Sood, A.K.; Hua, S. Advances and Challenges of Liposome Assisted Drug Delivery. *Front. Pharmacol.* **2015**, *6*, 286. [CrossRef]
9. Akbarzadeh, A.; Rezaei-Sadabady, R.; Davaran, S.; Joo, S.W.; Zarghami, N.; Hanifehpour, Y.; Samiei, M.; Kouhi, M.; Nejati-Koshki, K. Liposome: Classification, preparation, and applications. *Nanoscale Res. Lett.* **2013**, *8*, 102. [CrossRef] [PubMed]
10. Veatch, S.L. Electro-formation and fluorescence microscopy of giant vesicles with coexisting liquid phases. *Methods Mol. Biol.* **2007**, *398*, 59–72. [CrossRef] [PubMed]
11. Morales-Penningston, N.F.; Wu, J.; Farkas, E.R.; Goh, S.L.; Konyakhina, T.M.; Zheng, J.Y.; Webb, W.W.; Feigenson, G.W. GUV preparation and imaging: Minimizing artifacts. *Biochim. Biophys. Acta-Biomembr.* **2010**, *1798*, 1324–1332. [CrossRef]

12. Stein, H.; Spindler, S.; Bonakdar, N.; Wang, C. Production of Isolated Giant Unilamellar Vesicles under High Salt Concentrations. *Front. Physiol.* **2017**, *8*, 1–16. [CrossRef]
13. Has, C.; Sunthar, P. A comprehensive review on recent preparation techniques of liposomes. *J. Liposome Res.* **2019**, *0*, 1–30. [CrossRef]
14. Walde, P.; Cosentino, K.; Engel, H.; Stano, P. Giant vesicles: Preparations and applications. *ChemBioChem* **2010**, *11*, 848–865. [CrossRef] [PubMed]
15. Méléard, P.; Bagatolli, L.; Pott, T. Giant unilamellar vesicle electroformation from lipid mixtures to native membranes under physiological conditions. *Methods Enzymol.* **2009**, *465*, 161–176. [CrossRef] [PubMed]
16. Patil, Y.P.; Jadhav, S. Novel methods for liposome preparation. *Chem. Phys. Lipids* **2014**, *177*, 8–18. [CrossRef]
17. Mason, R.P.; Tulenko, T.N.; Jacob, R.F. Direct evidence for cholesterol crystalline domains in biological membranes: Role in human pathobiology. *Biochim. Biophys. Acta-Biomembr.* **2003**, *1610*, 198–207. [CrossRef]
18. Subczynski, W.K.; Pasenkiewicz-Gierula, M. Hypothetical Pathway for Formation of Cholesterol Microcrystals Initiating the Atherosclerotic Process. *Cell Biochem. Biophys.* **2020**, *78*, 241–247. [CrossRef] [PubMed]
19. Mainali, L.; Raguz, M.; O'Brien, W.J.; Subczynski, W.K. Properties of membranes derived from the total lipids extracted from clear and cataractous lenses of 61–70-year-old human donors. *Eur. Biophys. J.* **2014**, *44*, 91–102. [CrossRef]
20. Raguz, M.; Kumar, S.N.; Zareba, M.; Ilic, N.; Mainali, L.; Subczynski, W.K. Confocal Microscopy Confirmed that in Phosphatidylcholine Giant Unilamellar Vesicles with very High Cholesterol Content Pure Cholesterol Bilayer Domains Form. *Cell Biochem. Biophys.* **2019**, *77*, 309–317. [CrossRef]
21. Subczynski, W.K.; Raguz, M.; Widomska, J.; Mainali, L.; Konovalov, A. Functions of cholesterol and the cholesterol bilayer domain specific to the fiber-cell plasma membrane of the eye lens. *J. Membr. Biol.* **2012**, *245*, 51–68. [CrossRef] [PubMed]
22. Mainali, L.; Raguz, M.; Subczynski, W.K. Formation of cholesterol bilayer domains precedes formation of cholesterol crystals in cholesterol/dimyristoylphosphatidylcholine membranes: EPR and DSC studies. *J. Phys. Chem. B* **2013**, *117*, 8994–9003. [CrossRef]
23. Mainali, L.; Raguz, M.; O'Brien, W.J.; Subczynski, W.K. Properties of membranes derived from the total lipids extracted from the human lens cortex and nucleus. *Biochim. Biophys. Acta-Biomembr.* **2013**, *1828*, 1432–1440. [CrossRef] [PubMed]
24. Subczynski, W.K.; Mainali, L.; Raguz, M.; O'Brien, W.J. Organization of lipids in fiber-cell plasma membranes of the eye lens. *Exp. Eye Res.* **2017**, *156*, 79–86. [CrossRef] [PubMed]
25. Widomska, J.; Subczynski, W.K.; Mainali, L.; Raguz, M. Cholesterol Bilayer Domains in the Eye Lens Health: A Review. *Cell Biochem. Biophys.* **2017**, *75*, 387–398. [CrossRef]
26. Subczynski, W.K.; Pasenkiewicz-Gierula, M.; Widomska, J.; Mainali, L.; Raguz, M. High Cholesterol/Low Cholesterol: Effects in Biological Membranes Review. *Cell Biochem. Biophys.* **2017**, *75*, 369–385. [CrossRef] [PubMed]
27. Huang, J.; Buboltz, J.T.; Feigenson, G.W. Maximum solubility of cholesterol in phosphatidylcholine and phosphatidylethanolamine bilayers. *Biochim. Biophys. Acta-Biomembr.* **1999**, *1417*, 89–100. [CrossRef]
28. Boban, Z.; Puljas, A.; Kovač, D.; Subczynski, W.K.; Raguz, M. Effect of Electrical Parameters and Cholesterol Concentration on Giant Unilamellar Vesicles Electroformation. *Cell Biochem. Biophys.* **2020**, *78*, 157–164. [CrossRef] [PubMed]
29. Baykal-Caglar, E.; Hassan-Zadeh, E.; Saremi, B.; Huang, J. Preparation of giant unilamellar vesicles from damp lipid film for better lipid compositional uniformity. *Biochim. Biophys. Acta-Biomembr.* **2012**, *1818*, 2598–2604. [CrossRef] [PubMed]
30. Rodriguez, N.; Pincet, F.; Cribier, S. Giant vesicles formed by gentle hydration and electroformation: A comparison by fluorescence microscopy. *Colloids Surf. B Biointerfaces* **2005**, *42*, 125–130. [CrossRef]
31. Angelova, M.I.; Dimitrov, D.S. Liposome electroformation. *Faraday Discuss. Chem. Soc.* **1986**, *81*, 303–311. [CrossRef]
32. Dimitrov, D.S.; Angelova, M.I. Lipid swelling and liposome formation on solid surfaces in external electric fields. In *New Trends in Colloid Science*; Springer: Berlin/Heidelberg, Germany, 1987; pp. 48–56.
33. Has, C.; Pan, S. Vesicle formation mechanisms: An overview. *J. Liposome Res.* **2020**, *31*, 90–111. [CrossRef]
34. Li, W.; Wang, Q.; Yang, Z.; Wang, W.; Cao, Y.; Hu, N.; Luo, H.; Liao, Y.; Yang, J. Impacts of electrical parameters on the electroformation of giant vesicles on ITO glass chips. *Colloids Surf. B Biointerfaces* **2016**, *140*, 560–566. [CrossRef]
35. Li, Q.; Wang, X.; Ma, S.; Zhang, Y.; Han, X. Electroformation of giant unilamellar vesicles in saline solution. *Colloids Surf. B Biointerfaces* **2016**, *147*, 368–375. [CrossRef]
36. Angelova, M.; Dimitrov, D.S. A mechanism of liposome electroformation. In *Trends in Colloid and Interface Science II*; Springer: Berlin/Heidelberg, Germany, 1988; pp. 59–67.
37. Herold, C.; Chwastek, G.; Schwille, P.; Petrov, E.P. Efficient electroformation of supergiant unilamellar vesicles containing cationic lipids on ITO-coated electrodes. *Langmuir* **2012**, *28*, 5518–5521. [CrossRef]
38. Drabik, D.; Doskocz, J.; Przybyło, M. Effects of electroformation protocol parameters on quality of homogeneous GUV populations. *Chem. Phys. Lipids* **2018**, *212*, 88–95. [CrossRef]
39. Pereno, V.; Carugo, D.; Bau, L.; Sezgin, E.; Bernardino De La Serna, J.; Eggeling, C.; Stride, E. Electroformation of Giant Unilamellar Vesicles on Stainless Steel Electrodes. *ACS Omega* **2017**, *2*, 994–1002. [CrossRef] [PubMed]
40. Behuria, H.G.; Biswal, B.K.; Sahu, S.K. Electroformation of liposomes and phytosomes using copper electrode. *J. Liposome Res.* **2021**, *31*, 255–266. [CrossRef] [PubMed]
41. Ayuyan, A.G.; Cohen, F.S. Lipid peroxides promote large rafts: Effects of excitation of probes in fluorescence microscopy and electrochemical reactions during vesicle formation. *Biophys. J.* **2006**, *91*, 2172–2183. [CrossRef]

42. Zhou, Y.; Berry, C.K.; Storer, P.A.; Raphael, R.M. Peroxidation of polyunsaturated phosphatidyl-choline lipids during electroformation. *Biomaterials* **2007**, *28*, 1298–1306. [CrossRef] [PubMed]
43. Farkas, E.R.; Webb, W.W. Multiphoton polarization imaging of steady-state molecular order in ternary lipid vesicles for the purpose of lipid phase assignment. *J. Phys. Chem. B* **2010**, *114*, 15512–15522. [CrossRef]
44. Okumura, Y.; Sugiyama, T. Electroformation of Giant Vesicles on a Polymer Mesh. *Membranes* **2011**, *1*, 184–194. [CrossRef] [PubMed]
45. Okumura, Y.; Zhang, H.; Sugiyama, T.; Iwata, Y. Electroformation of giant vesicles on a non-electroconductive substrate. *J. Am. Chem. Soc.* **2007**, *129*, 1490–1491. [CrossRef] [PubMed]
46. Lefrançois, P.; Goudeau, B.; Arbault, S. Electroformation of phospholipid giant unilamellar vesicles in physiological phosphate buffer. *Integr. Biol.* **2018**, *10*, 429–434. [CrossRef]
47. Bi, H.; Yang, B.; Wang, L.; Cao, W.; Han, X. Electroformation of giant unilamellar vesicles using interdigitated ITO electrodes. *J. Mater. Chem. A* **2013**, *1*, 7125–7130. [CrossRef]
48. Zhao, J.; Wu, J.; Shao, H.; Kong, F.; Jain, N.; Hunt, G.; Feigenson, G. Phase studies of model biomembranes: Macroscopic coexistence of Lα + Lβ, with light-induced coexistence of Lα + Lo Phases. *Biochim. Biophys. Acta-Biomembr.* **2007**, *1768*, 2777–2786. [CrossRef]
49. Witkowska, A.; Jablonski, L.; Jahn, R. A convenient protocol for generating giant unilamellar vesicles containing SNARE proteins using electroformation. *Sci. Rep.* **2018**, *8*, 9422. [CrossRef]
50. Estes, D.J.; Mayer, M. Electroformation of giant liposomes from spin-coated films of lipids. *Colloids Surf. B Biointerfaces* **2005**, *42*, 115–123. [CrossRef]
51. Politano, T.J.; Froude, V.E.; Jing, B.; Zhu, Y. AC-electric field dependent electroformation of giant lipid vesicles. *Colloids Surf. B Biointerfaces* **2010**, *79*, 75–82. [CrossRef]
52. Angelova, M.I.; Soléau, S.; Méléard, P.; Faucon, F.; Bothorel, P. Preparation of giant vesicles by external AC electric fields. Kinetics and applications. In *Trends in Colloid and Interface Science VI*; Springer: Berlin/Heidelberg, Germany, 1992; pp. 127–131.
53. Ghellab, S.E.; Mu, W.; Li, Q.; Han, X. Prediction of the size of electroformed giant unilamellar vesicle using response surface methodology. *Biophys. Chem.* **2019**, *253*, 106217. [CrossRef] [PubMed]
54. Gracià, R.S.; Bezlyepkina, N.; Knorr, R.L.; Lipowsky, R.; Dimova, R. Effect of cholesterol on the rigidity of saturated and unsaturated membranes: Fluctuation and electrodeformation analysis of giant vesicles. *Soft Matter* **2010**, *6*, 1472–1482. [CrossRef]
55. Taylor, P.; Xu, C.; Fletcher, P.D.I.; Paunov, V.N. A novel technique for preparation of monodisperse giant liposomes. *Chem. Commun.* **2003**, *44*, 1732–1733. [CrossRef]
56. Berre, L.; Chen, Y.; Baigl, D. From Convective Assembly to Landau—Levich Deposition of Multilayered Phospholipid Films of Controlled Thickness. *Langmuir* **2009**, 2554–2557. [CrossRef]
57. Bagatolli, L.A.; Parasassi, T.; Gratton, E. Giant phospholipid vesicles: Comparison among the whole lipid sample characteristics using different preparation methods: A two photon fluorescence microscopy study. *Chem. Phys. Lipids* **2000**, *105*, 135–147. [CrossRef]
58. Collins, M.D.; Gordon, S.E. Giant liposome preparation for imaging and patch-clamp electrophysiology. *J. Vis. Exp.* **2013**, *76*, e50227. [CrossRef] [PubMed]
59. Oropeza-Guzman, E.; Riós-Ramírez, M.; Ruiz-Suárez, J.C. Leveraging the Coffee Ring Effect for a Defect-Free Electroformation of Giant Unilamellar Vesicles. *Langmuir* **2019**, *35*, 16528–16535. [CrossRef]
60. Bhatia, T.; Husen, P.; Brewer, J.; Bagatolli, L.A.; Hansen, P.L.; Ipsen, J.H.; Mouritsen, O.G. Preparing giant unilamellar vesicles (GUVs) of complex lipid mixtures on demand: Mixing small unilamellar vesicles of compositionally heterogeneous mixtures. *Biochim. Biophys. Acta-Biomembr.* **2015**, *1848*, 3175–3180. [CrossRef]
61. Girard, P.; Pécréaux, J.; Lenoir, G.; Falson, P.; Rigaud, J.L.; Bassereau, P. A new method for the reconstitution of membrane proteins into giant unilamellar vesicles. *Biophys. J.* **2004**, *87*, 419–429. [CrossRef] [PubMed]
62. Miele, Y.; Mingotaud, A.F.; Caruso, E.; Malacarne, M.C.; Izzo, L.; Lonetti, B.; Rossi, F. Hybrid giant lipid vesicles incorporating a PMMA-based copolymer. *Biochim. Biophys. Acta-Gen. Subj.* **2021**, *1865*, 129611. [CrossRef]
63. Magnani, C.; Mpntis, C.; Mangiapia, G.; Mingotaud, A.F.; Mingotaud, C.; Roux, C.; Joseph, P.; Berti, D.; Lonetti, B. Hybrid vesicles from lipids and block copolymers: Phase behavior from the micro- to the nano-scale. *Colloids Surf. B Biointerfaces* **2018**, *168*, 18–28. [CrossRef] [PubMed]
64. Nam, J.; Beales, P.A.; Vanderlick, T.K. Giant Phospholipid/Block Copolymer Hybrid Vesicles: Mixing Behavior and Domain Formation. *Langmuir* **2010**, *27*, 1–6. [CrossRef]
65. Le Meins, J.F.; Schatz, C.; Lecommandoux, S.; Sandre, O. Hybrid polymer/lipid vesicles: State of the art and future perspectives. *Mater. Today* **2013**, *16*, 397–402. [CrossRef]
66. Van Meer, G.; Voelker, D.R.; Feigenson, G.W. Membrane lipids: Where they are and how they behave. *Nat. Rev. Mol. Cell Biol.* **2008**, *9*, 112–124. [CrossRef]
67. Stevens, M.M.; Honerkamp-Smith, A.R.; Keller, S.L. Solubility limits of cholesterol, lanosterol, ergosterol, stigmasterol, and β-sitosterol in electroformed lipid vesicles. *Soft Matter* **2010**, *6*, 5882–5890. [CrossRef] [PubMed]
68. Li, L.-K.; So, L.; Spector, A. Membrane cholesterol and phospholipid in consecutive concentric sections of human lenses. *J. Lipid Res.* **1985**, *26*, 600–609. [CrossRef]

69. Li, L.K.; So, L. Age dependent lipid and protein changes in individual bovine lenses. *Curr. Eye Res.* **1987**, *6*, 599–605. [CrossRef] [PubMed]
70. Mainali, L.; Pasenkiewicz-Gierula, M.; Subczynski, W.K. Formation of cholesterol Bilayer Domains Precedes Formation of Cholesterol Crystals in Membranes Made of the Major Phospholipids of Human Eye Lens Fiber Cell Plasma Membranes. *Curr. Eye Res.* **2020**, *45*, 162–172. [CrossRef]
71. Kusumi, A.; Fujiwara, T.K.; Tsunoyama, T.A.; Kasai, R.S.; Koichiro, A.L.; Masanao, M.H.; Matsumori, N.; Komura, N.; Ando, H.; Suzuki, K.G.N. Defining raft domains in the plasma membrane. *Traffic* **2020**, *21*, 106–137. [CrossRef]
72. Dimova, R.; Aranda, S.; Bezlyepkina, N.; Nikolov, V.; Riske, K.A.; Lipowsky, R. A practical guide to giant vesicles. Probing the membrane nanoregime via optical microscopy. *J. Phys. Condens. Matter* **2006**, *18*, 1151–1176. [CrossRef]
73. Wang, Q.; Li, W.; Hu, N.; Chen, X.; Fan, T.; Wang, Z.; Yang, Z.; Cheney, M.A.; Yang, J. Biointerfaces Ion concentration effect (Na+ and Cl−) on lipid vesicle formation. *Colloids Surf. B Biointerfaces* **2017**, *155*, 287–293. [CrossRef] [PubMed]
74. Jiang, L.; Wang, Q.; Lei, J.; Tao, K.; Huang, J.; Zhao, S.; Hu, N.; Yang, J. Mechanism study of how lipid vesicle electroformation is suppressed by the presence of sodium chloride. *Colloids Surf. B Biointerfaces* **2021**, *206*, 111951. [CrossRef]
75. Estes, D.J.; Mayer, M. Giant liposomes in physiological buffer using electroformation in a flow chamber. *Biochim. Biophys. Acta-Biomembr.* **2005**, *1712*, 152–160. [CrossRef] [PubMed]
76. Montes, L.-R.; Alonso, A.; Goni, F.M.; Bagatolli, L.A. Giant unilamellar vesicles electroformed from native membranes and organic lipid mixtures under physiological conditions. *Biophys. J.* **2007**, *93*, 3548–3554. [CrossRef]
77. Hristova, N.I.; Angelova, M.I.; Tsoneva, I. An experimental approach for direct observation of the interaction of polyanions with sphingosine-containing giant vesicles. *Bioelectrochemistry* **2002**, *58*, 65–73. [CrossRef]
78. Bucher, P.; Fischer, A.; Luisi, P.L.; Oberholzer, T.; Walde, P. Giant vesicles as biochemical compartments: The use of microinjection techniques. *Langmuir* **1998**, *14*, 2712–2721. [CrossRef]
79. Wang, Q.; Hu, N.; Lei, J.; Qing, Q.; Huang, J.; Tao, K.; Zhao, S.; Sun, K.; Yang, J. Formation of Giant Lipid Vesicles in the Presence of Nonelectrolytes—Glucose, Sucrose, Sorbitol and Ethanol. *Processes* **2021**, *9*, 945. [CrossRef]
80. Grit, M.; Zuidam, N.J.; Underberg, W.J.M.; Crommelin, D.J.A. Hydrolysis of Partially Saturated Egg Phosphatidylcholine in Aqueous Liposome Dispersions and the Effect of Cholesterol Incorporation on Hydrolysis Kinetics. *J. Pharm. Pharmacol.* **1993**, *45*, 490–495. [CrossRef]
81. Veatch, S.L.; Keller, S.L. Separation of Liquid Phases in Giant Vesicles of Ternary Mixtures of Phospholipids and Cholesterol. *Biophys. J.* **2003**, *85*, 3074–3083. [CrossRef]
82. Juhasz, J.; Davis, J.H.; Sharom, F.J. Biochimica et Biophysica Acta Fluorescent probe partitioning in GUVs of binary phospholipid mixtures: Implications for interpreting phase behavior. *Biochim. Biophys. Acta-Biomembr.* **2012**, *1818*, 19–26. [CrossRef]
83. Betaneli, V.; Worch, R.; Schwille, P. Effect of temperature on the formation of liquid phase-separating giant unilamellar vesicles (GUV). *Chem. Phys. Lipids* **2012**, *165*, 630–637. [CrossRef]
84. Hossain, R.; Adamiak, K. Dynamic properties of the electric double layer in electrolytes. *J. Electrostat.* **2013**, *71*, 829–838. [CrossRef]
85. Breton, M.; Amirkavei, M.; Mir, L.M. Optimization of the Electroformation of Giant Unilamellar Vesicles (GUVs) with Unsaturated Phospholipids. *J. Membr. Biol.* **2015**, *248*, 827–835. [CrossRef]
86. Shimanouchi, T.; Umakoshi, H.; Kuboi, R. Kinetic Study on Giant Vesicle Formation with Electroformation Method. *Langmuir* **2009**, *25*, 4835–4840. [CrossRef] [PubMed]
87. Jørgensen, K.; Mouritsen, O.G. Phase separation dynamics and lateral organization of two-component lipid membranes. *Biophys. J.* **1995**, *69*, 942–954. [CrossRef]
88. De Almeida, R.F.M.; Loura, L.M.S.; Fedorov, A.; Prieto, M. Nonequilibrium Phenomena in the Phase Separation of a Two-Component Lipid Bilayer. *Biophys. J.* **2002**, *82*, 823–834. [CrossRef]
89. Cuevas, E.; Zaldivar, D.; Pérez-Cisneros, M.; Ramírez-Ortegón, M. Circle detection using discrete differential evolution optimization. *Pattern Anal. Appl.* **2011**, *14*, 93–107. [CrossRef]
90. Zupanc, J.; Drobne, D.; Ster, B. Markov random field model for segmenting large populations of lipid vesicles from micrographs. *J. Liposome Res.* **2011**, *21*, 315–323. [CrossRef]
91. Hermann, E.; Bleicken, S.; Subburaj, Y.; García-Sáez, A.J. Automated analysis of giant unilamellar vesicles using circular Hough transformation. *Bioinformatics* **2014**, *30*, 1747–1754. [CrossRef]
92. Schneider, C.A.; Rasband, W.S.; Eliceiri, K.W. NIH Image to ImageJ: 25 years of image analysis. *Nat. Methods* **2012**, *9*, 671–675. [CrossRef]
93. Witkowska, A. Guv Membrane Linearization Macro. Available online: https://zenodo.org/record/376618 (accessed on 14 January 2021).
94. Witkowska, A. Macro for Quantification of GUV Diameter, Membrane Fluorescence Intensity, and FRET. Available online: https://zenodo.org/record/1249321 (accessed on 14 January 2021).
95. Sych, T.; Schubert, T.; Vauchelles, R.; Madl, J.; Omidvar, R.; Thuenauer, R.; Richert, L.; Mély, Y.; Römer, W. GUV-AP: Multifunctional Fiji-based tool for quantitative image analysis of Giant Unilamellar Vesicles. *Bioinformatics* **2019**, *35*, 2340–2342. [CrossRef]
96. Carvalho, K.; Ramos, L.; Roy, C.; Picart, C. Giant Unilamellar Vesicles Containing Phosphatidylinositol(4,5)bisphosphate: Characterization and Functionality. *Biophys. J.* **2008**, *95*, 4348. [CrossRef] [PubMed]

97. Husen, P.; Arriaga, L.R.; Monroy, F.; Ipsen, J.H.; Bagatolli, L.A. Morphometric image analysis of giant vesicles: A new tool for quantitative thermodynamics studies of phase separation in lipid membranes. *Biophys. J.* **2012**, *103*, 2304–2310. [CrossRef]
98. Sendra, G.H.; Hoerth, C.H.; Wunder, C.; Lorenz, H. 2D map projections for visualization and quantitative analysis of 3D fluorescence micrographs. *Sci. Rep.* **2015**, *5*, 12457. [CrossRef]
99. Vorauer-Uhl, K.; Wagner, A.; Borth, N.; Katinger, H. Determination of liposome size distribution by flow cytometry. *Cytometry* **2000**, *39*, 166–171. [CrossRef]
100. Simonsen, J.B. A liposome-based size calibration method for measuring microvesicles by flow cytometry. *J. Thromb. Haemost.* **2016**, *14*, 186–190. [CrossRef]
101. Sato, K.; Obinata, K.; Sugawara, T.; Urabe, I.; Yomo, T. Quantification of structural properties of cell-sized individual liposomes by flow cytometry. *J. Biosci. Bioeng.* **2006**, *3*, 171–178. [CrossRef] [PubMed]
102. Hema Sagar, G.; Tiwari, M.D.; Bellare, J.R. Flow cytometry as a novel tool to evaluate and separate vesicles using characteristic scatter signatures. *J. Phys. Chem. B* **2010**, *114*, 10010–10016. [CrossRef] [PubMed]
103. Matsushita-Ishiodori, Y.; Hanczyc, M.M.; Wang, A.; Szostak, J.W.; Yomo, T. Using imaging flow cytometry to quantify and optimize giant vesicle production by water-in-oil emulsion transfer methods. *Langmuir* **2019**, *35*, 2375–2382. [CrossRef]
104. Nishimura, K.; Hosoi, T.; Sunami, T.; Toyota, T.; Fujinami, M.; Oguma, K.; Matsuura, T.; Suzuki, H.; Yomo, T. Population analysis of structural properties of giant liposomes by flow cytometry. *Langmuir* **2009**, *25*, 10439–10443. [CrossRef]
105. van der Pol, E.; Coumans, F.A.W.; Grootemaat, A.E.; Gardiner, C.; Sargent, I.L.; Harrison, P.; Sturk, A.; van Leeuwen, T.G.; Nieuwland, R. Particle size distribution of exosomes and microvesicles determined by transmission electron microscopy, flow cytometry, nanoparticle tracking analysis, and resistive pulse sensing. *J. Thromb. Haemost.* **2014**, *12*, 1182–1192. [CrossRef]
106. Hoffman, R.A. Pulse width for particle sizing. *Curr. Protoc. Cytom.* **2009**, *1*, 1–17. [CrossRef]
107. Kang, K.; Lee, S.B.; Yoo, J.H.; Nho, C.W. Flow cytometric fluorescence pulse width analysis of etoposide-induced nuclear enlargement in HCT116 cells. *Biotechnol. Lett.* **2010**, *32*, 1045–1052. [CrossRef]
108. Vembadi, A.; Menachery, A.; Qasaimeh, M.A. Cell Cytometry: Review and Perspective on Biotechnological Advances. *Front. Bioeng. Biotechnol.* **2019**, *7*, 147. [CrossRef] [PubMed]
109. Parigoris, E.; Dunkelmann, D.L.; Murphy, A.; Wili, N.; Kaech, A.; Dumrese, C.; Jimenez-Rojo, N.; Silvan, U. Facile generation of giant unilamellar vesicles using polyacrylamide gels. *Sci. Rep.* **2020**, *10*, 1–10. [CrossRef]
110. Buboltz, J.T.; Feigenson, G.W. A novel strategy for the preparation of liposomes: Rapid solvent exchange. *Biochim. Biophys. Acta-Biomembr.* **1999**, *1417*, 232–245. [CrossRef]
111. Buboltz, J.T. A more efficient device for preparing model-membrane liposomes by the rapid solvent exchange method. *Rev. Sci. Instrum.* **2009**, *80*, 124301. [CrossRef] [PubMed]

6 OPTIMIZATION OF GIANT UNILAMELLAR VESICLE ELECTROFORMATION FOR PHOSPHATIDYLCHOLINE/ SPHINGOMYELIN/CHOLESTEROL TERNARY MIXTURES

Reproduced from Boban, Z.; Mardešić, I.; Subczynski, W.K.; Jozić, D.; Raguz, M. Optimization of Giant Unilamellar Vesicle Electroformation for Phosphatidylcholine/Sphingomyelin/ Cholesterol Ternary Mixtures. Membranes (Basel). 2022, 12, 525, doi:10.3390/membranes12050525.

membranes

MDPI

Article

Optimization of Giant Unilamellar Vesicle Electroformation for Phosphatidylcholine/Sphingomyelin/Cholesterol Ternary Mixtures

Zvonimir Boban [1,2], Ivan Mardešić [1,2], Witold Karol Subczynski [3], Dražan Jozić [4] and Marija Raguz [1,*]

[1] Department of Medical Physics and Biophysics, University of Split School of Medicine, 21000 Split, Croatia; zvonimir.boban@mefst.hr (Z.B.); imardesi@mefst.hr (I.M.)
[2] Faculty of Science, University of Split, Doctoral Study of Biophysics, 21000 Split, Croatia
[3] Department of Biophysics, Medical College of Wisconsin, Milwaukee, WI 53226, USA; subczyn@mcw.edu
[4] Faculty of Chemistry and Technology, University of Split, 21000 Split, Croatia; jozicd@ktf-split.hr
* Correspondence: marija.raguz@mefst.hr; Tel.: +385-9876-8819

Abstract: Artificial vesicles are important tools in membrane research because they enable studying membrane properties in controlled conditions. Giant unilamellar vesicles (GUVs) are specially interesting due to their similarity in size to eukaryotic cells. We focus on optimization of GUV production from phosphatidylcholine/sphingomyelin/cholesterol mixtures using the electroformation method. This mixture has been extensively researched lately due to its relevance for the formation of lipid rafts. We measured the effect of voltage, frequency, lipid film thickness, and cholesterol (Chol) concentration on electroformation successfulness using spin-coating for reproducible lipid film deposition. Special attention is given to the effect of Chol concentrations above the phospholipid bilayer saturation threshold. Such high concentrations are of interest to groups studying the role of Chol in the fiber cell plasma membranes of the eye lens or development of atherosclerosis. Utilizing atomic force and fluorescence microscopy, we found the optimal lipid film thickness to be around 30 nm, and the best frequency–voltage combinations in the range of 2–6 V and 10–100 Hz. Increasing the Chol content, we observed a decrease in GUV yield and size. However, the effect was much less pronounced when the optimal lipid film thickness was used. The results underline the need for simultaneous optimization of both electrical parameters and thickness in order to produce high-quality GUVs for experimental research.

Keywords: GUVs; electroformation; cholesterol; sphingomyelin; phosphatidylcholine; film thickness; frequency; voltage; AFM

Citation: Boban, Z.; Mardešić, I.; Subczynski, W.K.; Jozić, D.; Raguz, M. Optimization of Giant Unilamellar Vesicle Electroformation for Phosphatidylcholine/Sphingomyelin/Cholesterol Ternary Mixtures. *Membranes* **2022**, *12*, 525. https://doi.org/10.3390/membranes12050525

Academic Editor: Katia Cortese

Received: 5 April 2022
Accepted: 13 May 2022
Published: 16 May 2022

1. Introduction

Membrane bilayers are crucial for the proper functioning of biological cells. However, due to their complexity, it is often hard to evaluate a specific property while controlling for all other properties that also might influence the measurement. This is why many studies concerned with specific membrane properties use artificial vesicles. Giant unilamellar vesicles (GUVs) are of special importance since their size in the range of 5–100 μm is comparable to the size of eukaryotic cells. Additionally, this size range is optimal for studies utilizing light microscopy.

The most commonly used method for growth of GUVs is electroformation. It was developed by Angelova and Dimitrov in 1986 [1] and has constantly been perfected and updated since. The method consists of depositing a lipid mixture of choice on a conductive substrate. The dried film is then hydrated, and an alternating current applied to detach the lipid film from the surface and form GUVs. Although quite simple at first glance, the method is influenced by many parameters, requiring optimization depending on the experimental setup [2]. We focus on the effect of lipid composition, lipid film thickness,

and electrical parameters (frequency and voltage) using a ternary mixture of 1-palmitoyl-2-oleoyl-glycero-3-phosphocholine/sphingomyelin/cholesterol (POPC/SM/Chol) (Figure 1). This mixture was chosen since these three type of lipids are the most abundant in biological membranes [3–5]. Of special interest currently is the state of liquid order–liquid disorder (Lo–Ld) phase separation which is important for the formation of lipid rafts [6]. Although substantial research has been conducted using GUVs of such compositions, we are aware of no study systematically dealing with optimization of the manufacturing process for those compositions using electroformation.

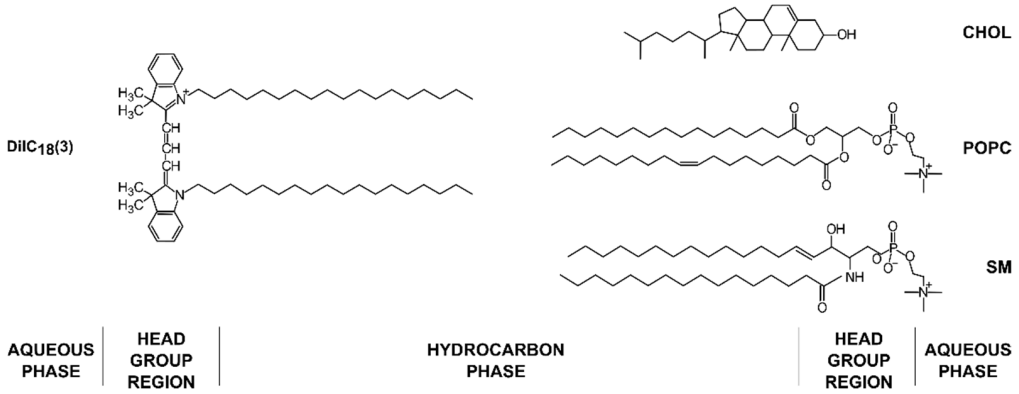

Figure 1. Chemical structures of lipids and the fluorescent dye used in the experiments with their approximate locations in the membrane bilayer.

In addition to frequency and voltage, lipid film thickness is an important electroformation parameter whose importance is often overlooked. Some studies dealing with electroformation optimization focused solely on optimizing the electrical parameters. This limits the usefulness of the results, since lipid film thickness inevitably affects the electric field and consequent membrane fluctuation [7,8]. Consequently, using different lipid thicknesses with the same electrical parameters should provide different results. Additionally, the traditional electroformation protocol uses drop deposition in which the lipids are simply dropped on the surface and the solvent is evaporated afterward. This leaves a lipid film of uneven thickness, reducing the homogeneity of obtained GUVs and reproducibility of the experiment. Several methods have been suggested for achieving reproducible lipid film thicknesses [9–11]. Here, we use the spin-coating method in which lipids are deposited onto the electrode and then spun at a high angular velocity in order to obtain a homogeneous lipid film for electroformation [9].

The effect of different Chol concentrations, including those exceeding its membrane saturation limits, is also explored. Such high Chol concentrations are interesting to researchers investigating the role of Chol in fiber cell plasma membranes of the eye lens [12–17] or the development of atherosclerosis [18,19]. Within the human eye lens, the Chol/phospholipid (Chol/PL) molar ratio is in the range of 1–2 in the lens cortex and 3–4 in the lens nucleus [20,21]. Such high Chol contents are thought to be crucial for maintaining lens transparency by enabling the formation of Chol bilayer domains (CBDs) which ensure that the surrounding phospholipid bilayer is saturated with Chol.

Applying traditional electroformation protocols for production of GUVs from mixtures containing large quantities of Chol leads to Chol demixing artefacts and formation of Chol crystals [13,22,23]. These issues were encountered when we tried to confirm the existence of CBDs in Chol/POPC GUVs using confocal microscopy [13]. We were able to observe CBDs, but only when the Chol/POPC mixing ratio was equal to or greater than 3. This was in contrast with our earlier studies showing that CBDs start to appear at a Chol/PL ratio of 1/1 (50 mol.% Chol) in multilamellar vesicles [15,24]. However, when producing multilamellar vesicles, the rapid solvent exchange method can be used [25,26], which has been shown to be effective at protecting against the Chol demixing artefact. This confirms the significant effect of Chol demixing during the drying phase of the protocol, resulting in

different lipid ratios inside the GUV membranes (molar ratios) compared to the initial ratios in the lipid mixture (mixing ratios). Consequently, in order to cover the Chol concentrations needed for CBD formation, we used mixing ratios of Chol/(POPC + SM) in the range of 0–3.5.

2. Materials and Methods

2.1. Materials

POPC, egg SM, and Chol were obtained from Avanti Polar Lipids Inc. (Alabaster, AL, USA). The fluorescent dye 1,1′-dioctade-cyl-3,3,3′,3′-tetramethylindocarbocyanine Perchlorate ($DiIC_{18}(3)$) (Figure 1) was purchased from Invitrogen, Thermo Fisher Scientific (Waltham, MA, USA). When not used, the lipids were stored at −20 °C. Other chemicals of at least reagent grade were obtained from Sigma-Aldrich (St. Louis, MO, USA). Indium tin oxide-coated glass (ITO, CG-90 INS 115) was purchased from Delta Technologies (Loveland, CO, USA). ITO glass dimensions were 25 mm × 75 mm × 1.1 mm. New ITO glass was used for each preparation in order to prevent coating deterioration [27]. Mili-Q deionized water was used as the internal chamber solution.

2.2. Deposition of the Lipid Film

The spin-coating method was used for lipid film deposition [9]. Prior to spin-coating, the glass was immersed in deionized water for at least 45 min before being wiped four times with 70% ethanol moistened lint-free wipes. Properties of samples with Chol/(POPC + SM) mixing ratios in the range of 0–3.5 were compared (0–77.8 mol.% Chol in the mixture). The POPC/$DiIC_{18}(3)$ molar ratio was always kept at 1/0.002. The POPC/SM mixing ratio is fixed at 1/1. Lipid mixtures were prepared in 95% chloroform and 5% acetonitrile solution [9]. The solution (350 µL) was deposited onto the ITO surface, and a thin lipid layer was created using a Sawatec SM-150 spin-coater (Sawatec, Sax, Switzerland). The glass was spun for 4 min at 600 rpm with the final velocity reached in 1 s. After coating, the lipid film was placed under vacuum for 30 min to evaporate any remaining solvent.

2.3. Electroformation Chamber

The electroformation chamber was made of two 25 mm × 37.5 mm ITO-coated glass electrodes separated by a 1.6 mm thick Teflon spacer (Figure 2). The electrodes were made by cutting a 25 mm × 75 mm ITO glass slide in half using a diamond pen cutter. After spin-coating lipids on one of the electrodes, the chamber was assembled by attaching the spacer to the electrodes using vacuum grease. Upon insertion, the stopper was also sealed with vacuum grease. In this way, contact between the grease and the internal solution was avoided, minimizing the possibility of harmful effects due to grease contamination [28]. Finally, the chamber was attached to a voltage source (UNI-T UTG9005C, Chengdu, China pulse generator or a Joy-IT PSG 9080, Neukirchen-Vluyn, Germany signal generator) and placed inside an incubator at a temperature of 60 °C. In order to assure good contact between the conductor wires and the electrodes, the outer edges of the electrodes were covered with copper tape. After 2 h, the voltage was turned off and the chamber was kept in an incubator for another hour. When examining the effect of Chol concentration on average GUV diameter, electroformation was performed simultaneously on six samples by connecting the chambers in parallel.

2.4. Thickness Measurements

Atomic force microscopy (AFM) images were obtained using a JPK NanoWizard 4 system (JPK/Bruker, Berlin, Germany). Imaging was carried out in tapping mode. The image resolution was 512 pixels per line. Analysis was performed using the Gwyddion 2.60 software. In order to obtain the thicknesses, a cut was made on the lipid film deposited on ITO glass. The depth of the cut was assessed by calculating the height difference between the bottom of the trough and the height of the plateau next to the cut (far away enough from the edge of the cut ensuring that the measurements represent the unperturbed lipid

film). Final thickness was an average obtained from measurements of five height profiles perpendicular to the cut. In order to confirm the flatness of the ITO layer prior to film deposition, we performed AFM measurements on clean ITO slides and found the surface roughness to be in the range of couple nanometers, in accordance with the results presented by Herold et al. [27].

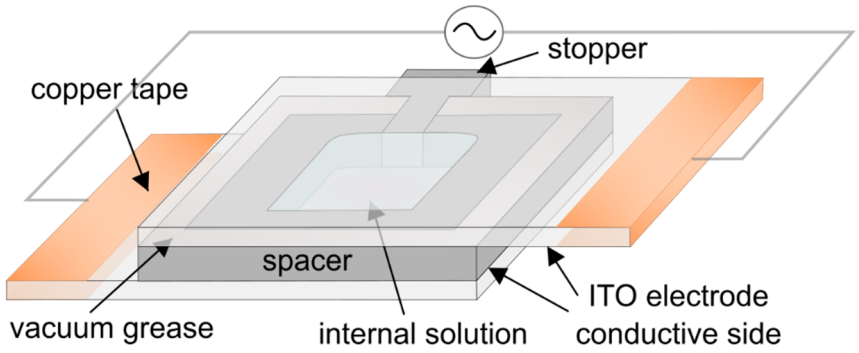

Figure 2. Schematic representation of the electroformation chamber used in the experiments.

The X-ray reflectivity (XRR) experiments were performed using an Empyrean X-ray diffraction system (Malvern PANalytical, Malvern, UK) with a programmable *xy*-platform and *z*-adjustment at the position of the sample holder. The instrument was equipped with a copper X-ray tube (CuKα = 1.541 Å), multicore optics iCore/dCore, and PIXcel3D detector with Medipix-3 technology. The X-ray beam was parallelized using iCore optics and XRR curves were recorded under the following operating conditions: 45 kV anode voltage and 40 mA anode current. Scans were made using an Omega-2Theta scan with a step size of 0.002° and a scanning angle in the range of −0.021° to 6°.

2.5. Fluorescence Imaging

In order to search the entire volume of the chamber, we collected images from 13 regions on the sample. If possible, up to 50 vesicles were tracked from each image. In order to reduce measurer's bias, the computer randomly chose 30 vesicles out of these 50. If the image did not contain 30 vesicles, all of the tracked vesicles from that image were counted. Images were obtained using an Olympus BX51 (Olympus, Tokyo, Japan) fluorescence microscope. Vesicle diameters were measured using the line tool in Fiji software [29].

2.6. Data Analysis

If not stated otherwise, numerical results are expressed as the mean ± standard error. Sample distribution normality was tested using the Shapiro–Wilk test. Difference of means for two groups was tested using Student's *t*-test. Goodness of linear fit was estimated using the coefficient of determination R^2. Data analysis and visualization were performed using the R programming language [30].

3. Results and Discussion

3.1. Effect of Electrical Parameters

In order to determine the optimal electrical parameters, we tested 25 frequency–voltage combinations with frequencies ranging from 1 to 1000 Hz and peak-to-peak voltages ranging from 0.5 to 20 V. A 3.75 mg/mL concentrated POPC/SM/Chol 1/1/1 mixture was used. Such a mixture should create GUVs in the Lo–Ld phase [31], which is important for studies of lipid rafts [6].

Electroformation successfulness was estimated from fluorescence images, taking into account the GUV population homogeneity, yield, and size, as well as the amount of defects. It is denoted in Figure 3 by circles, where a fuller circle indicates better successfulness. Empty circles represent conditions for which GUV formation did not occur or was sporadic.

The results indicate that the best frequency–voltage combinations were in the range of 10–100 Hz and 2–6 V (Figure 3a). For these combinations, the GUVs yield was high with sizes up to ~50 μm (Figure 3b). GUVs formation was observed for other combinations as well, but the successfulness was lower. It can also be noted that, in order to grow GUVs at higher voltages, higher frequencies were required. Such behavior can be explained through the effect of electrical parameters on lipid film fluctuations and lipid oxidation. Too strong electric fields can induce lipid oxidation [32,33] and tear the lipid film off the surface prematurely [34], negatively affecting GUV formation. Lipid film oscillations are important because they are responsible for lipid film bending and separation. These oscillations have been shown to rise with increasing electric fields and decrease with increasing frequencies [7,8,35]. This could explain why an increase in frequency is required in order to create GUVs at higher voltages. Increasing the frequency simultaneously with voltage keeps the oscillations in the optimal interval, ensuring that membrane fluctuations appear, but preventing an overly fast bilayer detachment. Furthermore, decreasing the voltage too much or overly increasing the frequency leads to too small membrane fluctuations, preventing the swelling required for GUV formation [36]. POPC and SM are monounsaturated lipids, and it has been shown that such lipids are not affected strongly by voltage-induced oxidation [33,37]. Consequently, the dominant effect here is probably related to oscillations intensity.

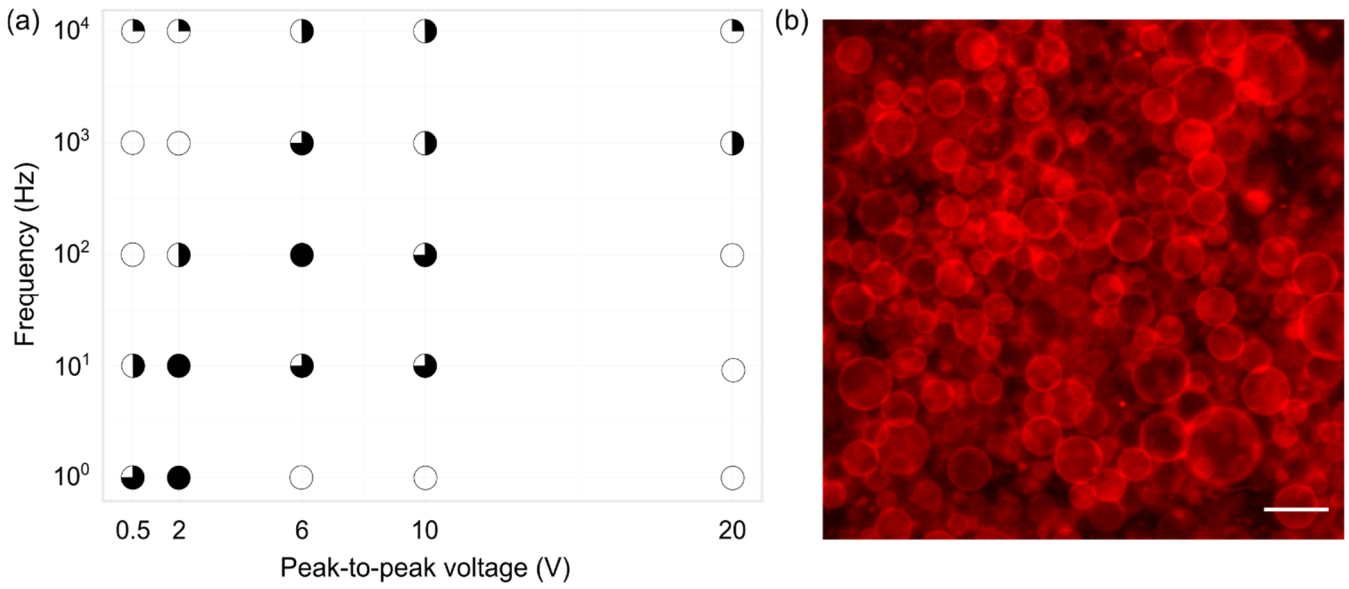

Figure 3. (**a**) Electroformation successfulness dependence on frequency–voltage combinations for a 1/1/1 POPC/SM/Chol mixture and a lipid concentration of 3.75 mg/mL. Successfulness takes into account the population homogeneity, yield, and size of GUVs, as well as the amount of defects. It is displayed here through circle fullness, where a fuller circle indicates better successfulness. Empty circles denote that no GUVs were formed or their number was negligible. (**b**) Fluorescence microscopy image of electroformed GUVs for a 10 Hz–2 V frequency–voltage combination. The scale bar in the bottom right corner denotes 50 μm.

3.2. Effect of Lipid Film Thickness

Along with voltage and frequency, lipid film thickness is also a crucial electroformation parameter, but studies optimizing lipid thickness are scarce. The reason is probably mostly historical, since researchers often use the traditional drop-deposition protocol, in which film thickness can only be crudely estimated from the mass of deposited lipids and the deposition area. Furthermore, both measuring the thickness and using alternative protocols which enable reproducible film deposition require special equipment, again making it harder to

conduct such experiments. Here, we utilized spin-coating [9] in order to test the effect of lipid film thickness on GUV electroformation from a ternary POPC/SM/Chol mixture.

We spin-coated the lipid solutions using four different lipid concentrations: 0.5, 2, 3.75, and 6 mg/mL. Two Chol/(POPC + SM) mixing ratios of 0.5 and 2 were inspected, giving a total of eight different parameter combinations tested. Measurements were performed three times for each different combination.

The lipid surface was imaged using AFM, and thicknesses were determined from height profiles of the cut in the film (Figure 4a). The depth of the cut was assessed from the height profiles by calculating the difference between the bottom of the trough and the height of the plateau next to the cut (Figure 4b). The plateau measurements were taken far away enough from the edge of the cut so we could be certain that the measurements represent the unperturbed lipid film. Obtained thicknesses displayed a linear dependence on lipid concentration for both mixtures (Figure 4c).

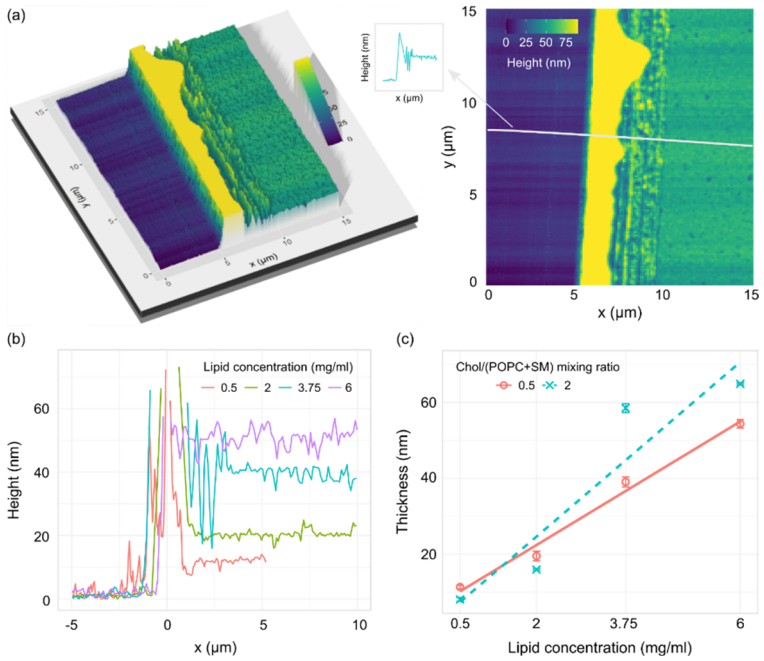

Figure 4. (**a**) 3D (left) and 2D (right) AFM images of a cut on a lipid film made from a 1/1/1 POPC/SM/Chol mixture with a lipid concentration of 3.75 mg/mL. The material buildup on the edge of the trough (yellow hill on the image) is cut off in order to better visualize the rest of the sample. The gray line on the 2D image shows the height profile position. The arrow points to a schematic representation of the height profile used for thickness measurements. (**b**) Representative AFM height profiles for a 1/1/1 POPC/SM/Chol mixture at different lipid concentrations. (**c**) Thickness of the lipid film for two POPC/SM/Chol mixtures depending on the concentration of lipids in the solution used for spin-coating. R^2 = 0.98 and 0.83 for Chol/(POPC + SM) mixing ratios of 0.5 and 2, respectively.

In addition to AFM, we performed XRR measurements for different lipid concentrations at the same Chol/(POPC + SM) mixing ratio (Figure S1). The measurements on uncoated ITO glass yielded thicknesses similar to those stated by the manufacturer (~25 nm) (Figure S1a). Using the XRR method on lipid films gave more than one value of thickness, which suggests some film inhomogeneity over larger scales. However, the results displayed a thickness trend corresponding to that obtained by AFM (Figure S1b).

Figure 5 shows the results of experiments performed using six lipid concentrations and two different Chol/(POPC + SM) mixing ratios. Measurements were repeated three times for every combination. All of the experiments were performed using a frequency–voltage combination of 10 Hz–2 V. At the top of the panels in Figure 5a, the average number of tracked vesicles per sample is displayed. Electroformation successfulness is

displayed at the bottom using the convention explained for Figure 3a. The trend was quite similar for both Chol/(POPC + SM) mixing ratios used. When we tested the lowest concentration of 0.5 mg/mL, practically no vesicles were observed due to a too small thickness of the film (~10 nm). The successfulness improved with increase in the lipid concentration, peaking at 2.75 mg/mL (film thickness ~30 nm) which seemed to be optimal for our mixtures. A decrease in successfulness then appeared as we moved on to the 3.75 and 6 mg/mL concentrations.

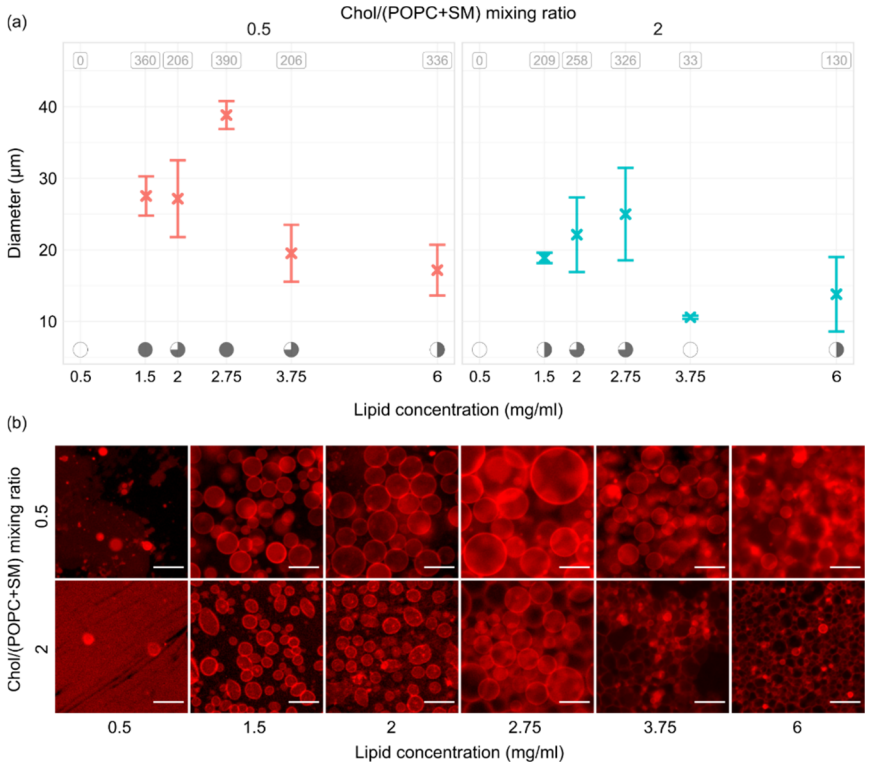

Figure 5. (**a**) GUV size depending on the thickness of the lipid film and Chol/(POPC + SM) mixing ratio. All of the experiments were performed using a frequency–voltage combination of 10 Hz–2 V. At the top of the panels, the average number of tracked vesicles per sample is displayed. Electroformation successfulness is displayed at the bottom of the panels. Successfulness takes into account the yield and size of GUVs and the amount of defects. It is displayed here through circle fullness, where a fuller circle indicates better successfulness. Empty circles denote that no GUVs were formed or electroformation efficiency was very low. (**b**) Representative fluorescence microscopy images for conditions displayed in the panels above. The scale bar in the bottom right of the images denotes 50 µm.

Observing Figure 5b, we can see that using the optimal lipid film thickness not only increases the yield and size of vesicles, but also contributes to a lower amount of defects in the sample. This was especially visible for the mixture with a higher concentration of Chol, where only the 2.75 mg/mL concentration seemed to provide the conditions for growth of dominantly defect-free vesicles.

3.3. Effect of Cholesterol Concentration

In order to see how electroformation results changed with varying Chol content, we inspected Chol/(POPC + SM) mixing ratios in the range of 0–3.5 (0–77.8 mol.%). The Chol/(POPC + SM) mixing ratios were chosen so that, above the mixture transition temperature, GUVs with all possible bilayer phase domains could be grown (Ld, Lo–Ld, Lo, and CBDs). In order to assess the effects of both lipid film thickness and voltage, the experiments were performed for lipid concentrations of 2.75 and 3.75 mg/mL and voltages of 2 and 6 V. A frequency of 10 Hz was used for all experiments, and each parameter

combination was tested three times. All three sets indicated a decrease in electroformation successfulness with increasing Chol content, with decreases in both GUV size and quality (Figure 6a,b). This is in agreement with our previous results using binary POPC/Chol mixtures [38], and it is probably due to large Chol concentrations increasing the rigidity of the lipid bilayer, causing more difficult bending during electroformation. Chol also has a condensing effect on the membrane, leading to smaller phospholipid surface coverage and thicker membranes [39].

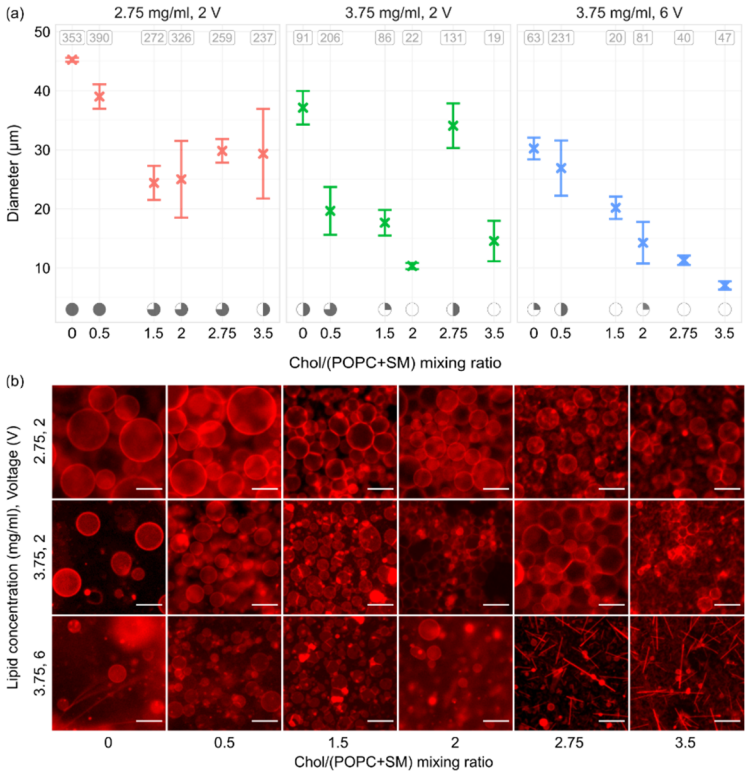

Figure 6. (**a**) GUVs sizes for different Chol concentrations, lipid concentrations (lipid film thicknesses), and voltages. All experiments were performed using a 1/1/1 POPC/SM/Chol mixture and a frequency of 10 Hz. At the top of the panels, the average number of tracked vesicles per sample is displayed. Electroformation successfulness is displayed at the bottom of the panels. Successfulness takes into account the yield and size of GUVs and the amount of defects. It is displayed here through circle fullness, where a fuller circle indicates better successfulness. Empty circles denote that no GUVs were formed or electroformation efficiency was very low. (**b**) Representative fluorescence microscopy images for conditions displayed in the panels above. The scale bar in the bottom right of the images denotes 50 µm.

Interestingly, even though a concentration of 3.75 mg/mL yielded poor results with the POPC/SM/Chol mixture, our earlier experiments using POPC/Chol binary mixtures were quite successful at that concentration [35]. A comparison of thicknesses of 2/1 POPC/Chol and 1/1/1 POPC/SM/Chol mixtures at 3.75 mg/mL showed a slight increase after addition of SM (33.2 ± 0.3 vs. 39 ± 1 nm, respectively, $p = 0.009$). A recent molecular simulation study found that introduction of SM to POPC/Chol bilayers increases hydrocarbon chain order, condenses the bilayer, and reduces water permeability [40]. The effect of SM is, thus, similar to the effect of Chol. Consequently, the decrease in electroformation successfulness when SM is added to the mixture can be explained through the effects of SM on bilayer properties and the difference in lipid film thickness.

In accordance with the results for different film thicknesses, the results for the 2.75 mg/mL concentration were superior to other combinations. The difference was most prominent at higher Chol concentrations, where different combinations showed very poor GUV quality.

Moreover, after the Chol/(POPC + SM) mixing ratio reached 2.75, crystal-like patterns started appearing over the lipid-deposited surface. These probably represent Chol crystals forming due to the Chol demixing artefact (Figure 6b) [13,22,23]. Comparing the results between two different voltages for a lipid concentration of 3.75 mg/mL, we can see that using the optimal electrical parameters of 10 Hz–2 V as determined above did somewhat improve the quality of GUV preparations. However, successfulness for Chol/(POPC + SM) mixing ratios higher than 2 was still unsatisfactory, with low GUV yields and a large amount of defects. The 2.75 mg/mL concentration proved to be superior in this aspect as well, allowing the formation of a large number of GUVs with a much lower amount of defects. These findings show that optimizing the lipid film thickness is at least as important as optimizing the electrical parameters and should be performed for every new mixture used in order to maximize electroformation successfulness.

4. Conclusions

Combining spin-coating with the electroformation method, we investigated the effect of electrical parameters, film thickness, and Chol concentration on GUV production. The best frequency–voltage combinations were in the ranges 2–6 V and 10–100 Hz. Using AFM, we found the optimal film thickness to be approximately 30 nm. This thickness was achieved for a lipid solution concentration of 2.75 mg/mL at 600 rpm. Compared to binary POPC/Chol mixtures, SM seemed to make it harder for GUVs to form. Additionally, increasing the Chol concentration also led to lower-quality GUVs and a larger amount of defects. However, the effect was much less pronounced when the optimal film thickness was used during electroformation. At very high Chol concentrations (above a Chol/(POPC + SM) mixing ratio of 2.75), needle-like shapes started showing up on fluorescence microscopy images of lipid film surfaces. These most likely appeared due to Chol demixing during lipid film drying. Alternative protocols bypassing the dry lipid film state, such as those laid out by Baykal-Caglar et al. [23], could be applied to such mixtures. On the basis of their results for mixtures with lower Chol concentrations, we think that the protocol could be extended to concentrations exceeding the Chol saturation threshold.

In conclusion, the article presented the optimal values of several key electroformation parameters. The results confirm the need to optimize the protocol for every new mixture used and underlines the importance of lipid film thickness in the process.

Supplementary Materials: The following supporting information can be downloaded at https://www.mdpi.com/article/10.3390/membranes12050525/s1: Figure S1: XRR analysis of spin-coated lipid films thicknesses. The right column shows the raw data, and the left one the normalized Fourier transform intensity. (a) Measurements for an ITO sample. (b) Measurements for different lipid concentrations using a Chol/(POPC+SM) mixing ratio of 0.75.

Author Contributions: Z.B., conceptualization, investigation, writing—original draft preparation, writing—review and editing, and visualization; I.M., investigation and writing—review and editing; W.K.S., writing—review and editing; D.J., investigation and writing—review and editing; M.R., conceptualization, writing—review and editing, project administration, and funding acquisition. All authors have read and agreed to the published version of the manuscript.

Funding: Research reported in this publication was supported by the Croatian Science Foundation (Croatia) under Grant IP-2019-04-1958.

Data Availability Statement: The data presented in this study are available upon reasonable request from the corresponding author.

Acknowledgments: We thank Ante Bilušić and Lucija Krce for access to their lab equipment and helpful discussions and comments.

Conflicts of Interest: The authors declare no conflict of interest.

References

1. Angelova, M.I.; Dimitrov, D.S. Liposome Electro formation. *Faraday Discuss. Chem. Soc.* **1986**, *81*, 303–311. [CrossRef]
2. Boban, Z.; Mardešić, I.; Subczynski, W.K.; Raguz, M. Giant Unilamellar Vesicle Electroformation: What to Use, What to Avoid, and How to Quantify the Results. *Membranes* **2021**, *11*, 860. [CrossRef] [PubMed]
3. Watson, H. Biological membranes. *Essays Biochem.* **2015**, *59*, 43–70. [CrossRef]
4. Van Meer, G.; Voelker, D.R.; Feigenson, G.W. Membrane lipids: Where they are and how they behave. *Nat. Rev. Mol. Cell Biol.* **2008**, *9*, 112–124. [CrossRef] [PubMed]
5. Lorent, J.H.; Levental, K.R.; Ganesan, L.; Rivera-Longsworth, G.; Sezgin, E.; Doktorova, M.; Lyman, E.; Levental, I. Plasma membranes are asymmetric in lipid unsaturation, packing and protein shape. *Nat. Chem. Biol.* **2020**, *16*, 644–652. [CrossRef]
6. Kusumi, A.; Fujiwara, T.K.; Tsunoyama, T.A.; Kasai, R.S.; Koichiro, A.L.; Masanao, M.H.; Matsumori, N.; Komura, N.; Ando, H.; Suzuki, K.G.N. Defining raft domains in the plasma membrane. *Traffic* **2020**, *21*, 106–137. [CrossRef]
7. Lecuyer, S.; Fragneto, G.; Charitat, T. Effect of an electric field on a floating lipid bilayer: A neutron reflectivity study. *Eur. Phys. J. E* **2006**, *21*, 153–159. [CrossRef]
8. Li, Q.; Wang, X.; Ma, S.; Zhang, Y.; Han, X. Electroformation of giant unilamellar vesicles in saline solution. *Colloids Surf. B Biointerfaces* **2016**, *147*, 368–375. [CrossRef]
9. Estes, D.J.; Mayer, M. Electroformation of giant liposomes from spin-coated films of lipids. *Colloids Surf. B Biointerfaces* **2005**, *42*, 115–123. [CrossRef]
10. Oropeza-Guzman, E.; Riós-Ramírez, M.; Ruiz-Suárez, J.C. Leveraging the Coffee Ring Effect for a Defect-Free Electroformation of Giant Unilamellar Vesicles. *Langmuir* **2019**, *35*, 16528–16535. [CrossRef]
11. Berre, L.; Chen, Y.; Baigl, D. From Convective Assembly to Landau—Levich Deposition of Multilayered Phospholipid Films of Controlled Thickness. *Langmuir* **2009**, *25*, 2554–2557. [CrossRef]
12. Mainali, L.; Raguz, M.; O'Brien, W.J.; Subczynski, W.K. Properties of membranes derived from the total lipids extracted from clear and cataractous lenses of 61–70-year-old human donors. *Eur. Biophys. J.* **2014**, *44*, 91–102. [CrossRef] [PubMed]
13. Raguz, M.; Kumar, S.N.; Zareba, M.; Ilic, N.; Mainali, L.; Subczynski, W.K. Confocal Microscopy Confirmed that in Phosphatidylcholine Giant Unilamellar Vesicles with very High Cholesterol Content Pure Cholesterol Bilayer Domains Form. *Cell Biochem. Biophys.* **2019**, *77*, 309–317. [CrossRef] [PubMed]
14. Subczynski, W.K.; Raguz, M.; Widomska, J.; Mainali, L.; Konovalov, A. Functions of cholesterol and the cholesterol bilayer domain specific to the fiber-cell plasma membrane of the eye lens. *J. Membr. Biol.* **2012**, *245*, 51–68. [CrossRef] [PubMed]
15. Mainali, L.; Raguz, M.; O'Brien, W.J.; Subczynski, W.K. Properties of membranes derived from the total lipids extracted from the human lens cortex and nucleus. *Biochim. Biophys. Acta-Biomembr.* **2013**, *1828*, 1432–1440. [CrossRef]
16. Subczynski, W.K.; Mainali, L.; Raguz, M.; O'Brien, W.J. Organization of lipids in fiber-cell plasma membranes of the eye lens. *Exp. Eye Res.* **2017**, *156*, 79–86. [CrossRef] [PubMed]
17. Widomska, J.; Subczynski, W.K.; Mainali, L.; Raguz, M. Cholesterol Bilayer Domains in the Eye Lens Health: A Review. *Cell Biochem. Biophys.* **2017**, *75*, 387–398. [CrossRef] [PubMed]
18. Mason, R.P.; Tulenko, T.N.; Jacob, R.F. Direct evidence for cholesterol crystalline domains in biological membranes: Role in human pathobiology. *Biochim. Biophys. Acta-Biomembr.* **2003**, *1610*, 198–207. [CrossRef]
19. Subczynski, W.K.; Pasenkiewicz-Gierula, M. Hypothetical Pathway for Formation of Cholesterol Microcrystals Initiating the Atherosclerotic Process. *Cell Biochem. Biophys.* **2020**, *78*, 241–247. [CrossRef]
20. Li, L.K.; So, L.; Spector, A. Membrane cholesterol and phospholipid in consecutive concentric sections of human lenses. *J. Lipid Res.* **1985**, *26*, 600–609. [CrossRef]
21. Li, L.-K.; So, L.; Spector, A. Age-dependent changes in the distribution and concentration of human lens cholesterol and phospholipids. *Biochim. Biophys. Acta (BBA)-Lipids Lipid Metab.* **1987**, *917*, 112–120. [CrossRef]
22. Huang, J.; Buboltz, J.T.; Feigenson, G.W. Maximum solubility of cholesterol in phosphatidylcholine and phosphatidylethanolamine bilayers. *Biochim. Biophys. Acta (BBA)-Biomembr.* **1999**, *1417*, 89–100. [CrossRef]
23. Baykal-Caglar, E.; Hassan-Zadeh, E.; Saremi, B.; Huang, J. Preparation of giant unilamellar vesicles from damp lipid film for better lipid compositional uniformity. *Biochim. Biophys. Acta-Biomembr.* **2012**, *1818*, 2598–2604. [CrossRef] [PubMed]
24. Mainali, L.; Pasenkiewicz-Gierula, M.; Subczynski, W.K. Formation of cholesterol Bilayer Domains Precedes Formation of Cholesterol Crystals in Membranes Made of the Major Phospholipids of Human Eye Lens Fiber Cell Plasma Membranes. *Curr. Eye Res.* **2020**, *45*, 162–172. [CrossRef]
25. Buboltz, J.T.; Feigenson, G.W. A novel strategy for the preparation of liposomes: Rapid solvent exchange. *Biochim. Biophys. Acta (BBA)-Biomembr.* **1999**, *1417*, 232–245. [CrossRef]
26. Buboltz, J.T. A more efficient device for preparing model-membrane liposomes by the rapid solvent exchange method. *Rev. Sci. Instrum.* **2009**, *80*, 124301. [CrossRef]
27. Herold, C.; Chwastek, G.; Schwille, P.; Petrov, E.P. Efficient electroformation of supergiant unilamellar vesicles containing cationic lipids on ITO-coated electrodes. *Langmuir* **2012**, *28*, 5518–5521. [CrossRef]
28. Veatch, S.L. Electro-formation and fluorescence microscopy of giant vesicles with coexisting liquid phases. *Methods Mol. Biol.* **2007**, *398*, 59–72. [CrossRef]
29. Schindelin, J.; Arganda-Carreras, I.; Frise, E.; Kaynig, V.; Longair, M.; Pietzsch, T.; Preibisch, S.; Rueden, C.; Saalfeld, S.; Schmid, B.; et al. Fiji: An open-source platform for biological-image analysis. *Nat. Methods* **2012**, *9*, 676. [CrossRef]

30. R Development Core Team. *R: A Language and Environment for Statistical Computing*; R Development Core Team: Vienna, Austria, 2008.
31. De Almeida, R.F.M.; Fedorov, A.; Prieto, M. Sphingomyelin/phosphatidylcholine/cholesterol phase diagram: Boundaries and composition of lipid rafts. *Biophys. J.* **2003**, *85*, 2406–2416. [CrossRef]
32. Zhou, Y.; Berry, C.K.; Storer, P.A.; Raphael, R.M. Peroxidation of polyunsaturated phosphatidyl-choline lipids during electroformation. *Biomaterials* **2007**, *28*, 1298–1306. [CrossRef]
33. Breton, M.; Amirkavei, M.; Mir, L.M. Optimization of the Electroformation of Giant Unilamellar Vesicles (GUVs) with Unsaturated Phospholipids. *J. Membr. Biol.* **2015**, *248*, 827–835. [CrossRef]
34. Li, W.; Wang, Q.; Yang, Z.; Wang, W.; Cao, Y.; Hu, N.; Luo, H.; Liao, Y.; Yang, J. Impacts of electrical parameters on the electroformation of giant vesicles on ITO glass chips. *Colloids Surf. B Biointerfaces* **2016**, *140*, 560–566. [CrossRef] [PubMed]
35. Dimitrov, D.S.; Angelova, M.I. Lipid swelling and liposome formation on solid surfaces in external electric fields. In *New Trends in Colloid Science*; Springer: Berlin/Heidelberg, Germany, 1987; pp. 48–56.
36. Politano, T.J.; Froude, V.E.; Jing, B.; Zhu, Y. AC-electric field dependent electroformation of giant lipid vesicles. *Colloids Surf. B Biointerfaces* **2010**, *79*, 75–82. [CrossRef] [PubMed]
37. Drabik, D.; Doskocz, J.; Przybyło, M. Effects of electroformation protocol parameters on quality of homogeneous GUV populations. *Chem. Phys. Lipids* **2018**, *212*, 88–95. [CrossRef] [PubMed]
38. Boban, Z.; Puljas, A.; Kovač, D.; Subczynski, W.K.; Raguz, M. Effect of Electrical Parameters and Cholesterol Concentration on Giant Unilamellar Vesicles Electroformation. *Cell Biochem. Biophys.* **2020**, *78*, 157–164. [CrossRef]
39. Hung, W.-C.; Lee, M.-T.; Chen, F.-Y.; Huang, H.W. The Condensing Effect of Cholesterol in Lipid Bilayers. *Biophys. J.* **2007**, *92*, 3960. [CrossRef]
40. Saeedimasine, M.; Montanino, A.; Kleiven, S.; Villa, A. Role of lipid composition on the structural and mechanical features of axonal membranes: A molecular simulation study. *Sci. Rep.* **2019**, *9*, 8000. [CrossRef]

Supplementary Material

Optimization of Giant Unilamellar Vesicle Electroformation for Phosphatidylcholine/Sphingomyelin/Cholesterol Ternary Mixtures

Zvonimir Boban [1,2], Ivan Mardešić [1,2], Witold Karol Subczynski [3], Dražan Jozić [4] and Marija Raguz [1,*]

[1] Department of Medical Physics and Biophysics, University of Split School of Medicine, Split, Croatia; zvonimir.boban@mefst.hr; ivan.mardesic@mefst.hr; marija.raguz@mefst.hr
[2] University of Split, Faculty of Science, Doctoral study of Biophysics, Split, Croatia
[3] Department of Biophysics, Medical College of Wisconsin, Milwaukee, WI, USA; subczyn@mcw.edu
[4] University of Split, Faculty of Chemistry and Technology, Split, Croatia; jozicd@ktf-split.hr
***Correspondence: marija.raguz@mefst.hr; Tel.: +38598768819**

Figure S1 shows thicknesses obtained using XRR measurements. The right column shows the raw data, and the left one the normalized Fourier transform intensity. Curves for the ITO sample show a dominant peak centered at ~ 25 μm, with an additional smaller peak at ~ 55 μm (Figure S1a).

Figure S1b compares the thicknesses measurements between films made using three different lipid film concentrations and a Chol/(POPC+SM) mixing ratio of 0.75. The results for the 2 mg/ml concentration show an additional hump around 20 μm. This is the dominant peak when we account the ITO signal and its value is in agreement with the AFM measurements. The middle concentration mostly restores the symmetrical shape of the main ITO peak, with a dominant lipid film peak occuring at ~ 35 μm. The highest measured concentration seems to be the least homogenous, but an increase in thickness compared to lower concentrations is evident from the wide peak appearing at ~ 70 μm. The results are in line with the trend of increasing thickness with increasing lipid concentration suggested by the AFM results in the main text.

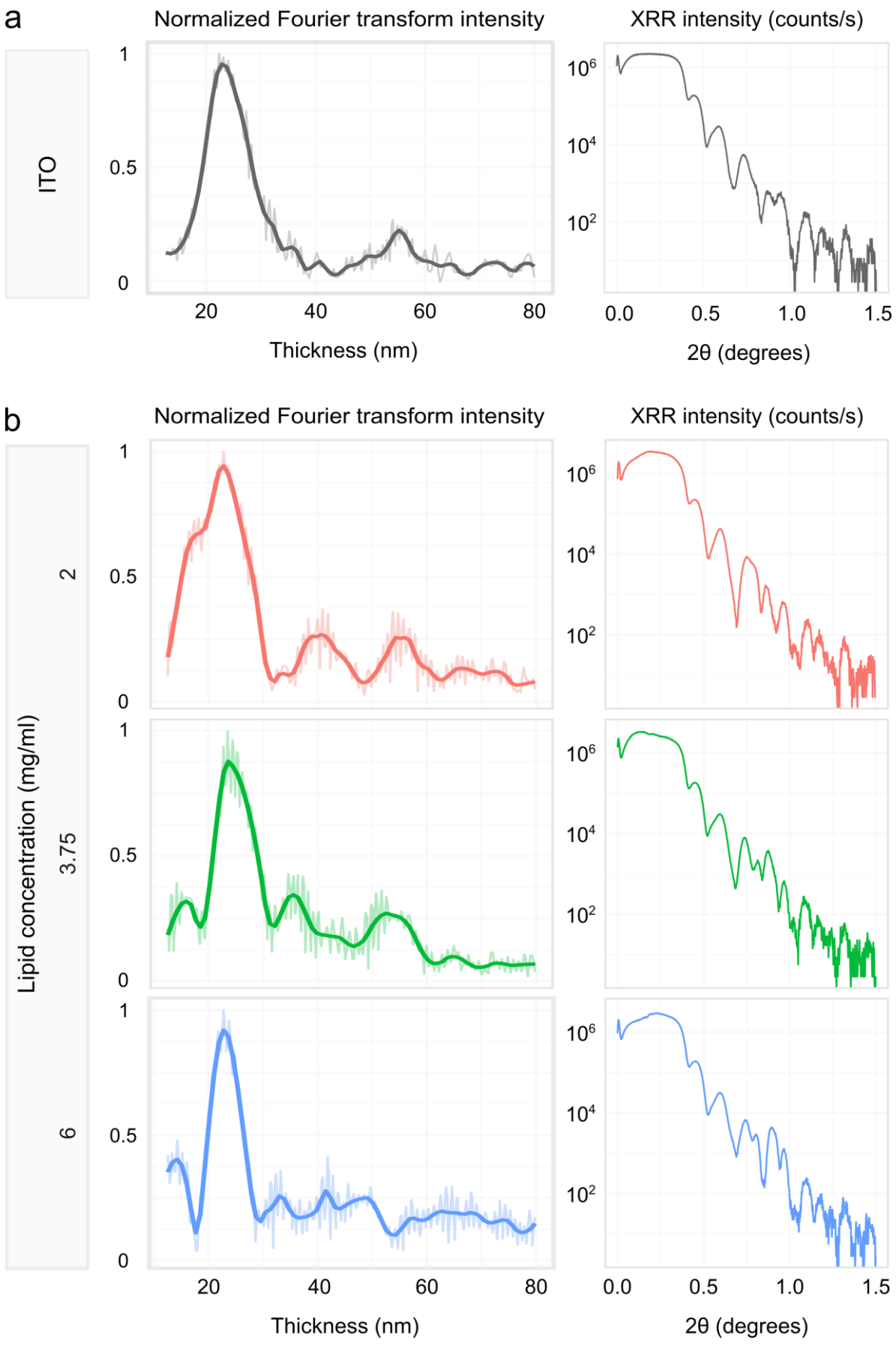

Figure S1. XRR analysis of spin-coated lipid films thickness. The right column shows the raw data, and the left one the normalized Fourier transform intensity. **(a)** Measurements for an ITO sample. **(b)** Measurements for different lipid concentrations using a Chol/(POPC+SM) mixing ratio of 0.75.

7 ELECTROFORMATION OF GIANT UNILAMELLAR VESICLES FROM DAMP LIPID FILMS FORMED BY VESICLE FUSION

Boban, Z.; Mardešić, I.; Perinović Jozić, S.; Šumanovac, J.; Subczynski, W.K.; Raguz, M. Electroformation of Giant Unilamellar Vesicles from Damp Lipid Films Formed by Vesicle Fusion. Membranes (Basel). 2023, 13, 352, doi: 10.3390/membranes13030352.

membranes

MDPI

Article

Electroformation of Giant Unilamellar Vesicles from Damp Lipid Films Formed by Vesicle Fusion

Zvonimir Boban [1,2], Ivan Mardešić [1,2], Sanja Perinović Jozić [3], Josipa Šumanovac [4], Witold Karol Subczynski [5] and Marija Raguz [1,*]

[1] Department of Medical Physics and Biophysics, University of Split School of Medicine, 21000 Split, Croatia; zvonimir.boban@mefst.hr (Z.B.); imardesi@mefst.hr (I.M.)
[2] Faculty of Science, University of Split, Doctoral Study of Biophysics, 21000 Split, Croatia
[3] Department of Organic Technology, Faculty of Chemistry and Technology, University of Split, 21000 Split, Croatia
[4] Department of Physics, Faculty of Science, University of Split, 21000 Split, Croatia
[5] Department of Biophysics, Medical College of Wisconsin, Milwaukee, WI 53226, USA; subczyn@mcw.edu
* Correspondence: marija.raguz@mefst.hr; Tel.: +385-9876-8819

Abstract: Giant unilamellar vesicles (GUVs) are artificial membrane models which are of special interest to researchers because of their similarity in size to eukaryotic cells. The most commonly used method for GUVs production is electroformation. However, the traditional electroformation protocol involves a step in which the organic solvent is completely evaporated, leaving behind a dry lipid film. This leads to artifactual demixing of cholesterol (Chol) in the form of anhydrous crystals. These crystals do not participate in the formation of the lipid bilayer, resulting in a decrease of Chol concentration in the bilayer compared to the initial lipid solution. We propose a novel electroformation protocol which addresses this issue by combining the rapid solvent exchange, plasma cleaning and spin-coating techniques to produce GUVs from damp lipid films in a fast and reproducible manner. We have tested the protocol efficiency using 1/1 phosphatidylcholine/Chol and 1/1/1 phosphatidylcholine/sphingomyelin/Chol lipid mixtures and managed to produce a GUV population of an average diameter around 40 μm, with many GUVs being larger than 100 μm. Additionally, compared to protocols that include the dry film step, the sizes and quality of vesicles determined from fluorescence microscopy images were similar or better, confirming the benefits of our protocol in that regard as well.

Keywords: GUV; electroformation; cholesterol; damp lipid film; rapid solvent exchange; plasma cleaning; cholesterol crystals; vesicle fusion

Citation: Boban, Z.; Mardešić, I.; Jozić, S.P.; Šumanovac, J.; Subczynski, W.K.; Raguz, M. Electroformation of Giant Unilamellar Vesicles from Damp Lipid Films Formed by Vesicle Fusion. *Membranes* **2023**, *13*, 352. https://doi.org/10.3390/membranes13030352

Academic Editor: Maria João Moreno

Received: 20 February 2023
Revised: 14 March 2023
Accepted: 16 March 2023
Published: 18 March 2023

1. Introduction

Liposomes are commonly used by researchers investigating membrane properties in a controlled environment. Based on their structure, we classify vesicles into unilamellar, multilamellar, and oligolamellar vesicles. Unilamellar vesicles only have a single outer bilayer, multilamellar vesicles contain multiple bilayers arranged in concentric circles, and oligolamellar vesicles enclose smaller ones inside. Unilamellar vesicles are further sorted by size into small (<100 nm), large (100 nm–1 μm), and giant unilamellar vesicles (GUVs, >1 μm). Small and large unilamellar vesicles are more often studied in the context of drug delivery applications and GUVs are more interesting to researchers studying membrane properties and organization because of the similarity in size to eukaryotic cells [1]. An additional advantage of GUV size is the possibility to observe them using light microscopy techniques.

Historically, GUVs were first produced using the natural swelling method introduced by Reeves and Dowben in 1969 [2]. Using this method, the vesicles are formed primarily due to osmotic pressure driving the aqueous solution in between the stacked lipid bilayers,

causing them to close up into vesicles. However, the proportion of GUVs that can be generated using this method is small, as most of them are either multilamellar or display other types of defects [3].

Nowadays, one of the most commonly used methods for production of GUVs is electroformation, which facilitates the production of vesicles by applying an electric field to the lipid film [4]. Briefly, the lipids dissolved in an organic solvent are deposited onto the electrode. The organic solvent evaporates, and the remaining traces are vacuumed away, leaving a dry lipid film on the electrode surface. The coated electrode is used to construct a chamber which is then filled with an internal solution of choice and connected to an alternating current generator. Film hydration aided by the influence of an external electric field detaches the lipids from the surface, producing vesicles which can be observed under a microscope [5]. Compared to vesicles grown using the gentle hydration method, the electroformation method reduces the compositional heterogeneity of the vesicles [6] and increases the proportion of unilamellar vesicles [3]. The method has evolved significantly over the years, with many potential pitfalls identified and protocol modifications tested [7–9]. The most important issues are related to the use of organic solvents during lipid film deposition, reproducibility of the conventional film deposition technique, and the step in which the lipid film is completely dried.

Researchers tried to replace the organic solvent with an aqueous solution during the film deposition step [10,11]. They concluded that using aqueous solutions improved the efficiency of GUV formation in water as well as in buffers at physiologically relevant concentrations [10,12]. This was attributed to the ability of aqueous dispersions to produce well-oriented membrane stacks on the electrode [10]. Additionally, removal of organic solvents from the process should be beneficial for protocols dealing with protein reconstitution into GUVs due to reduced protein denaturation [12–16].

Regarding the lipid film deposition step, most electroformation protocols still use the drop-deposition method for preparation of the lipid film [4,8]. However, that approach results in films of nonuniform thickness [17]. Consequently, GUVs with a wide size distribution and different compositions are created and the experiment reproducibility is very low. Over the years, multiple attempts have been made to address this issue [8,17–20]. One of these was a study by Estes and Mayer who tested lipid film deposition using the spin-coating method [17]. The lipid solution is dropped onto a flat indium-tin oxide (ITO) coated glass surface, which is subsequently spun at a large angular velocity in order to obtain a film of uniform thickness. The uniformity of the lipid film and method reproducibility were validated by ellipsometry and atomic force microscopy. The method has been accepted by several groups using a wide range of lipid compositions to produce GUVs [17,21–24].

Another issue is the dry film step of the traditional protocol. This step creates a problem when working with lipid solutions containing high amounts of cholesterol (Chol). In such situations, some Chol demixes and forms anhydrous Chol crystals [11,25,26]. Once the film is rehydrated, these crystals do not participate in the formation of the lipid bilayer, resulting in an artifactual decrease of Chol concentration in the bilayer compared to the initial mixing ratio in the lipid solution. An example of Chol demixing was described in a study which utilized confocal microscopy to detect pure Chol bilayer domains in GUVs formed from a mixture of Chol and 1-palmitoyl-2-oleoyl-glycero-3-phosphocholine (POPC) using the traditional electroformation method (with the dry lipid film step) [26]. Chol bilayer domains were observed only for about 75 mol% of Chol in the initial mixture (Chol/POPC mixing ratio of 3/1), and not at 50 mol% as expected.

A method called the rapid solvent exchange (RSE) can be utilized to bypass the dry phase. During the procedure, chloroform-dissolved lipids are first mixed with an aqueous medium and the chloroform is then rapidly evaporated from the mixture [27]. The method has proven effective against the Chol demixing artifact [11,25,28]. However, it results in the formation of smaller multilamellar vesicles (MLVs), not GUVs. Paramagnetic resonance measurements on MLVs produced using the RSE method showed that pure Chol

bilayer domains start to form at 50 mol% of Chol (at a Chol/phospholipid molar ratio of 1/1) [28,29]. Comparison of the amount of Chol in the initial lipid mixture needed for detection of Chol bilayer domains in RSE MLVs and GUVs produced with the conventional electroformation protocol attests to the severity of Chol demixing during the lipid film drying step.

Baykal-Caglar et al. have attempted electroformation from damp lipid films obtained by depositing an aqueous RSE-produced solution of MLVs onto the electrode and then slowly drying it under high-humidity conditions [11]. Their results show a decrease in the average transition temperature of GUVs made from damp compared to dry lipid films, implying a higher Chol concentration in GUVs made from the damp film. The main disadvantage of their approach is the long preparation time due to prolonged drying (22–25 h) in high-humidity conditions. Additionally, the obtained lipid film would inevitably display nonuniformities due to using the drop-deposition technique for the deposition of the suspension of MLVs.

Advancements to the traditional protocol have been proposed regarding the electrode-cleaning approaches as well. Traditionally, electrodes are cleaned prior to film deposition by applying organic solvents and then drying them. Plasma cleaning has also been tried out on ITO glass as an alternative and has proved to be very effective [30]. Moreover, treating the electrodes with plasma has enabled researchers to efficiently produce GUVs containing buffers with physiological levels of charged particles, which was very hard to achieve using conventional protocols [30]. The improvement has been attributed to easier hydration of the lipid film and subsequent formation of lipid bilayers [30]. However, this experiment used plasma treatments only as a method for electrode cleaning, and traditional film deposition which uses organic solvents was used in the protocol.

In this article, we introduce a novel electroformation protocol which includes the most useful modifications to the traditional protocol and combines them in a novel way in order to bypass the dry film phase. As far as we know, no one before tried to produce lipid films by depositing an aqueous suspension of liposomes on plasma-cleaned surfaces. Our approach was inspired by the vesicle fusion method which is often used for preparation of supported bilayer membranes [31]. The method involves the deposition of an aqueous suspension of vesicles on a hydrophilized surface. The interaction of the hydrophilic surface with the vesicles causes them to rupture, creating a surface bilayer.

Compared to the approach used by Baykal-Caglar et al., the new protocol significantly reduces the preparation time and increases the experiment reproducibility. Consequently, amongst other benefits, the protocol improves the electroformation of GUVs with higher Chol concentrations. Such GUVs are interesting to researchers investigating the role of Chol in fiber cell plasma membranes of the eye lens [26,32,33] or the development of atherosclerosis [34,35]. Moreover, bypassing the dry state results in a protocol more compatible with protein insertion into GUVs [13]. The advantage of such protocols is reduced protein denaturation, which occurs when preparing GUVs from lipids dissolved in an organic solvent or during film drying.

2. Materials and Methods

2.1. Materials

1-palmitoyl-2-oleoyl-glycero-3-phosphocholine (POPC), egg sphingomyelin (SM), and Chol were obtained from Avanti Polar Lipids Inc. (Alabaster, AL, USA). The fluorescent dye 1,1-dioctade-cyl-3,3,3,3-tetramethylindocarbocyanine Perchlorate ($DiIC_{18}(3)$) was purchased from Invitrogen, Thermo Fisher Scientific (Waltham, MA, USA). When not used, the lipids were stored at −20 °C. The purity of chloroform (BDH Prolabo) was greater than 99.8%. ITO glass (ICG-90 INS 115, resistance 70–100 Ω) was purchased from Delta Technologies (Loveland, LO, USA). ITO glass dimensions were 25 × 75 × 1.1 mm. New ITO glass was used for each preparation in order to prevent coating deterioration [36]. Mili-Q (Merck, Rahway, NJ, USA) deionized water preheated to 60 °C was used as the internal chamber solution.

2.2. Preparation of the Suspension of Large Unilamellar Vesicles

MLVs were first prepared using a home-built RSE device to bypass the dry phase and the Chol demixing artifact. The chloroform dissolved lipid mixture was produced from 25 mg/mL POPC, 25 mg/mL SM, 20 mg/mL Chol, and 1 mg/mL $DiIC_{18}(3)$ stocks. The POPC/Chol molar ratio was 1/1 and the POPC/SM/Chol ratio 1/1/1. The molar ratio of the fluorescent probe with respect to POPC was 1/500. The total lipid mass was 2.1 mg. This resulted in an organic solution of lipids with a volume of 94.4 µL for the POPC/Chol mixture and 90.4 µL for the POPC/SM/Chol mixture. A volume of 400 µL Mili-Q deionized water was then added to the solution and the resulting mixture was vortexed (Vortex IR, Star Lab, Blakelands, UK) at a velocity of 2200 rpm. After initiating the vortexing, the pressure was slowly decreased to a approximately 0.05 bar using a vacuum pump (HiScroll 6, Pfeiffer Vacuum, Asslar, Germany). After reaching the desired pressure, the vortexed sample was kept under vacuum for an additional 90 s. The obtained suspension of MLVs was extruded using an Avanti Mini Extruder (Avanti Polar Lipids, Inc, Alabaster, AL.). The suspension was passed through a 100 nm polycarbonate (Nuclepore Track-Etch Membrane, Whatman, UK) filter 15 times in order to obtain a homogeneous large unilamellar vesicle (LUV) suspension. In order to prevent the loss of lipids during the initial wetting of the filtering segment, before extruding the suspension, deionized water was passed through the filter to pre-wet the extruder parts. Finally, extra water was added in order to achieve a final lipid concentration of 3.5 mg/mL.

2.3. Preparation of the Damp Lipid Film

Prior to spin-coating, the ITO glass was immersed in deionized water for at least 45 min before being wiped four times with 70% ethanol moistened lint-free wipes. The glass was then plasma-cleaned with oxygen for 1 min using a plasma cleaner (PDC-002-HPCE with the PLASMAFLO PDC-FMG-2 attachment, Harrick Plasma, Ithaca, NY, USA) attached to a vacuum pump (HiScroll 6, Pfeiffer Vacuum, Assler, Germany).

Following that, 550 µL of the LUV suspension was deposited onto the electrode and spin-coated using a spin-coater (SM-150, Sawatec, Sax, Switzerland) to obtain the damp lipid film. The glass was spun at 600 rpm with the final velocity reached in 1 s. In order to prevent any unwanted evaporation, following spin-coating, the coated ITO glass was placed in a Petri dish and immediately used for the assembly of an electroformation chamber.

2.4. Electroformation Protocol

The electroformation chamber is made of two 25 × 37.5 mm ITO-coated glass electrodes separated by a 1.6 mm thick teflon spacer. The electrodes were made by cutting a 25 × 75 mm ITO glass slide in half using a diamond pen cutter. After lipid deposition, the chamber was assembled by attaching the spacer to the electrodes using vacuum grease. Upon insertion, the stopper was also sealed with vacuum grease. This way, contact between the grease and the internal solution is avoided, minimizing the possibility of harmful effects due to grease contamination [28]. The structure of the chamber is further secured by binding clips attached at three points on the electrodes—two next to the stopper, and one at the opposite side. Finally, the chamber was attached to a pulse generator (UTG9005C, UNI-T, Dongguan City, China or PSG 9080, Joy-IT, Neukirchen-Vluyn, Germany) and placed inside an incubator at a temperature of 60 °C. In order to assure good contact between the conductor wires and the electrodes, the outer edges of the electrodes were covered with copper tape. Based on experience from our previous electroformation studies [21,22], the electrical parameters were set to 2 V and 10 Hz. After 2 h, the voltage was turned off and the chamber was kept in the incubator for another hour.

2.5. Fourier Transform Infrared Spectroscopy

Attenuated total reflection Fourier transform infrared spectroscopy (ATR-FTIR) was used to obtain spectra of solutions before and after the RSE procedure, and spectra of glass slides before and after spin-coating. We used the Spectrum Two (Perkin-Elmer, Waltham,

MA, USA) spectrometer.. The scans were performed for wavenumbers ranging from 4000 to 450 cm^{-1} at a resolution of 4 cm^{-1} in 5 scans at 25 °C. A diamond was used as the reflection crystal. The obtained spectra were compared with each other and with the reference spectra in the Spectrum IR library to confirm the composition of the samples.

2.6. Fluorescence Imaging and Data Analysis

In order to search the entire volume of the chamber, we collected images from 13 regions on the sample. One hundred vesicles were randomly chosen from the images. If the images did not contain 100 vesicles, all observed vesicles were tracked. Images were obtained using a fluorescence microscope (Olympus BX51, Olympus, Tokyo, Japan). Vesicle diameters were measured using the line tool in the Fiji software [37].

2.7. Dynamic Light Scattering

The measurement of the hydrodynamic diameter and polydispersity index of liposome suspensions was performed using dynamic light scattering (Litesizer 500, Anton Paar, Graz, Austria). For the measurements, 100 µL of the liposome suspension was mixed with 900 µL of phosphate buffer.

2.8. Data Analysis

If not explicitly stated otherwise, numerical results are expressed as mean ± standard deviation. Sample distribution normality was assessed visually through histograms and formally by using the Shapiro–Wilk test. Depending on whether or not the normality assumption was violated, the difference of means for two groups was tested using the Student's t-test or the Wilcoxon rank sum test. All data analysis and visualization was performed using the R programming language [38].

3. Results and Discussion

3.1. The New Protocol

We present a novel protocol for production of GUVs from damp lipid films. In order to bypass the dry phase, an aqueous suspension of MLVs is obtained using the RSE method (Figure 1a) and then passed through an extruder in order to obtain a population of large unilamellar vesicles (LUVs) (Figure 1b,c).

The LUV suspension is deposited onto an indium tin oxide (ITO) coated glass which was previously plasma-cleaned, making the surface hydrophilic (Figure 2a,b). The interaction of the vesicle bilayers with the hydrophilic surface causes them to rupture during spin-coating, leaving behind a thin damp lipid film on the electrode. This electrode is then used in construction of the electroformation chamber which is subsequently placed in an incubator and connected to an alternating current source in order to form GUVs (Figure 2c).

We have confirmed that chloroform has successfully been removed from the solution using ATR-FTIR spectroscopy (Figure 3a). Compared to the solution containing chloroform, after applying the RSE method, there are no absorption peaks at around 700 and 1200 cm^{-1} due to CCl_3-stretching and CH-bending in the fingerprint region of the spectrum (Figure 3a,b), respectively. The remaining signal corresponds to the water spectrum from the database (Figure 3c), with characteristic peaks around 3400 and 1650 cm^{-1}.

In order to prove that the film remained damp after spin-coating, we have also compared ATR-FTIR spectra of glass before and after spin-coating (Figure 4). The blue curve, representing the sample after spin-coating, displays an additional broad peak around 3400 cm^{-1} due to the O-H stretching vibrations and another one around 1650 cm^{-1} corresponding to absorption due to H-O-H bending, confirming the presence of water. Both curves display multiple peaks between 2300 and 1900 cm^{-1} representing the absorption bands of diamond. In this region, diamond does not have full transmission capability, and the bands from the ATR reflection crystal are visible. The downward slope in the region from 2000 to 1500 cm^{-1} appears due to the glass on which the coating was performed.

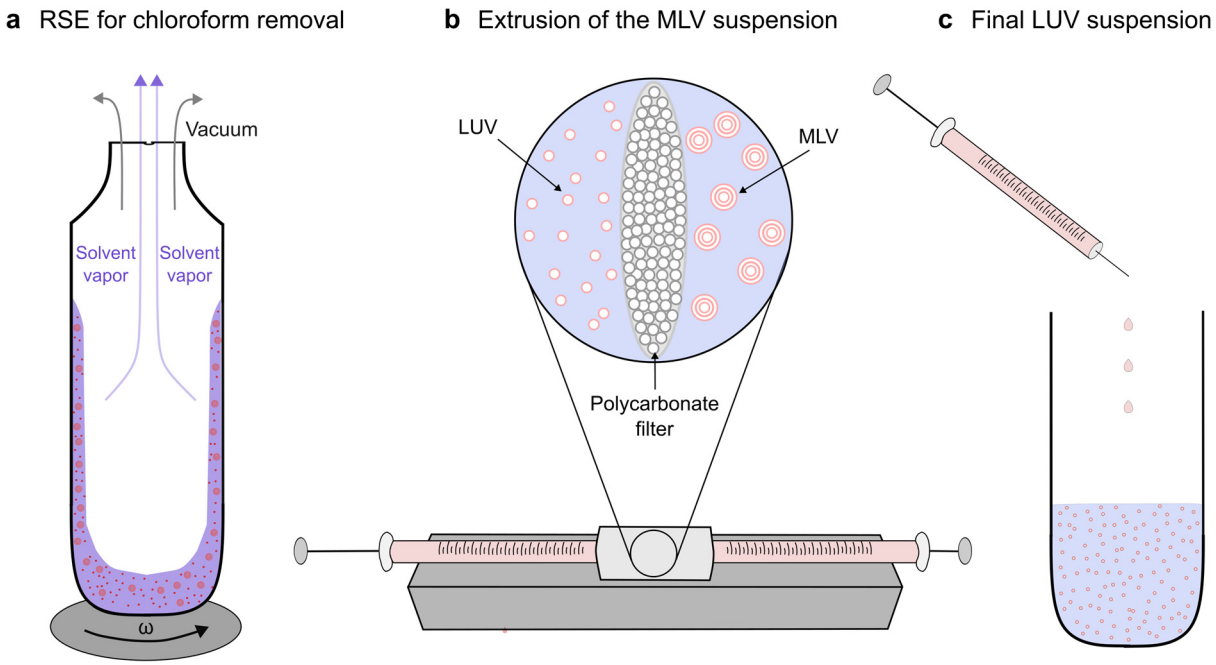

Figure 1. Preparation of the LUV solution. (**a**) MLVs are first prepared using the RSE method by rapidly evaporating chloroform from the mixture. (**b**) MLVs are passed through a polycarbonate filter an uneven number of times in order to obtain LUVs. (**c**) The obtained LUV solution is stored for later use in preparation of the damp lipid film.

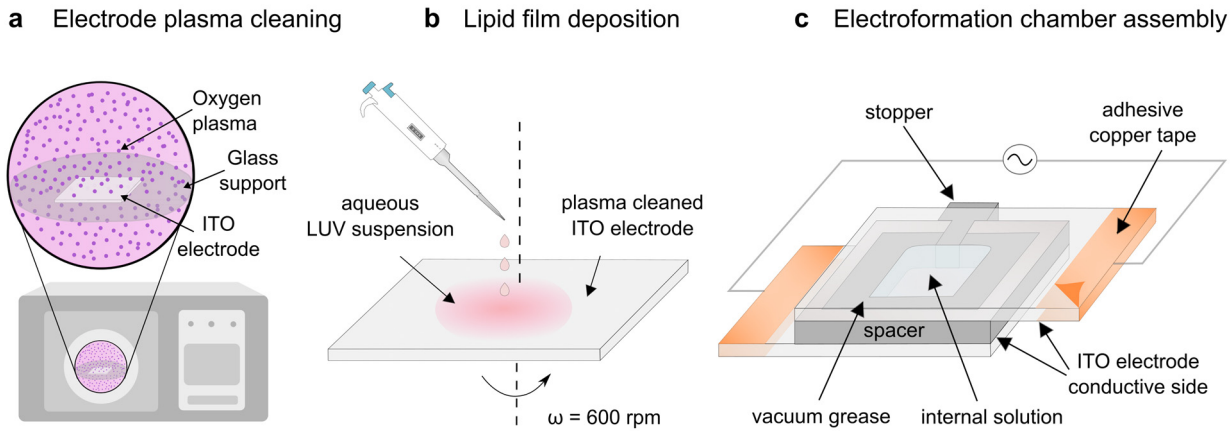

Figure 2. Electroformation from a damp lipid film. (**a**) The ITO electrode is hydrophilized using a plasma cleaner. (**b**) The LUV suspension is deposited onto a plasma cleaned ITO coated glass and spin-coated to obtain a damp lipid film. (**c**) The coated electrode is used to assemble the electroformation chamber.

This confirms that our approach avoids the dry film phase just like that of Baykal-Caglar et al., so it should also result in increased compositional homogeneity of the GUVs and reduction of the demixing artefact [11]. The great advantage of our protocol is a significant decrease in preparation time (22–25 h of drying compared to spin-coating, which lasts up to a couple of minutes) and the potential to create more homogeneous lipid films. Furthermore, aside from inducing vesicle rupture, treating the electrodes with plasma has also been proven beneficial for electroformation efficiency, enabling the production of GUVs with charged lipids and solutions containing high ion concentrations. The effect has been attributed to easier hydration of the lipid film and subsequent formation of lipid bilayers [30].

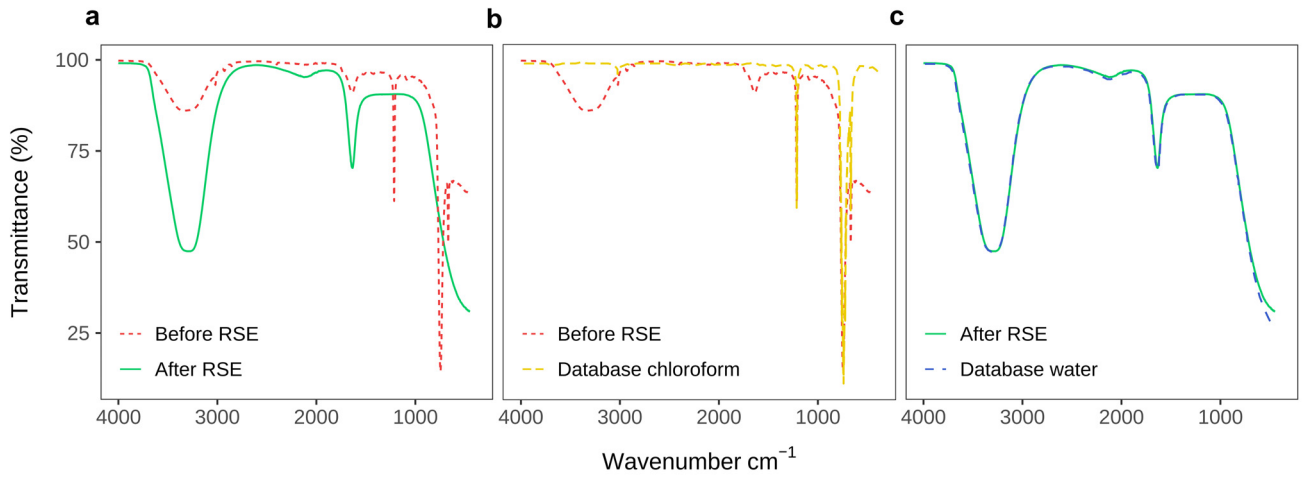

Figure 3. Confirmation of chloroform removal by the RSE method from a mixture of water and chloroform dissolved lipids. (**a**) Comparison of FTIR spectra before and after performing RSE. (**b**) FTIR spectrum before RSE compared to the database curve for chloroform. (**c**) FTIR spectrum of a sample after performing the RSE method compared with the database spectrum of water.

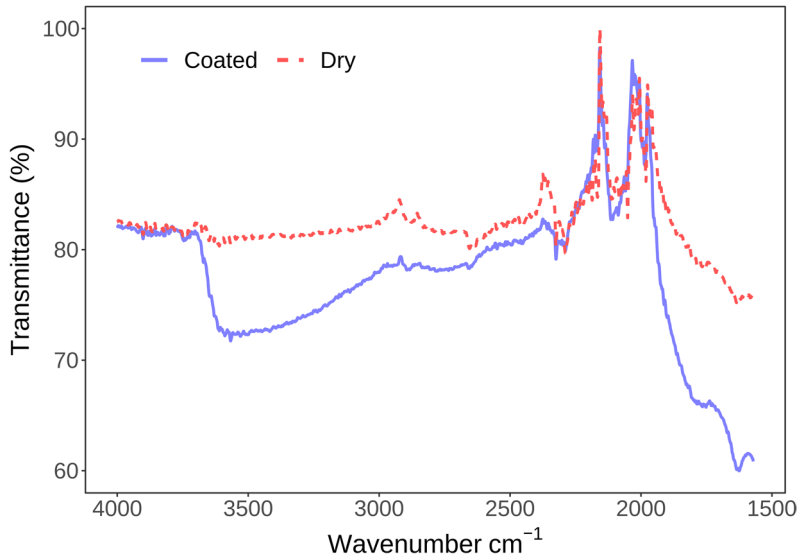

Figure 4. Confirmation of water presence before (red) and after (blue) one minute of water spin-coating on coverslip glass. Aside from the water peaks, there are also additional absorption peaks due to the diamond and glass absorption bands.

3.2. The Effect of Spin-Coating Duration

To demonstrate the efficiency of the new protocol, we produced GUVs from a 1/1 POPC/Chol molar ratio lipid mixture. The hydrodynamic diameter of the RSE-produced MLVs was 1401.2 nm with a polydispersity index of 0.3. After extrusion, the diameter of obtained LUVs was 136 nm with a polydispersity index of 0.11. The observation that the average size of LUVs is larger than the 100 nm pore size of the polycarbonate filter can be attributed to elastic deformations of LUVs [39].

Using different durations of spin-coating, ranging from 0 s to 3 min, we tested the effect of spin-coating duration on the efficiency of GUV formation (Figure 5a). The 0 s case involves no spin-coating, but the LUV suspension is instead simply dropped onto the plasma-cleaned electrode and the excess liquid is shaken off after 10 s. We performed three experiments for every duration of spin-coating. The obtained mean size and standard deviation ranged from 21 $\pm$ 16 m to 48 $\pm$ 20 m for the 0 s and 3 min groups of samples, respectively (Figure 5a). The average size shows a clear dependence on spin-coating

duration with longer drying being more favorable for production of GUV populations with larger size and yield.

Compared to previous research from our group which dealt with optimization of GUV electroformation from a dry lipid film [21,22], the sizes and quality of vesicles determined using fluorescence microscopy images were similar or better for both durations of spin-coating, confirming the benefits of our protocol in that regard as well (Figure 5b).

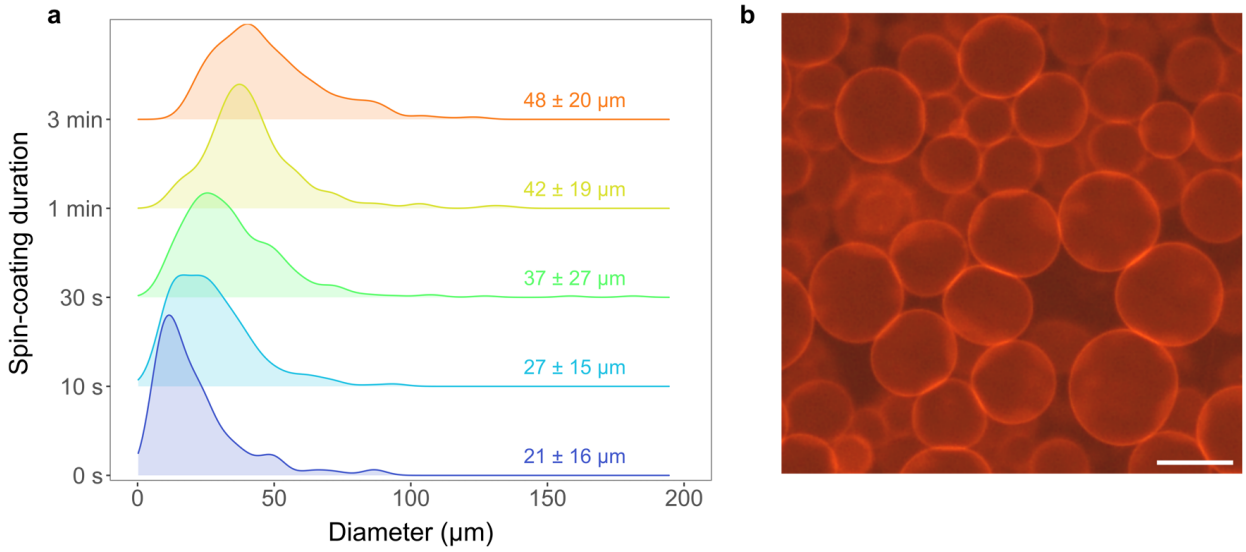

Figure 5. Size distribution densities of GUVs produced using the new protocol. (**a**) Comparison of size distributions for five spin-coating durations ranging from 0 s to 3 min. Each distribution represents 300 randomly selected vesicles from three independent samples (100 vesicles per sample). If the sample did not contain 100 vesicles, all vesicles from that sample were taken into account. (**b**) Fluorescence microscopy image of GUVs produced using the new protocol with 3 min of spin coating. The scale bar represents 50 m.

3.3. GUVs Grown from Different Lipid Mixtures

Aside from the binary 1/1 POPC/Chol mixture, we have also produced GUVs from a ternary 1/1/1 POPC/SM/Chol mixture which is important for researchers studying lipid rafts [40–42]. The hydrodynamic diameter of SM-containing LUVs was measured at 136 nm with a polydispersity index of 0.11. Using a spin-coating duration of 1 min, we have successfully produced GUVs from this mixture as well. We obtained an average diameter of 35 $\pm$ 21 . Comparing this to the corresponding result for the POPC/Chol mixture of 42 $\pm$ 19 m, we can see that the vesicles were smaller after inclusion of SM (p = 2) (Figure 6). This is consistent with our previous research, showing that inclusion of SM in the lipid mixture makes it harder to produce GUVs with large average size and yield [21,22]. The average size of the SM-containing GUV population is also on par with the best results obtained using the conventional lipid film deposition methods [21].

We observed no lateral phase separation in GUVs produced from the ternary POPC/SM/Chol mixture (Figure 6b). Depending on the membrane model type and method used, different phase diagrams have been reported for similar mixtures [41–43]. A study performed on GUVs produced from a 1/1/1 mixture of POPC/palmitoyl sphingomyelin/Chol showed that they should undergo phase separation at a transition temperature of approximately 20 °C [42]. Therefore, the temperature at which the GUV microscopy was performed might have been too high to observe the separation. Moreover, they used palmitoyl sphingomyelin and not egg sphingomyelin, so that could also affect the expected phase behavior. Additionally, all mentioned studies used a protocol which contained a dry film step [41–43], so the Chol content specified in the diagrams might have actually been lower due to demixing.

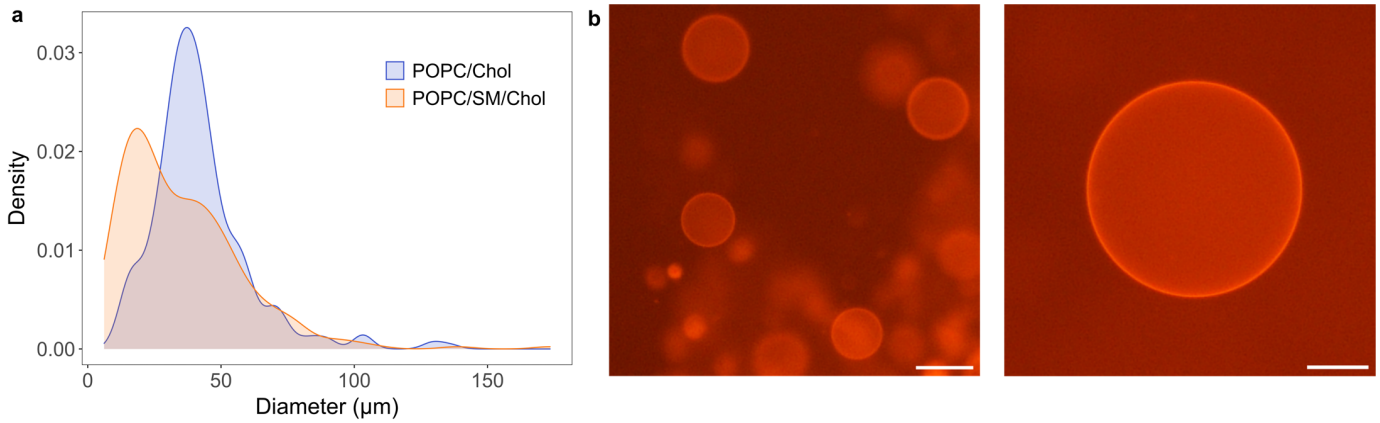

Figure 6. (**a**) Comparison of size distribution densities for GUVs produced from 1/1 POPC/Chol and 1/1/1 POPC/SM/Chol mixtures with a spin-coating duration of 1 min. (**b**) Fluorescence microscopy images of GUVs for the POPC/SM/Chol mixture. The scale bar represents 50 μm.

The proposed protocol should help reduce the Chol demixing artifact and improve the ability to produce high quality GUV populations under different conditions and from different lipid mixtures. However, a tradeoff seems to be involved. On one hand, in order to increase the certainty that Chol will not crystallize, the lipid film should remain as wet as possible. On the other hand, we have shown that shorter drying times result in lower yields and smaller average GUV diameters. If the lipid mixture contains no Chol, or small quantities of Chol, there is no reason not to dry the lipid film. However, if that is not the case, Chol demixing will certainly be an issue. The RSE technique is included to prevent Chol demixing during preparation of the MLV suspension, and keeping the lipid film damp should prevent Chol demixing during lipid film deposition. It should be noted that we have not quantified the exact Chol content in produced GUVs. However, to address this in the future, we plan to perform confocal fluorescence microscopy experiments using two fluorescent dyes—a phospholipid and a Chol analogue. Comparison of fluorescence intensity profiles between GUVs grown using the conventional and our newly developed protocol should reveal the level of demixing. Moreover, if our protocol reduced the demixing artifact, pure Chol bilayer domains should form between 50 and 66 mol% of Chol in the initial lipid mixture.

We have also successfully produced high quality POPC GUVs by eliminating the RSE step of the protocol and using the gentle hydration approach to produce MLVs instead (Supplementary Figure S1). Additionally, in the previous subsection, we have shown that spin-coating can be avoided as well by simply dropping the LUV suspension on the plasma-cleaned electrode and shaking off the excess liquid after 10 s. Alternatively, the LUV suspension could simply be directly deposited into a chamber with a plasma-cleaned electrode. However, this approach hampers subsequent microscopy due to a strong signal from LUVs that remain in the solution. Therefore, sample dilution or an additional purification step are required to adequately visualize the results. Both approaches reduce the yield and size of the obtained GUV population.

We believe that this new improved electroformation protocol will allow us to successfully study models of eye lens fiber cell membranes with their very high Chol content [32,33,44–46]. Furthermore, both using aqueous solutions and treating the electrodes with plasma have proven beneficial for electroformation efficiency, allowing for production of GUVs with charged lipids and solutions containing high ion concentrations [10,30]. Since it avoids organic solvents and lipid film drying, the protocol could also be adapted for protein reconstitution into GUVs.

4. Conclusions

We introduced a new improved electroformation protocol which bypasses the dry lipid film phase of the traditional approach by combining the plasma-cleaning, RSE, and spin-coating techniques. The protocol consists of 6 main steps:

1. The lipid solution is prepared from chloroform dissolved lipid stocks.
2. The obtained solution is mixed with deionized water and RSE is then used to obtain the MLV suspension.
3. MLVs are extruded by passing the solution through a polycarbonate filter in order to produce a homogeneous LUV solution.
4. The ITO electrodes which were stored in deionized water are cleaned by swabbing with ethanol moistened wipes and then plasma cleaned for additional cleaning and surface hydrophilization.
5. The LUV suspension is deposited onto the hydrophilic ITO electrode surface and spin-coated to produce a lipid film. The film is created due to vesicles rupturing in contact with the hydrophilic surface.
6. The coated electrode is used in construction of the electroformation chamber which is subsequently connected to an alternatincg current source in order to produce GUVs.

Previous studies have shown that electroformation from damp lipid films increases the compositional uniformity of the resulting GUV population and reduces the artifactual Chol demixing. Compared to the earlier damp lipid film protocol, our method significantly decreases the preparation time by eliminating the 24 h high-humidity drying phase and replacing it with a short duration of spin-coating. Furthermore, compared to the drop-deposition method, spin-coating can lead to higher experiment reproducibility. We believe that this new improved electroformation protocol will allow us to successfully study the physical properties, lateral organization and domain function of cell membranes with very high Chol such as the eye lens fiber cell membranes [32,33,44–46]. Additionally, both using aqueous solutions and treating the electrodes with plasma have proven beneficial for electroformation efficiency, allowing for production of GUVs with charged lipids and solutions containing high ion concentrations The protocol could also be adapted for protein insertion into GUVs with reduced protein denaturation due to the avoidance of organic solvents and lipid film drying.

Supplementary Materials: The following supporting information can be downloaded at: https://www.mdpi.com/article/10.3390/membranes13030352/s1, Figure S1: Size distribution density for GUVs produced from POPC with a spin-coating duration of 2 min. The lipid concentration was 3 mg/mL.

Author Contributions: Conceptualization, Z.B.; methodology, Z.B., I.M., S.P.J.; software, Z.B.; validation, Z.B., I.M., J.Š.; formal analysis, Z.B.; investigation, Z.B., I.M., S.P.J., J.Š.; resources, M.R., S.P.J.; data curation, Z.B.; writing—original draft preparation, Z.B.; writing—review and editing, Z.B., I.M., M.R., W.K.S., S.P.J.; visualization, Z.B.; supervision, M.R., Z.B.; project administration, M.R.; funding acquisition, M.R. All authors have read and agreed to the published version of the manuscript.

Funding: Research reported in this publication was supported by the Croatian Science Foundation (Croatia) under Grant IP-2019-04-1958.

Institutional Review Board Statement: Not applicable.

Data Availability Statement: The data presented in this study are available upon reasonable request from the corresponding author.

Acknowledgments: We thank Ante Bilušić for access to his lab equipment.

Conflicts of Interest: The authors declare no conflict of interest.

References

1. Rideau, E.; Dimova, R.; Schwille, P.; Wurm, F.R.; Landfester, K. Liposomes and Polymersomes: A Comparative Review towards Cell Mimicking. *Chem. Soc. Rev.* **2018**, *47*, 8572–8610. [CrossRef]
2. Reeves, J.P.; Dowben, R.M. Formation and Properties of Thin-Walled Phospholipid Vesicles. *J. Cell. Physiol.* **1969**, *73*, 49–60. [CrossRef] [PubMed]
3. Rodriguez, N.; Pincet, F.; Cribier, S. Giant Vesicles Formed by Gentle Hydration and Electroformation: A Comparison by Fluorescence Microscopy. *Colloids Surf. B Biointerfaces* **2005**, *42*, 125–130. [CrossRef] [PubMed]
4. Angelova, M.I.; Dimitrov, D.S. Liposome Electroformation. *Faraday Discuss. Chem. Soc.* **1986**, *81*, 303. [CrossRef]
5. Dimitrov, D.S.; Angelova, M.I. Lipid Swelling and Liposome Formation Mediated by Electric Fields. *J. Electroanal. Chem.* **1988**, *253*, 323–336. [CrossRef]
6. Grusky, D.S.; Bhattacharya, A.; Boxer, S.G. Examining Compositional Variability of Giant Unilamellar Vesicles via Secondary Ion Mass Spectrometry. *Biophys. J.* **2023**, *122*, 81a. [CrossRef]
7. Boban, Z.; Mardešić, I.; Subczynski, W.K.; Raguz, M. Giant Unilamellar Vesicle Electroformation: What to Use, What to Avoid, and How to Quantify the Results. *Membranes* **2021**, *11*, 860. [CrossRef] [PubMed]
8. Veatch, S.L. Electro-Formation and Fluorescence Microscopy of Giant Vesicles with Coexisting Liquid Phases. In *Lipid Rafts*; Springer: Humana Totowa, NJ, USA, 2007; pp. 59–72.
9. Morales-Penningston, N.F.; Wu, J.; Farkas, E.R.; Goh, S.L.; Konyakhina, T.M.; Zheng, J.Y.; Webb, W.W.; Feigenson, G.W. GUV Preparation and Imaging: Minimizing Artifacts. *Biochim. Biophys. Acta-Biomembr.* **2010**, *1798*, 1324–1332. [CrossRef]
10. Pott, T.; Bouvrais, H.; Méléard, P. Giant Unilamellar Vesicle Formation under Physiologically Relevant Conditions. *Chem. Phys. Lipids* **2008**, *154*, 115–119. [CrossRef]
11. Baykal-Caglar, E.; Hassan-Zadeh, E.; Saremi, B.; Huang, J. Preparation of Giant Unilamellar Vesicles from Damp Lipid Film for Better Lipid Compositional Uniformity. *Biochim. Biophys. Acta-Biomembr.* **2012**, *1818*, 2598–2604. [CrossRef]
12. Méléard, P.; Bagatolli, L.A.; Pott, T. Giant Unilamellar Vesicle Electroformation. From Lipid Mixtures to Native Membranes Under Physiological Conditions. *Methods Enzymol.* **2009**, *465*, 161–176. [CrossRef]
13. Witkowska, A.; Jablonski, L.; Jahn, R. A Convenient Protocol for Generating Giant Unilamellar Vesicles Containing SNARE Proteins Using Electroformation. *Sci. Rep.* **2018**, *8*, 9422. [CrossRef]
14. Collins, M.D.; Gordon, S.E. Giant Liposome Preparation for Imaging and Patch-Clamp Electrophysiology. *J. Vis. Exp.* **2013**, *76*, e50227. [CrossRef]
15. Bhatia, T.; Husen, P.; Brewer, J.; Bagatolli, L.A.; Hansen, P.L.; Ipsen, J.H.; Mouritsen, O.G. Preparing Giant Unilamellar Vesicles (GUVs) of Complex Lipid Mixtures on Demand: Mixing Small Unilamellar Vesicles of Compositionally Heterogeneous Mixtures. *Biochim. Biophys. Acta-Biomembr.* **2015**, *1848*, 3175–3180. [CrossRef]
16. Girard, P.; Pécréaux, J.; Lenoir, G.; Falson, P.; Rigaud, J.L.; Bassereau, P. A New Method for the Reconstitution of Membrane Proteins into Giant Unilamellar Vesicles. *Biophys. J.* **2004**, *87*, 419–429. [CrossRef] [PubMed]
17. Estes, D.J.; Mayer, M. Electroformation of Giant Liposomes from Spin-Coated Films of Lipids. *Colloids Surf. B Biointerfaces* **2005**, *42*, 115–123. [CrossRef]
18. Oropeza-Guzman, E.; Riós-Ramírez, M.; Ruiz-Suárez, J.C. Leveraging the Coffee Ring Effect for a Defect-Free Electroformation of Giant Unilamellar Vesicles. *Langmuir* **2019**, *35*, 16528–16535. [CrossRef]
19. Berre, L.; Chen, Y.; Baigl, D. From Convective Assembly to Landau-Levich Deposition of Multilayered Phospholipid Films of Controlled Thickness. *Langmuir* **2009**, *25*, 2554–2557. [CrossRef]
20. Taylor, P.; Xu, C.; Fletcher, P.D.I.; Paunov, V.N. A Novel Technique for Preparation of Monodisperse Giant Liposomes. *Chem. Commun.* **2003**, *44*, 1732–1733. [CrossRef] [PubMed]
21. Boban, Z.; Mardešić, I.; Subczynski, W.K.; Jozić, D.; Raguz, M. Optimization of Giant Unilamellar Vesicle Electroformation for Phosphatidylcholine/Sphingomyelin/Cholesterol Ternary Mixtures. *Membranes* **2022**, *12*, 525. [CrossRef] [PubMed]
22. Boban, Z.; Puljas, A.; Kovač, D.; Subczynski, W.K.; Raguz, M. Effect of Electrical Parameters and Cholesterol Concentration on Giant Unilamellar Vesicles Electroformation. *Cell Biochem. Biophys.* **2020**, *78*, 157–164. [CrossRef]
23. Politano, T.J.; Froude, V.E.; Jing, B.; Zhu, Y. AC-Electric Field Dependent Electroformation of Giant Lipid Vesicles. *Colloids Surf. B Biointerfaces* **2010**, *79*, 75–82. [CrossRef] [PubMed]
24. Billerit, C.; Jeffries, G.D.M.; Orwar, O.; Jesorka, A. Formation of Giant Unilamellar Vesicles from Spin-Coated Lipid Films by Localized IR Heating. *Soft Matter* **2012**, *8*, 10823. [CrossRef]
25. Huang, J.; Buboltz, J.T.; Feigenson, G.W. Maximum Solubility of Cholesterol in Phosphatidylcholine and Phosphatidylethanolamine Bilayers. *Biochim. Biophys. Acta-Biomembr.* **1999**, *1417*, 89–100. [CrossRef] [PubMed]
26. Raguz, M.; Kumar, S.N.; Zareba, M.; Ilic, N.; Mainali, L.; Subczynski, W.K. Confocal Microscopy Confirmed That in Phosphatidylcholine Giant Unilamellar Vesicles with Very High Cholesterol Content Pure Cholesterol Bilayer Domains Form. *Cell Biochem. Biophys.* **2019**, *77*, 309–317. [CrossRef] [PubMed]
27. Buboltz, J.T. A More Efficient Device for Preparing Model-Membrane Liposomes by the Rapid Solvent Exchange Method. *Rev. Sci. Instrum.* **2009**, *80*, 124301. [CrossRef]
28. Mainali, L.; Raguz, M.; Subczynski, W.K. Formation of Cholesterol Bilayer Domains Precedes Formation of Cholesterol Crystals in Cholesterol/Dimyristoylphosphatidylcholine Membranes: EPR and DSC Studies. *J. Phys. Chem. B* **2013**, *117*, 8994–9003. [CrossRef]

29. Mainali, L.; Pasenkiewicz-Gierula, M.; Subczynski, W.K. Formation of Cholesterol Bilayer Domains Precedes Formation of Cholesterol Crystals in Membranes Made of the Major Phospholipids of Human Eye Lens Fiber Cell Plasma Membranes. *Curr. Eye Res.* **2020**, *45*, 162–172. [CrossRef]
30. Li, Q.; Wang, X.; Ma, S.; Zhang, Y.; Han, X. Electroformation of Giant Unilamellar Vesicles in Saline Solution. *Colloids Surf. B Biointerfaces* **2016**, *147*, 368–375. [CrossRef]
31. Hardy, G.J.; Nayak, R.; Zauscher, S. Model Cell Membranes: Techniques to Form Complex Biomimetic Supported Lipid Bilayers via Vesicle Fusion. *Curr. Opin. Colloid Interface Sci.* **2013**, *18*, 448–458. [CrossRef]
32. Mainali, L.; Raguz, M.; O'Brien, W.J.; Subczynski, W.K. Properties of Membranes Derived from the Total Lipids Extracted from Clear and Cataractous Lenses of 61–70-Year-Old Human Donors. *Eur. Biophys. J.* **2014**, *44*, 91–102. [CrossRef]
33. Mainali, L.; Raguz, M.; O'Brien, W.J.; Subczynski, W.K. Properties of Membranes Derived from the Total Lipids Extracted from the Human Lens Cortex and Nucleus. *Biochim. Biophys. Acta-Biomembr.* **2013**, *1828*, 1432–1440. [CrossRef]
34. Mason, R.P.; Tulenko, T.N.; Jacob, R.F. Direct Evidence for Cholesterol Crystalline Domains in Biological Membranes: Role in Human Pathobiology. *Biochim. Biophys. Acta-Biomembr.* **2003**, *1610*, 198–207. [CrossRef]
35. Subczynski, W.K.; Pasenkiewicz-Gierula, M. Hypothetical Pathway for Formation of Cholesterol Microcrystals Initiating the Atherosclerotic Process. *Cell Biochem. Biophys.* **2020**, *78*, 241–247. [CrossRef]
36. Herold, C.; Chwastek, G.; Schwille, P.; Petrov, E.P. Efficient Electroformation of Supergiant Unilamellar Vesicles Containing Cationic Lipids on ITO-Coated Electrodes. *Langmuir* **2012**, *28*, 5518–5521. [CrossRef]
37. Schindelin, J.; Arganda-Carreras, I.; Frise, E.; Kaynig, V.; Longair, M.; Pietzsch, T.; Preibisch, S.; Rueden, C.; Saalfeld, S.; Schmid, B.; et al. Fiji: An Open-Source Platform for Biological-Image Analysis. *Nat. Methods* **2012**, *9*, 676. [CrossRef]
38. R Development Core Team. *R: A Language and Environment for Statistical Computing*; R Foundation for Statistical Computing: Vienna, Austria, 2020.
39. Ong, S.; Chitneni, M.; Lee, K.; Ming, L.; Yuen, K. Evaluation of Extrusion Technique for Nanosizing Liposomes. *Pharmaceutics* **2016**, *8*, 36. [CrossRef] [PubMed]
40. Kusumi, A.; Fujiwara, T.K.; Tsunoyama, T.A.; Kasai, R.S.; Liu, A.; Hirosawa, K.M.; Kinoshita, M.; Matsumori, N.; Komura, N.; Ando, H.; et al. Defining Raft Domains in the Plasma Membrane. *Traffic* **2020**, *21*, 106–137. [CrossRef]
41. de Almeida, R.F.M.; Fedorov, A.; Prieto, M. Sphingomyelin/Phosphatidylcholine/Cholesterol Phase Diagram: Boundaries and Composition of Lipid Rafts. *Biophys. J.* **2003**, *85*, 2406–2416. [CrossRef] [PubMed]
42. Veatch, S.L.; Keller, S.L. Miscibility Phase Diagrams of Giant Vesicles Containing Sphingomyelin. *Phys. Rev. Lett.* **2005**, *94*, 3–6. [CrossRef] [PubMed]
43. Ionova, I.V.; Livshits, V.A.; Marsh, D. Phase Diagram of Ternary Cholesterol/Palmitoylsphingomyelin/Palmitoyloleoyl-Phosphatidylcholine Mixtures: Spin-Label EPR Study of Lipid-Raft Formation. *Biophys. J.* **2012**, *102*, 1856–1865. [CrossRef] [PubMed]
44. Li, L.K.; So, L.; Spector, A. Membrane Cholesterol and Phospholipid in Consecutive Concentric Sections of Human Lenses. *J. Lipid Res.* **1985**, *26*, 600–609. [CrossRef] [PubMed]
45. Li, L.-K.; So, L.; Spector, A. Age-Dependent Changes in the Distribution and Concentration of Human Lens Cholesterol and Phospholipids. *Biochim. Biophys. Acta-Lipids Lipid Metab.* **1987**, *917*, 112–120. [CrossRef] [PubMed]
46. Deeley, J.M.; Mitchell, T.W.; Wei, X.; Korth, J.; Nealon, J.R.; Blanksby, S.J.; Truscott, R.J.W. Human Lens Lipids Differ Markedly from Those of Commonly Used Experimental Animals. *Biochim. Biophys. Acta-Mol. Cell Biol. Lipids* **2008**, *1781*, 288–298. [CrossRef] [PubMed]

Supplementary Material

Electroformation of Giant Unilamellar Vesicles from Damp Lipid Films Formed by Vesicle Fusion

Zvonimir Boban [1,2], Ivan Mardešić [1,2], Sanja Perinović Jozić [3], Josipa Šumanovac [4], Witold Karol Subczynski [5] and Marija Raguz [1,*]

[1] Department of Medical Physics and Biophysics, University of Split School of Medicine, 21000 Split, Croatia; zvonimir.boban@mefst.hr (Z.B.); imardesi@mefst.hr (I.M.); marija.raguz@mefst.hr (M.R.)
[2] Faculty of Science, University of Split, Doctoral Study of Biophysics, 21000 Split, Croatia
[3] Department of Organic Technology, Faculty of Chemistry and Technology, University of Split, 21000 Split, Croatia
[4] Faculty of Science, University of Split, Department of Physics, 21000 Split, Croatia
[5] Department of Biophysics, Medical College of Wisconsin, Milwaukee, WI 53226, USA; subczyn@mcw.edu
* Correspondence: marija.raguz@mefst.hr; Tel.: +385-9876-8819

Supplementary Figure S1 shows the size density distribution of GUVs produced from POPC. Instead of RSE, the gentle hydration method was used to produce MLVs. All other steps were the same as in other experiments. The average GUV diameter (mean ± sd) was 55 ± 31 μm, with many GUVs larger than 100 μm and even as large as 300 μm being produced. There is no need to use the RSE method if no Chol, or small amount of Chol is present in the mixture. However, if that is not the case, since the gentle hydration protocol also involves a lipid film drying step, the Chol demixing will certainly be an issue. The RSE technique is included to assure that the Chol concentration in initial MLVs is the same as the concentration of Chol in the initial mixture of lipids dissolved in an organic solvent.

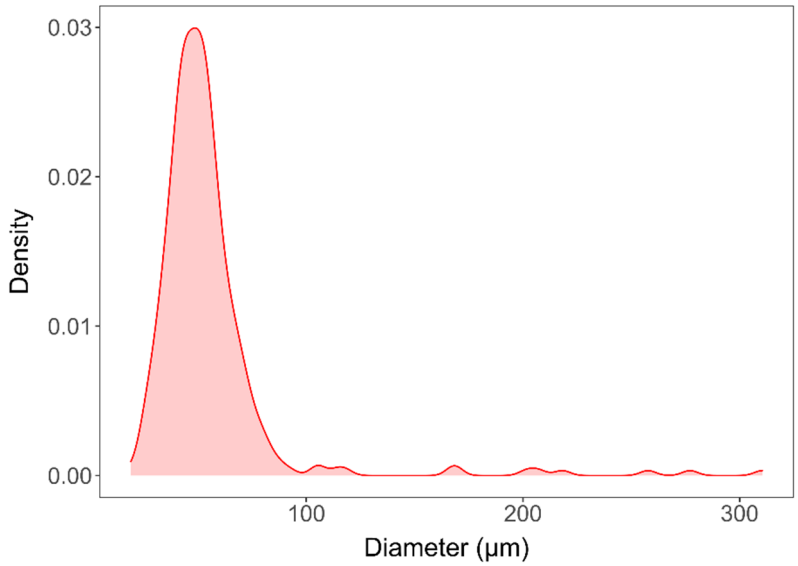

Figure S1. Size distribution density for GUVs produced from POPC with a spin-coating duration of 2 min. The lipid concentration was 3 mg/mL.

8 CONCLUSIONS AND OUTLOOKS

We have performed experiments in order to optimize and advance the electroformation of GUVs containing different phospholipids and Chol concentrations reaching and surpassing the Chol saturation threshold. The traditional electroformation protocol has low reproducibility and yields GUV populations with a wide size distribution. After upgrading the electroformation chamber and replacing the traditional drop-deposition method with spin-coating, we optimized the electrical parameters to produce GUVs from binary POPC/Chol and ternary POPC/sphingomyelin/Chol mixtures with high Chol concentrations. Analyzing fluorescence microscopy images of obtained samples, we found the optimal electrical parameters to be 10 Hz and 2 V. Lipid film thickness for which best results were achieved was estimated at approximately 30 nm from atomic force microscopy and X-ray reflectometry measurements.

However, these modifications could not address the issue of Chol demixing during the dry lipid film step of the protocol. Consequently, we proposed a new protocol which bypasses this phase by combining plasma-cleaning, RSE, and spin-coating techniques for production of GUVs from aqueous damp lipid films. We believe that this new improved electroformation protocol will enable successful studies of physical properties, lateral organization and domain function of cell membranes with very high Chol such as the eye lens fiber cell membranes. Additionally, both using aqueous solutions and treating the electrodes with plasma have been proven beneficial for electroformation efficiency, allowing for production of GUVs with charged lipids and solutions containing high ion concentrations. The protocol could also be adapted for protein insertion into GUVs with reduced protein denaturation due to the avoidance of organic solvents and lipid film drying.

9 CURRICULUM VITAE

EXPERIENCE

NOVEMBER 2017 - PRESENT

RESEARCH AND TEACHING ASISSTANT

UNIVERSITY OF SPLIT SCHOOL OF MEDICINE

DEPARTMENT OF MEDICAL PHYSICS AND BIOPHYSICS

EDUCATION

JANUARY 2019 - PRESENT

DOCTORAL STUDY OF BIOPHYSICS,

FACULTY OF SCIENCE, UNIVERSITY OF SPLIT

OCTOBER 2012 - JUNE 2017

MASTER OF PHYSICS

FACULTY OF SCIENCE, UNIVERSITY OF ZAGREB

Graduated Magna Cum Laude

GPA 4.8/5.0

AWARDS

SEPTEMBER 2017

YOUNG INVESTIGATOR AWARD FOR BEST POSTER

SECOND ADRIATIC SYMPOSIUM ON BIOPHYSICAL APPROACHES IN BIOMEDICAL STUDIES

Poster title: “The mitotic spindle is chiral due to torques generated by motor proteins”

BOOKS

JULY 2022

UVOD U RUDARENJE PODATAKA R-OM (INTRODUCTION TO DATA MINING WITH R)

Authors: Hrvoje Kalinić and Zvonimir Boban

Publisher: Element, Zagreb

The first university textbook on R in Croatian

ARTICLES

1. Boban, Z.; Mardešić, I.; Perinović Jozić, S.; Šumanovac, J.; Subczynski, W.K.; Raguz, M. Electroformation of Giant Unilamellar Vesicles from Damp Lipid Films Formed by Vesicle Fusion. *Membranes (Basel).* **2023**, *13*, 352, doi: 10.3390/membranes13030352.

2. Mardešić, I.; Boban, Z.; Subczynski, W.K.; Raguz, M. Membrane Models and Experiments Suitable for Studies of the Cholesterol Bilayer Domains. *Membranes (Basel).* **2023**, *13*, 320, doi:10.3390/membranes13030320.

3. Boban, D.; Dželalija, A.M.; Gujinović, D.; Benzon, B.; Ključević, N.; Boban, Z.; Mudnić, I.; Grković, I. Differential Effects of White Wine and Ethanol Consumption on Survival of Rats after a Myocardial Infarction. *Appl. Sci.* **2023**, *13*, 1450, doi:10.3390/app13031450.

4. Vrdoljak, J.; Boban, Z.; Barić, D.; Šegvić, D.; Kumrić, M.; Avirović, M.; Perić Balja, M.; Periša, M.M.; Tomasović, Č.; Tomić, S.; et al. Applying Explainable Machine Learning Models for Detection of Breast Cancer Lymph Node Metastasis in Patients Eligible for Neoadjuvant Treatment. *Cancers (Basel).* **2023**, *15*, 634, doi:10.3390/cancers15030634.

5. Nazlić, J.; Jurić, D.; Mudnić, I.; Boban, Z.; Dželalija, A.M.; Tandara, L.; Šupe-Domić, D.; Gugo, K.; Boban, M. Effects of Moderate Consumption of Red Wine on Hepcidin Levels in Patients with Type 2 Diabetes Mellitus. *Foods* **2022**, *11*, 1881, doi:10.3390/foods11131881.

6. Boban, Z.; Mardešić, I.; Subczynski, W.K.; Jozić, D.; Raguz, M. Optimization of Giant Unilamellar Vesicle Electroformation for Phosphatidylcholine/Sphingomyelin/ Cholesterol Ternary Mixtures. Membranes (Basel). **2022**, 12, 525, doi:10.3390/membranes12050525.

7. Boban, Z.; Mardešić, I.; Subczynski, W.K.; Raguz, M. Giant Unilamellar Vesicle Electroformation: What to Use, What to Avoid, and How to Quantify the Results. Membranes (Basel). **2021**, 11, 860, doi:10.3390/membranes11110860.

8. Boban, Z.; Puljas, A.; Kovač, D.; Subczynski, W.K.; Raguz, M. Effect of Electrical Parameters and Cholesterol Concentration on Giant Unilamellar Vesicles Electroformation. Cell Biochem. Biophys. **2020**, 78, 157–164, doi:10.1007/s12013-020-00910-9.

9. Novak, M.; Polak, B.; Simunić, J.; Boban, Z.; Kuzmić, B.; Thomae, A.W.; Tolić, I.M.; Pavin, N. The Mitotic Spindle Is Chiral Due to Torques within Microtubule Bundles. *Nat. Commun.* **2018**, *9*, 3571, doi:10.1038/s41467-018-06005-7.